

DISCOVERY OF NOVEL GENETIC
MODULATORS OF RESPONSE TO
CYTARABINE AND IMMUNE EVASION IN
ACUTE MYELOID LEUKEMIA

Maja Jankovic

Department of Medicine

Division of Experimental Medicine

McGill University

Montréal, Québec, Canada

August, 2023

A thesis submitted to McGill University in partial fulfillment of the requirements of the
degree of Doctor of Philosophy

© Maja Jankovic 2023

1 Table of Contents

<u>LIST OF ABBREVIATIONS</u>	<u>VII</u>
<u>ABSTRACT.....</u>	<u>XII</u>
<u>RÉSUMÉ</u>	<u>XIV</u>
<u>ACKNOWLEDGEMENTS</u>	<u>XVII</u>
<u>CONTENTS OF MANUSCRIPT.....</u>	<u>XVIII</u>
<u>PREFACE AND FORMAT OF THE THESIS.....</u>	<u>XVIII</u>
<u>CONTRIBUTION OF AUTHORS</u>	<u>XX</u>
CHAPTER 1: INTRODUCTION	XX
CHAPTER 2: HERC1	XX
CHAPTER 3: SLC25A19	XX
CHAPTER 4: DISCUSSION	XXI
CONTRIBUTIONS TO ORIGINAL KNOWLEDGE.....	XXII
<u>1. CHAPTER: GENERAL INTRODUCTION</u>	<u>1</u>
1.1 HEMATOPOIESIS.....	2
1.1.1 INTRODUCTION TO HEMATOPOIESIS AND HSCs.....	2
1.1.2 HIERARCHICAL ORGANIZATION OF HEMATOPOIESIS	4
1.1.3 IDENTIFICATION OF HSCs	4

1.1.4	THE BONE MARROW NICHE.....	6
1.1.5	GENOME INSTABILITY IN HSCs.....	7
1.1.6	DISORDERS OF BLOOD PRODUCTION	9
1.2	ACUTE MYELOID LEUKEMIA	12
1.2.1	INTRODUCTION TO ACUTE MYELOID LEUKEMIA.....	12
1.2.13	AML BIOLOGY	25
1.3	AML SUBTYPES AND DIAGNOSIS.....	30
1.4	TREATMENT	34
1.4.5	INTRODUCTION TO NUCLEOSIDE ANALOGUES.....	38
1.4.6	INTRACELLULAR NUCLEOSIDE METABOLISM.....	41
1.5	MURINE AML MODELS	42
1.6	CRISPR/CAS9-BASED GENETIC SCREENING IN AML.....	44
1.7	UBIQUITIN-PROTEASOME SYSTEM.....	46
1.8	HYPOTHESIS AND RESEARCH OBJECTIVES.....	50
2	<u>CHAPTER 2: THE E3 UBIQUITIN LIGASE HERC1 MODULATES THE RESPONSE TO</u>	
	<u>NUCLEOSIDE ANALOGS IN ACUTE MYELOID LEUKEMIA</u>	<u>51</u>
2.1	PREFACE TO THE MANUSCRIPT.....	52
2.2	ABSTRACT	55
2.3	STATEMENT OF SIGNIFICANCE	56
2.4	INTRODUCTION	57
2.5	MATERIALS AND METHODS.....	58
2.6	RESULTS	70
2.6.1	CRISPR SCREENING IDENTIFIES HERC1 AS A MODULATOR OF ARA-C IN AML CELLS	70

2.6.2	LOSS OF HERC1 INCREASES THE SENSITIVITY OF MURINE AML CELL TO NUCLEOSIDE ANALOGS <i>IN VITRO</i>	74
2.6.3	TARGETING THE E3 UB LIGASE HERC1 EXACERBATES ARA-C-INDUCED APOPTOSIS IN AML CELLS	78
2.6.4	HERC1 CONTROLS DCK PROTEIN LEVELS IN MURINE AML CELLS	82
2.6.5	TARGETING HERC1 MODULATES ARA-C RESPONSE <i>IN VIVO</i>	85
2.7	DISCUSSION	88
2.8	DISCLOSURE OF CONFLICTS OF INTEREST	90
2.9	AUTHORSHIP CONTRIBUTIONS	90
2.10	ACKNOWLEDGMENTS	91
2.11	REFERENCES	92
2.12	SUPPLEMENTARY DATA	95
3	<u>CHAPTER 3: IMPORTANCE OF THE MITOCHONDRIAL TRANSPORTER SLC25A19 IN AML</u>	<u>106</u>
3.1	ABSTRACT.....	109
3.2	INTRODUCTION	110
3.3	MATERIALS AND METHODS	111
3.4	RESULTS	118
3.4.1	FOCUSED BASED-DROPOUT SCREEN TARGETS DIFFERENT COMPONENTS OF AML BIOLOGY.....	118
3.4.2	CRISPR SCREENING IDENTIFIES <i>Slc25a19</i> AS AN IMMUNE REGULATOR IN AML.	121
3.5	DISCUSSION	127
3.6	ACKNOWLEDGMENTS	129
3.7	AUTHORSHIP	129
3.8	REFERENCES	130

3.9	SUPPLEMENTARY FIGURES	133
4	<u>CHAPTER: DISCUSSION AND FUTURE DIRECTIONS</u>	<u>136</u>
4.1	HERC1 IN AML AND NUCLEOSIDE ANALOGUE TREATMENT.....	137
4.1.3	PROTEASOMAL DEGRADATION OF DCK AS A NOVEL REGULATORY STEP IN ARA-C RESISTANCE 139	
4.1.4	HERC1 AS A CANDIDATE REGULATOR OF DCK ACTIVITY	141
4.1.5	THE POTENTIAL ROLE OF HERC1 IN NUCLEOTIDE METABOLISM AT STEADY STATE AND CHEMORESISTANCE.....	141
4.1.6	POTENTIAL PLEOTROPIC EFFECTS IN HERC1-DEPLETED MA CELLS	143
4.1.7	LIMITATIONS OF THE STUDY	145
4.1.8	THERAPEUTIC IMPLICATIONS	145
4.2	CRISPR/CAS9-BASED SCREENING APPROACH FOR THE DISCOVERY OF IMMUNE REGULATORY GENES	146
4.2.1	NEW POTENTIAL OF CELLULAR IMMUNE THERAPIES IN THE TREATMENT OF AML	149
4.2.2	OTHER IMMUNE TARGETS	151
4.2.3	LIMITATIONS OF THE STUDY	151
4.2.4	THERAPEUTIC IMPLICATIONS	152
4.3	CONCLUSION AND SUMMARY	152
5	<u>REFERENCES</u>	<u>154</u>

List of Figures

Figure 1. 1 The classical model of hematopoiesis.	5
Figure 1. 2 Sources of genome instability in HSC.....	9
Figure 1. 3 AML development and clonal architecture, adapted from [87]. Created with BioRender.com.	15
Figure 1. 4 Intracellular metabolism of Ara-C.....	40
Figure 2. 1 CRISPR screen identifies HERC1 as modulator of Ara-C.	73
Figure 2. 2 Loss of Herc1 increases the sensitivity of murine AML cell to nucleoside analogs <i>in vitro</i>	76
Figure 2. 3 Targeting the E3 Ub ligase Herc1 exacerbates Ara-C-induced apoptosis in AML cells.	80
Figure 2. 4 Herc1 controls Dck protein levels in murine AML.....	84
Figure 2. 5 Loss of Herc1 <i>in vivo</i> sensitizes AML to Ara-C.....	87
Supplementary Figure 2. 1 Gene editing of Herc1.	95
Figure 3.1 Generation of focused <i>in vivo</i> library.....	121
Figure 3.2 <i>In vivo</i> CRISPR/Cas9 library targets different components of AML biology.	124
Figure 3.3 CRISPR/Cas9 mediated KO of Slc25a19 is lethal in immune competent mice.	126
Supplementary Figure 3. 1 Engraftment efficiency of library transduced MA-Cas9 cells.	133
Supplementary Figure 3. 2 Loss of Slc25a19 is essential in immune competent BL6 mice.....	134

Figure 4. 1 Model of the contribution of HERC1 in the nucleotide salvage pathway..... 143

List of Tables

Table 1. 1 Top mutated genes and chromosomal rearrangements, data generated using cBioPortal using Beat AML, TCGA and TARGET data set. AML categories based on [88]. 17

Table 1. 2 5th edition WHO diagnosis criteria for AML types defined by genetic abnormalities, adapted from [216]..... 33

Table 1. 3 5th edition WHO diagnosis criteria for AML types defined by differentiation, adapted from [192] 34

Table 2-1 sgRNAs human and mouse 62

Table 2-2 Primer for TIDE analysis..... 63

Table 2-3 MS significant hits..... 96

Table 2-4 Overlap proteomics and RNA seq 103

List of Abbreviations

Abbreviation	Definition
2-HG	2-hydroxyglutarate
2'-O-Me	rRNA 2'-O-methylation
5-Aza-C	Azacytidine
5mC	5-methylcytosine
ABL	Abelson murine leukemia gene
ALDH	Aldehyde dehydrogenase
ALL	Acute lymphoid leukemia
AML	Acute myeloid leukemia
AMP	Adenosine monophosphate
APL	Promyelocytic leukemia
Ara-C	Cytarabine
Ara-U	Uracil Arabinoside
ARCH	Age-related clonal hematopoiesis
ARG	Arginase
ASXL1	Additional sex combs like transcriptional regulator 1
ATM	Ataxia-telangiectasia-mutated
ATO	Arsenic trioxide
ATP	Adenosine triphosphate
ATP	Adenosine triphosphate
ATR	Ataxia telangiectasia and rad3 related
ATRA	All-trans retinoic acid
BCL-2	B-Cell lymphoma 2
BCR	Breakpoint cluster region gene
BER	Base excision repair
BM	Bone marrow
BME	Bone marrow microenvironment
BMN	Bone marrow niche
BrdU	Bromodeoxyuridine
CBF-AML	Core-binding factor complex AML
CBFB/MYH11	Core-binding factor subunit beta/myosin heavy chain
CDA	Cytidine deaminase
CDP	Cytidine diphosphate
CEBPA	CCAT/enhancer binding protein α
CEBPE	CCAAT Enhancer Binding Protein Epsilon
CH3	Methyl groups

CHIP	Clonal hematopoiesis of indeterminate potential
CLP	Common lymphoid progenitors
CMP	Chronic myeloid leukemia
CMP	Common myeloid progenitors
CNTs	Concentrative nucleoside transporters
CR	Complete remission
CREB	CAMP response element-binding protein
CRISPR	Clustered regularly interspaced short palindromic repeats
CRISPRa	CRISPR activation
CRISPRi	CRISPR interference
CTP	Cytidine triphosphate
dCAS9	Endonuclease dead Cas9
DCK	Deoxycytidine kinase
DDR	DNA damage response
DGK	Deoxyguanosine kinase
dhmC	5-hydroxymethylcytosine
DNMT3A	DNA (cytosine-5)-methyltransferase 3A
dNTP	Deoxynucleotides
DSB	Double strand break
dsDNA	Double strand DNA
DUBS	Deubiquitinating enzymes
E1	Ub-activating enzymes
E2	Ub-conjugating enzymes
E3	Ub-ligating enzymes
ELN	European LeukemiaNET
ENT	Equilibrative nucleoside transporter
ET	Essential thrombocythemia
ETC	Electron transport chain
EVs	Extracellular vesicles
EZH2	Zeste 2 polycomb repressive complex 2 subunit
FAB	French-American-British
FACS	Fanconi anemia
FACS	Fluorescence-activated cell sorting
FISH	Fluorescent in situ hybridization
FLT3	Fms-like kinase 3
FLT3-ITD	FLT3-Internal Tandem duplication
GEMMs	Genetically-engineered mouse models
GMP	Granulocyte-monocyte progenitors
GMP	Guanosine monophosphate
H2O2	Hydrogen peroxide

HDAC	Histone deacetylases
HECT	Homologous to the E6-AP carboxyl terminus HECT and RLD domain containing E3 ubiquitin protein ligase family
HERC1	member 1
HIF	Hypoxia inducible factor
HIF1 α	Hypoxia-inducible factor 1 alpha
HM	HOXA9-MEIS1 cell line
HMA	Hypomethylating agents
HOX	Homeobox gene
HR	Homologous recombination
HSC	Hematopoietic stem cell
ICL	Interstrand crosslink
IDH	Isocitrate dehydrogenase
IDO1	Indoleamine 2,3-dioxygenase-1
IFN	Interferon
IL	Interleukin
IMP	Inosine monophosphate
INDEL	Insertion-deletion
iPSCs	Induced pluripotent stem cells
IR	Ionizing radiation
JARID2	Jumonji AT-rich interactive domain 2
KI	Knock-in
KIT	Tyrosine kinase kit
KMT2A	Lysine methyltransferase 2A
KO	Knock-out
KRAB	Kruppel associated box domain
LDHA	Lactate dehydrogenase A
LSCs	Leukemic stem cells
LSK	Lin ⁻ /Sca1 ⁺ /ckit ⁺ hematopoietic stem cells
MA	MLL-AF9 cell line
MA	MLL-AF9
MDS	Myelodysplastic syndrome
MEIS1	Meis Homoeobox 1
MEP	Erythrocyte-megakaryocyte progenitors
MHC	Major histocompatibility complex
MK	Megakaryocytes
MLL	Mixed-lineage leukemia
MLL-PTD	Partial tandem duplications of MLL
MMR	Mismatch repair
MOMP	Mitochondrial outer membrane permeabilization

MPN	Myeloproliferative neoplasm
MPO	Myeloperoxidase
MPP	Multipotent progenitors
MRD	Residual disease
MS	Mass spectrometry
MTORC1	MTOR complex1
NER	Nucleotide excision repair
NES	Nuclear export signal
NGS	Next generation sequencing
NHEJ	Non-homologous end joining
NHEJ	Non-homologous end joining
NKG2CL	NKG2D ligand
NKG2D	Natural Killer Group 2D
NPM1	Nucleophosmin
NPM1c+	Cytosolic nucleophosmin
NSG	NOD- <i>scid-IL2Rgc</i> ^{-/-}
OXPHOS	Oxidative phosphorylation
P2X7	Purinergic Receptor P2X 7
PARP1	Poly ADP-ribose Polymerase 1
PB	Peripheral blood
PDH	Pyruvate dehydrogenase
Ph ⁺	Philadelphia Chromosome
PHGDH	Phosphoglycerate dehydrogenase
PKM2	Pyruvate kinase muscle isoform M2
PMF	Primary myelofibrosis
PML	Promyelocytic leukemia gene
PRC	Polycomb repressor complex
PTM	Post-transcriptional modification
PTPN1	Protein tyrosine phosphatase non-receptor 11
PV	Polycythemia vera
RAD21	RAD21 Cohesin Complex Component
RAR α	Retinoic acid receptor α
RAS	Rat sarcoma virus gene
RBR	Ring between ring fingers
RING	Really interesting new gene family
RNAi	RNA interference
RNP	CRISPR/Cas9:sgRNA ribonucleoprotein
RNR	Ribonucleotide reductase
ROS	Reactive oxygen species
RUNX1	RUNX family transcription factor

RUNX1T1	RUNX1 partner transcriptional co-repressor 1
s-AML	secondary AML
SAA	Serum amyloid A
SAA	Acute-phase protein serum amyloid
SAMHD1	Sterile alpha motif and HD domain-containing protein 1
SLAM	CD150 ⁺ /CD48 ⁺ /CD34 ^{low}
SLC25A19	Solute carrier family 25 member 19
SMC	Structural maintenance of chromosomes proteins
snRNA	U1 spliceosomal RNA
SNV	Single nucleotide variant
SoNar	Senor of NAD(H) redox
SRSF2	Serine and arginine rich splicing factor 2
SSB	Single strand break
ssDNA	Single strand DNA
STAG2	Cohesion subunit SA-2
SUZ12	SUZ12 polycomb repressive complex 2 subunit
t-AML	Therapy-related AML
TCA	Tricarboxylic acid cycle/ Citric acid cycle
TCGA	The Cancer Genome Atlas Research Network
TET2	Ten-eleven translocation 2
TF	Transcription factor
TK	Thymidine kinase
TLS	Translesion synthesis
TNF	Tumor necrosis factor
TPP	Thiamine pyrophosphate
U2AF	U2 small nuclear ribonucleoprotein auxiliary factor
Ub	Ubiquitin
UDP	Uridine diphosphate
UMP	Uridine monophosphate
UPS	Ubiquitin-Proteasom system
VAF	Variant allele fraction
WHO	World Health Organization
WT	Wilms tumor gene
α-KG	Alpha-ketoglutarate

Abstract

Acute myeloid leukemia (AML) is a hematological malignancy characterized by aberrant self-renewal and a block in the differentiation of myeloid progenitors. Chemotherapy remains the current standard of care for most patients with AML and this regimen is often composed of several DNA-damaging agents, including the pyrimidine nucleoside analog cytarabine (Ara-C). Unfortunately, approximately half of AML patients treated with chemotherapy ultimately relapse. Moreover, Ara-C-based therapy is associated with adverse side effects, including severe cytopenias and infections that limit its administration to older patients. Understanding the genetic factors within AML cells that influence Ara-C response both *in vitro* and *in vivo* may allow us to better identify patients who are likely to benefit from Ara-C treatment.

Immunotherapy has revolutionized the care of solid tumors and lymphomas and has shown some promising results in the treatment of AML. However, targeted immunotherapy in AML is currently challenged by the lack of AML-specific target antigens and the complex *in vivo* architecture of AML. Thus, deciphering the genetic vulnerabilities of AML under the pressure of the immune system is critical to establish more effective immune-based therapies for the treatment of AML patients.

CRISPR/Cas9-based dropout screening is a powerful discovery tool, which allows us to identify novel genetic vulnerabilities in combination with different therapies *in vitro* and *in vivo*. **The goal of my doctoral studies has been to utilize this technology in experimental models of AML to identify (i) drug-gene interactions in the context of Ara-C exposure *in vitro* (Chapter 2); and (ii) genetic vulnerabilities in the context of the immune system *in vivo* (Chapter 3).** As part of Chapter 2, I performed a genome-wide CRISPR-Cas9 screen in two murine AML cell lines, driven by the oncogenes MLL/AF9 and HoxA9/Meis1, to identify the landscape of genes

modulating Ara-C response. Using this approach, I identified the E3 ubiquitin ligase Herc1 as a regulator of sensitivity to pyrimidine and purine analogues. Treatment with Ara-C led to impaired cell cycle progression in Herc1-depleted murine AML cells and enhanced Ara-C-induced apoptosis. To identify Herc1 substrate(s) that could mediate the response to Ara-C in murine AML cells, I performed comparative transcriptomic and proteomic analyses between Herc1-depleted and wild-type murine AML cells. This multi-omics integrative analysis identified 96 protein candidates that are differentially regulated at the post-transcriptional level in Herc1-depleted cells, including deoxycytidine kinase (Dck), the enzyme that phosphorylates Ara-C and promote its incorporation into DNA,. Increased abundance of Dck protein levels was confirmed in murine Herc1-depleted AML cells both *in vitro* and *in vivo*. Importantly, the loss of Herc1 *in vivo* confirmed increased sensitivity of Ara-C, demonstrating its therapeutic relevance. As part of Chapter 3, I completed a focused CRISPR-based dropout screen *in vivo* to compare genetic vulnerabilities of AML in immune-competent and -deficient mice. This screen targeted 126 genes encompassing different components of AML biology *in vivo*, including cell adhesion, immune response, and metabolism. As expected, genetic targeting of immune-related processes such as MHC class I, complement factor, and CD47 signaling, led to AML depletion in immune-competent mice, confirming the validity of the approach. Furthermore, I identified the mitochondrial thiamine transporter *Slc25a19* as an immune-specific vulnerability in AML. Overall, I established two CRISPR screening pipelines in therapeutically relevant contexts and discovered two novel promising targets for the treatment of AML: the E3 ligase Herc1 and the mitochondrial transporter *Slc25a19*. Further investigation will provide better insight about the relevance of both targets for the diagnosis and treatment of AML in humans.

Résumé

La leucémie aiguë myéloïde (LAM) est une hémopathie maligne caractérisée par un auto-renouvellement aberrant et un blocage de la différenciation des progéniteurs myéloïdes. La chimiothérapie reste la norme de soins actuelle pour la plupart des patients atteints de LAM et ce régime est composé de plusieurs agents endommageant l'ADN, y compris la cytarabine (Ara-C), un analogue du nucléoside pyrimidique. Malheureusement, environ la moitié des patients atteints de LAM traités par chimiothérapie finissent par rechuter. De plus, la thérapie à base d'Ara-C peut être associée à des effets secondaires indésirables, notamment des nausées, des vomissements et de la fièvre graves qui peuvent limiter sa mise en œuvre chez les patients âgés. Par conséquent, la compréhension des facteurs génétiques qui influencent la réponse de l'Ara-C à la fois *in vitro* et *in vivo* peut permettre de combler cette lacune clinique non comblée.

L'immunothérapie a révolutionné la prise en charge des tumeurs solides et des lymphomes et a montré des résultats prometteurs dans le traitement de la LAM. Cependant, l'immunothérapie ciblée dans la LAM est actuellement mise au défi par le manque d'antigènes cibles spécifiques à la LAM et l'architecture *in vivo* complexe de la LAM. Ainsi, déchiffrer les vulnérabilités génétiques de la LAM sous différents niveaux d'immunité est essentiel pour établir des thérapies immunitaires plus efficaces pour le traitement des patients atteints de LAM. Le dépistage d'abandon basé sur CRISPR/Cas9 est un outil puissant qui nous permet d'identifier de nouvelles vulnérabilités en combinaison avec différents modèles biologiques *in vitro* et *in vivo*. L'objectif de mes études doctorales a été d'utiliser cette technologie dans des modèles expérimentaux de LAM pour identifier (i) les interactions médicament-gène dans le contexte de l'exposition à l'Ara-C *in vitro* (Chapitre 2) ; et (ii) les vulnérabilités génétiques sous différents niveaux d'immunité *in vivo* (Chapitre 3). Dans le cadre du chapitre 2, j'ai effectué un criblage CRISPR-Cas9 à l'échelle

du génome dans deux lignées cellulaires AML murines pilotées par les oncogènes MLL/AF9 et HoxA9/Meis1 pour identifier le paysage des gènes modulant la réponse Ara-C. En utilisant cette approche, j'ai identifié l'ubiquitine ligase E3 Herc1 comme un nouveau sensibilisateur des cellules AML murines à la pyrimidine et aux analogues de purine. Le traitement par Ara-C a entraîné une altération de la progression du cycle cellulaire dans les cellules AML murines appauvries en Herc1 et une apoptose induite par Ara-C améliorée. Pour identifier le ou les substrats Herc1 susceptibles de répondre à Ara-C dans les cellules AML murines, des analyses comparatives transcriptomiques et protéomiques ont été effectuées entre des cellules AML murines appauvries en Herc1 et de type sauvage. Cette analyse d'intégration de données multi-omiques a identifié 96 protéines candidates exclusivement régulées au niveau post-transcriptionnel, dont la désoxycytidine kinase (Dck), connue pour phosphoryler l'Ara-C et favoriser son incorporation dans l'ADN, influençant ainsi la réponse de Cellules AML à Ara-C. L'augmentation de l'abondance des niveaux de protéine Dck a été confirmée dans les cellules AML appauvries en Herc1 murines, à la fois *in vitro* et *in vivo*. Fait important, la perte de Herc1 *in vivo* a confirmé une sensibilité accrue de l'Ara-C. Dans le cadre du chapitre 3, j'ai effectué un criblage d'abandon ciblé basé sur CRISPR *in vivo* pour explorer les vulnérabilités génétiques chez les souris immunocompétentes et déficientes. Cette bibliothèque contenait 126 gènes ciblant différents composants de la biologie de la LAM *in vivo*, notamment l'adhésion cellulaire, la réponse immunitaire et le métabolisme. Comme prévu, le ciblage génétique de processus liés au système immunitaire, tels que le CMH de classe I, le facteur complémentaire et la signalisation CD47, a conduit à une déplétion de l'AML chez des souris immunocompétentes, confirmant ainsi la validité de l'approche. De plus, j'ai identifié le transporteur de thiamine mitochondrial Slc25a19, comme une dépendance immuno-sélective dans la LAM. Dans l'ensemble, j'ai établi deux pipelines de dépistage systématique et découvert deux

nouvelles cibles prometteuses pour le traitement de la LMA : la ligase E3 HERC1 et le transporteur mitochondrial Slc25a19. Une enquête plus approfondie permettra de mieux comprendre la pertinence de cibler les deux résultats pour le diagnostic et le traitement de la LAM.

Acknowledgements

I would like to express my deepest gratitude to all those who have supported and contributed to the completion of my thesis.

First and foremost, I am immensely grateful to my supervisors Dr. Francois Mercier and Dr. Alexandre Orthwein, for their invaluable guidance, encouragement, and expertise throughout the entire duration of my graduate studies. When I began my graduate studies at the Lady Davis Institute, Francois and Alex provided me with the opportunity to learn and grow as a scientist. I would also like to thank my thesis advisory committee, Drs. Javier Di Noia, Brian Wilhelm and Josie Ursini-Siegel for their insightful feedback, support and invaluable expertise, which played a pivotal role in shaping my projects.

I would also like to extend my appreciation to the members of my laboratories, especially Gabriela Galicia-Vazquez, William Poon, Steven Findlay, Joey Heath, Vincent Luo for their collaborative efforts, support, and thought-provoking discussions. You guys are the best, and my thesis would have not been possible without you all.

Furthermore, I would like to acknowledge the assistance provided by the staff and resources of the Lady Davis Institute, especially Christian Young, whose support facilitated the smooth progress of this research.

To my parents Manda and Goran, and my brother Alex, a big hug and thank you! You have supported me throughout my entire life, including the last steps of my thesis. I am grateful for your continuous encouragement throughout this journey.

To my husband Hugo, for your constant belief in me and all your support. There are many things I could write, but I will only say one: I love you!

To my children Sofia and Matias, you are the light in my life and have been my biggest motivation throughout this journey.

Contents of Manuscript

Preface and Format of the thesis

This is a manuscript-based thesis consisting of two to-be-submitted research articles.

Chapter 2

Jankovic, M., Poon, W.L., Gonzales-Losada, C., Galicia Vazquez, G., Sharif-Askar, B., Ding Y., D., Desombre, C., Iliac, A., Shi, J., Orthwein, A., Mercier, F.E. (2023). The E3 ubiquitin ligase Herc1 modulates the response to nucleoside analogs in acute myeloid leukemia (To be submitted for publication).

Chapter 3

Jankovic, M., Poon, W.L., Galicia Vazquez, G., Desombre, C., Ding Y., Shi, J., Orthwein, A., Mercier, F.E. (2023). In vivo CRISPR/Cas9 systematic mapping uncovers *SLC25a19* as potential immune regulator in murine leukemia (To be submitted for publication).

Publications that include work performed by Maja Jankovic but not included in this dissertation:

Worme S, Jessa S, Poon W, **Jankovic M**, Vazquez GG, Bazinet A, Fooks K, Iasenza I, Arrebatutusaus P, Eppert K, Ragoussis I, Wang YC, Johnson NA, Assouline SE, Kleinman CL, Mercier FE. Single-Cell Transcriptomic Profiling of De Novo and Relapsed Acute Myeloid Leukemia Identifies a Leukemic Stemness Program Shared across Diverse Phenotypes. (Manuscript in preparation)

Abusarah J, Cui Y, El-Hachem N, El-Kadiry AE, Hammond-Martel I, Wurtele H, Beaudry A, Raynal NJ, Robert F, Pelletier J, **Jankovic M**, Mercier F, Kamyabiazar S, Annabi B, Rafei M. TACIMA-218: A Novel Pro-Oxidant Agent Exhibiting Selective Antitumoral Activity. *Mol Cancer Ther.* 2021 Jan;20(1):37-49. Doi: 10.1158/1535-7163.MCT-20-0333. Epub 2020 Oct 21. PMID: 33087510.

Mercier FE, Shi J, Sykes DB, Oki T, **Jankovic M**, Man CH, Kfoury YS, Miller E, He S, Zhu A, Vasic R, Doench J, Orthwein A, Michor F, Scadden DT. In vivo genome-wide CRISPR screening in murine acute myeloid leukemia uncovers microenvironmental dependencies. *Blood Adv.* 2022 Sep 13;6(17):5072-5084. Doi: 10.1182/bloodadvances.2022007250. PMID: 35793392; PMCID: PMC9631646.

Contribution of authors

Chapter 1: Introduction

MJ wrote this chapter under the guidance and editorial supervision of FM and AO.

Chapter 2: HERC1

Chapter 2 contains scientific material that is included in a manuscript in preparation to be submitted as an original research article. Conception and design of the work was done by MJ, FM, and AO. Most of the experiments in this study were designed, executed, and analyzed by MJ under the supervision of FM and AO. WP performed *in vitro* culture, lentiviral transduction, and DNA isolation. MJ performed the computational analysis of CRISPR/Cas9 screening data and performed single-sgRNA validation experiments. MJ designed and performed *in vivo* experiments. CGL assisted with western blot experiments. MJ designed experiments and performed *in vitro* experiments for RNA sequencing and Mass spectrometry. RNA sequencing was performed and analyzed by the genomics platform of the Institute de recherche en immunologie et cancerologie (IRIC). DY and SJ assisted with TCGA data analysis and pathway enrichment analysis of RNA seq data. Mass spectrometry was performed and analyzed by the Proteomics and Molecular Analysis Platform at the Centre universitaire de sante McGill (MUHC). The composition of the manuscript and design of experimental figures were done under the supervision of FM and AO.

Chapter 3: SLC25A19

Chapter 3 contains scientific material that is included in a manuscript that is currently in preparation as an original research article. Conception and design of the work was done by MJ, FM and AO. Library was designed and cloned by MJ. In vivo screen was performed and analyzed by MJ. DY and SJ assisted with analysis and performed survival analysis. Most of the experiments in this study were designed, executed, and analyzed by MJ under the supervision of FM and AO.

The composition of the manuscript and design of experimental figures were done under the supervision of FM and AO.

Chapter 4: Discussion

MJ wrote the complete chapter under the guidance of FM and AO.

Contributions to original knowledge

Chapter 2:

- Completed genome-wide CRISPR/Cas9 screen in two murine AML cell lines under Ara-C treatment *in vitro*.
- Identified the ubiquitin ligase Herc1 as a sensitizer to Ara-C and other nucleoside analogs.
- Identified Dck as a target of Herc1.
- Identified that loss of Herc1 provides sensitivity to Ara-C in murine AML *in vivo*.

Chapter 3:

- Curated CRISPR/Cas9 library targeting *in vivo* components of AML biology.
- Developed systematic screening pipeline in immune competent and immune deficient mice.
- Identified 5 novel gene candidates sensitizing AML to immune cells.
- Identified the mitochondrial transporter Slc25a19 as immune sensitizer in AML
- Linked mitochondrial metabolism to the immune compartment.

1. Chapter: General Introduction

1.1 Hematopoiesis

1.1.1 Introduction to hematopoiesis and HSCs

Hematopoiesis is the process of blood cell formation, which takes place in the bone marrow in human adults [1]. The hematopoietic system is responsible for the production of cells with distinct functions, such as leukocytes responsible for innate and adaptive immunity, erythrocytes that transport oxygen and carbon dioxide, and megakaryocytes that generate platelets for blood clotting and wound healing. The hematopoietic system is organized in a hierarchical manner, in which two main lineages of blood cells- the lymphoid and myeloid lineages- arise from multipotent hematopoietic stem cells (HSCs) at the apex. Depending on physiological needs, HSCs can self-renew through symmetrical cell division and expand the stem cell pool or undergo asymmetric cell divisions and give rise to committed progenitors. While the hematopoietic system is highly regenerative and responsible for generating approximately 500 billion blood cells every day, HSCs are rare within the bone marrow (1 in 100,000) [2]. It is estimated that humans have between 50,000-200,000 HSCs and mice have approximately 5,000 HSCs [3, 4]. In 1961, Till and McCulloch described HSC properties for the first time, by transplanting serially diluted bone marrow cells in lethally irradiated mice and observing that shortly after transplantation, small hematopoietic colonies grew in the spleen of recipient mice, later known as colony-forming unit-spleen (CFU-S) [5]. Furthermore, they noted that not every bone marrow cell gave rise to progenitor cells and that there is a positive linear relationship between the number of cells transplanted and the number of CFU-S. Earlier work by E. Donnell Thomas in 1957 provided evidence that human HSCs show a similar potential to reconstitute the hematopoietic system upon transplantation and described their clinical application as first cellular therapy in monozygotic twins [6]. The advancement of fluorescence-activated cell sorting (FACS) in combination with

antibodies directed against cell surface markers allowed the identification and purification of murine and human HSCs and progenitor cell populations from the bone marrow [7-9]. Since the 1960s, the functional study of HSCs in mice and in humans has primarily relied on transplantation experiments to assess two essential properties: self-renewal and multipotency [7]. Upon transplantation, murine HSCs can be distinguished from progenitors if they engraft long-term (> 4 months) and repopulate all blood lineages. Human HSCs engraft in xenogeneic hosts such as immune-deficient mouse strains (e.g., NOD-*scid-IL2Rgc^{-/-}*; NSG) for at least 24 weeks and successfully generate all blood cell types, which demonstrates the considerable conservation between mouse and human hematopoiesis [10, 11]. Proliferation analysis using the thymidine analog bromodeoxyuridine (BrdU) and label-retaining studies using transgenic mice demonstrated that HSCs lie in a quiescent state with low mitochondrial activity to protect themselves from stem cell exhaustion [12]. Subsequent studies demonstrated that the repopulation capacity of HSCs is related to their quiescent state, and showed that HSCs in adult mice divide only about 5 times during the lifespan to maintain hematopoiesis [12-14]. In contrast to adult HSCs, fetal liver and postnatal HSCs are highly proliferative, to expand the HSCs pool during ontogeny and to adapt to the needs of the developing fetus [15-17]. More recently, lineage tracing experiments in mice confirmed that maintenance of adult hematopoiesis at steady state is mostly driven by multipotent progenitors [18, 19], whereas quiescent HSCs act as a reserve pool of stem cells that can be robustly activated to proliferate in response to injury [12]. It is intriguing to discover that adult HSCs are not simply dormant but rather in a state of deep inactivity characterized by reduced metabolic activity, ribosomal biogenesis, and DNA replication. This state of dormancy is critical for protecting these cells, which possess the highest capacity for self-renewal among all blood cells, from any potential mutations that could lead to uncontrolled proliferation and leukemia [20].

1.1.2 Hierarchical organization of hematopoiesis

Through cell division, HSCs give rise to various types of progenitors with gradually decreasing multi-lineage potential and limitation in self-renewal capacity (**Figure 1.1**). Those heterogeneous progenitor cells are also known as multipotent progenitors (MPPs). MPPs give rise to committed progenitors, forming either common lymphoid progenitors (CLPs) or common myeloid progenitors (CMPs). CLPs can differentiate into B cells (B), T cells (T), natural killer cells (NK) and plasmacytoid dendritic cells (DC). CMPs give rise to oligopotent granulocyte-monocyte progenitors (GMPs) and erythrocyte-megakaryocyte progenitors (MEPs). GMPs differentiate into dendritic cells (DC), monocytes (M) and granulocytes (G). and MEPs differentiate into megakaryocytes (MK) and erythrocytes. Recent development in single-cell sequencing and murine lineage tracing has led to an ongoing re-definition of the classical model of hematopoiesis, for example, by the identification of direct trajectories from HSCs to MK, bypassing all progenitor states [21, 22].

1.1.3 Identification of HSCs

HSCs and MPPs express a combination of cell surface antigens that can be identified through FACS. Multiple cell surface markers in HSCs have been discovered over the past decades, allowing for the enrichment of HSCs with great levels of purity [4, 23, 24]. In murine systems, immature HSCs and MPPs are often isolated using cell surface expression of CD117 (c-Kit) and stem cell antigen (Sca)-1 together with the absence of lineage markers of mature cells (Lin⁻), which are often referred to as LSKs. To further distinguish LSK subtypes, the cell surface markers CD150⁺/CD48⁺/CD34^{low} (SLAM) are commonly used to identify long-term repopulating HSCs [25, 26]. In humans, HSCs and MPPs are identified by FACS by the expression of the cell surface

markers CD34⁺/CD38⁻. Long term repopulating HSCs can be further enriched based on CD90⁺/CD45RA⁻/CD49f⁺ [11, 22].

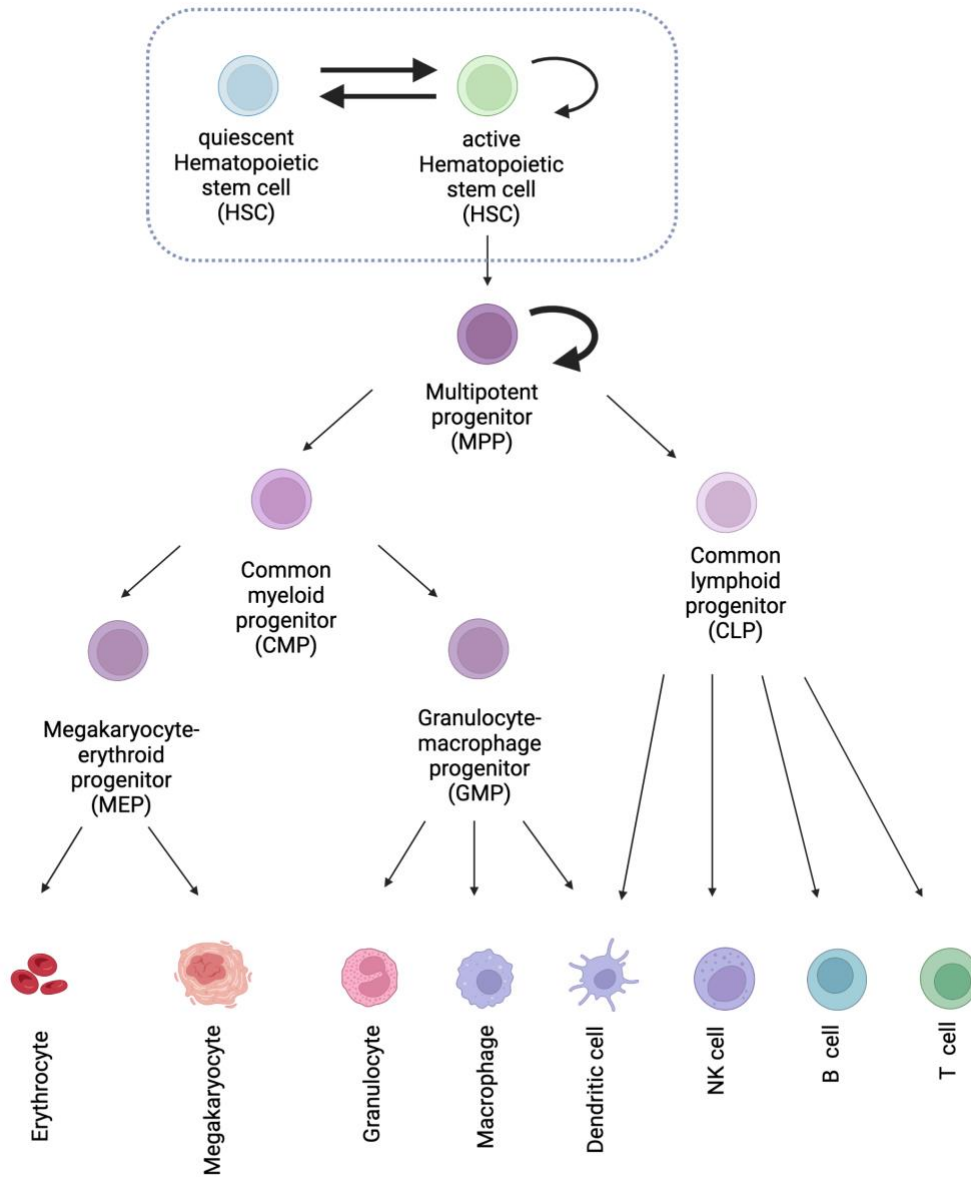


Figure 1. 1 The classical model of hematopoiesis.

Schematic representing adult hematopoiesis in the bone marrow. At the apex of the hierarchy reside multipotent HSCs. Most of the HSCs are quiescent and divide rarely (dormant), very few

are active. MPPs are highly proliferative and the drivers of native hematopoiesis. Created with BioRender.com.

1.1.4 The bone marrow niche

In 1978, R. Schofield proposed the concept of “the HSC niche” to describe the cell-extrinsic factors that regulate and direct HSC self-renewal and differentiation [27]. The bone marrow microenvironment, also often referred to as the bone marrow (BM) niche, is a multicellular network including differentiated blood and immune cells, osteoblasts, mesenchymal stem cells, endothelial cells, adipocytes, perivascular cells, and the sympathetic nerve [28]. Hematopoiesis takes place in the central part of the bone. In mice, HSCs can be found in all bones regardless of the anatomical structure, and interestingly, most HSCs can be enriched using similar immunophenotypic profiles and expression of a core set of “stemness”-associated genes [25]. Human hematopoiesis is found predominantly in the axial skeleton (which includes the cranium, sternum, ribs, vertebrae, and ilium) [28, 29]. The BM niche is not only defined through the physical presence of HSCs but is further characterized by functional properties that maintain HSC characteristics [28]. Genetic manipulation can be used to ablate candidate niche cells *in vivo* and evaluate the effect on HSCs and hematopoiesis. Cre recombinase-mediated labeling of HSCs and surrounding niche cells has helped to identify various cell types and secreted factors contributing to HSC maintenance [27, 28, 30-34]. For instance, MKs are predominantly localized in the perivascular zone adjacent to quiescent HSCs, and it has been shown that MKs secrete chemokine C-X-C motif ligand 4 (CXCL4) and transforming growth factor beta (TGF- β) to regulate HSCs [28, 35, 36]. The targeted elimination of MKs using an inducible Mk lineage *Platelet factor 4 (Pff4)-cre* reporter line resulted in the activation of previously dormant HSCs [28, 36]. Furthermore, Schwann-cells have been found to regulate HSC quiescence through transforming growth factor

beta (TGF- β) and SMAD signaling [28, 37], and a subtype of Foxp3⁺ T regulatory cells (Tregs), through adenosine [28, 38, 39].

1.1.5 Genome instability in HSCs

HSCs are exposed to different sources of DNA damage, leading to genome instability. Endogenous physiological sources of DNA damage are reactive oxygen species (ROS), aldehydes and replication stress. Examples of ROS include hydrogen peroxide (H₂O₂) and superoxide anion radical O₂⁻, which are primarily produced intracellularly by the mitochondria [40]. ROS cause accumulation of base pair anomalies, such as O⁶-methylguanine and 8-oxoguanine [41], which can lead to nucleotide mismatch or DNA inter-strand cross-link adducts (ICL) if the lesion is not repaired efficiently. ICLs refer to covalent linkages between DNA strands that can lead to single-strand breaks (SSBs) and double-strand breaks (DSBs). While ICL-mediated repair is commonly used to resolve such damage, it can result in delayed replication and transcription, thereby eventually leading to apoptosis [23-26]. Aldehydes are formed when alcohol is oxidized by various aldehyde dehydrogenases during the metabolism of carbohydrates, lipids, and amino acids. These aldehydes can also cause ICL. Inborn errors of aldehyde metabolism can lead to increased apoptosis of HSCs and bone marrow failure. This has been observed in both human patients and mouse models with mutations in aldehyde dehydrogenase 2 (ALDH2) and aldehyde dehydrogenase 5 (ALDH5) [42-44]. In comparison to other cell types, HSCs are more sensitive to replication stress, which is caused by decreased expression of DNA damage response genes and delayed DNA damage repair [43]. In experimental models, these altered dynamics of DNA replication forks produced a decline in the self-renewal and the repopulation capacity of murine HSCs [43]. HSCs repair DNA damage using different DNA repair mechanisms depending on their state of proliferation. Quiescent HSCs predominantly repair DNA double-strand-breaks (DSB) by

non-homologous end joining (NHEJ) [45, 46], whereas active cycling HSCs predominately repair DNA breaks using homologous recombination (HR). Irradiation experiments of murine quiescent HSCs have revealed that quiescent HSCs accumulate DSB while in G0 and repair DNA damage upon entry into the cell cycle [47, 48]. DNA damage in quiescent HSCs results in higher frequencies of DSB and chromosomal translocations (**Figure 1.2**). It is also known that patients with solid cancers who have undergone chemotherapy or radiation treatment have a higher risk of developing secondary myeloid neoplasms or AML with complex cytogenetics and poor outcomes [49]. Various studies have identified balanced translocations involving the MLL gene locus as a common consequence of therapy-related leukemia, especially after treatment with topoisomerase II inhibitors [49-52], highlighting the detrimental consequences of DNA-damaging agents on HSCs.

Overall, mutations in genes of DNA repair often result in bone marrow failure and the predisposition to hematopoietic malignancies. First observations came from studies of patients with Fanconi Anemia (FA). FA is characterized by several physical abnormalities, but the most predominant complication is BM failure at a young age and susceptibility to AML. Several genes (FANC genes) have been identified in FA patients, and knock-out studies in murine models confirmed defective repair of DNA cross-links resulting in apoptosis of HSCs [53]. Additionally, it has been demonstrated that FANC genes repair ICL arising from aldehydes [54]. Other studies in mice revealed that the genetic KO of *ataxia telangiectasia mutated (Atm)* in HSCs results in self-renewal and repopulation deficiency leading ultimately to HSC exhaustion [55].

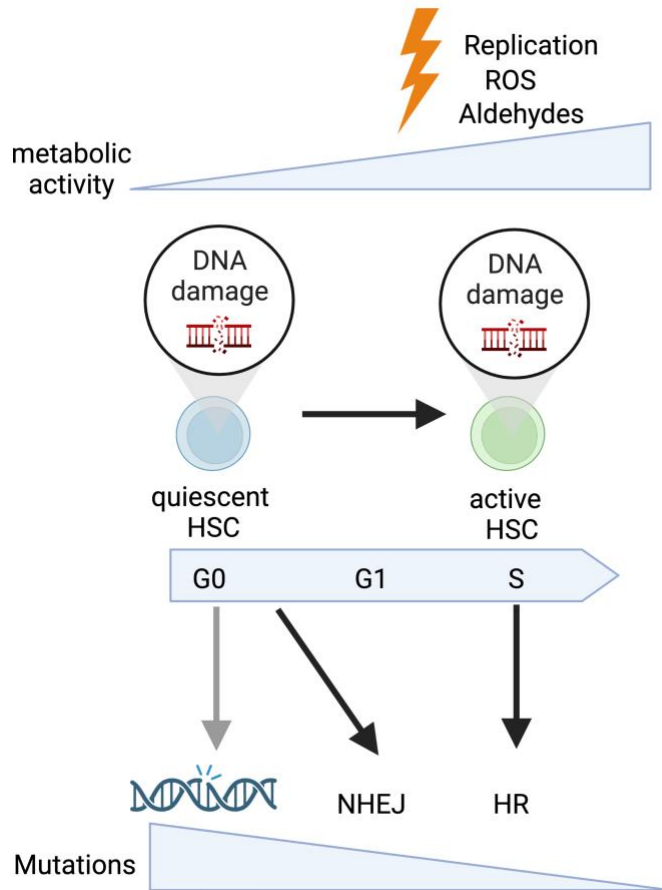


Figure 1. 2 Sources of genome instability in HSC.

HSCs are exposed to physiological sources of DNA damage including replication stress, ROS, and aldehydes. Quiescent HSCs accumulate DNA damage during G0, and repair DNA damage predominantly using NHEJ when entering the cell cycle in G1. Active HSCs are vulnerable to more endogenous stress, but repair DNA damage predominantly using HR. Created with BioRender.com.

1.1.6 Disorders of blood production

1.1.7 Hematopoietic aging and clonal hematopoiesis

Hematopoietic aging refers to the changes and decline in the function of the hematopoietic system over the lifespan of the organism. During aging, several changes occur in HSCs, such as a decline in stem-cell function, accumulation of genetic mutations, and alterations in the clonal

composition of HSCs. Age-related clonal hematopoiesis (ARCH) or clonal hematopoiesis of indeterminate potential (CHIP) is characterized by the presence of a dominant clonal population derived from a single HSC. Originally, ARCH was determined by a threshold of 2% variant allele fraction (VAF) in clinical samples, related to the technological limit of detection of a clonal population to >2% using next generation sequencing (NGS). With the advancement in targeted sequencing, researchers can now detect smaller clonal populations with VAF of 0.03 % or less [56].

Humans have between 50,000-200,000 HSCs [3], and it is estimated that each HSC acquires one exonic mutation per decade of life [57], corresponding to 350,000 to 1.4 million mutations for the entire HSC compartment [58]. Mutations in ARCH-related genes lead to a competitive advantage and result in the expansion of clones of HSCs [59-61]. A considerable portion of ARCH can be attributed to loss-of-function mutations in two enzymes that are responsible for DNA methylation, namely *DNA (cytosine-5)-methyltransferase 3A (DNMT3A)* and *Ten eleven translocation 2 (TET2)*. These mutations are predominantly somatic and often caused by single-nucleotide base-pair changes of cytosine to thymine (C->T) [62]. The methyltransferase DNMT3A is responsible for *de novo* CpG islands methylation, while TET2 catalyzes demethylation from CpG islands by catalyzing the oxidation of 5-methylcytosine (5mC) to 5-hydroxymethylcytosine (dhmC) [63, 64]. ARCH is associated with an ~10-fold increased risk of developing AML or other hematopoietic malignancies [59, 60]. Patients who have ARCH and undergo treatment with cytotoxic drugs for solid malignancies are more susceptible to acquiring mutations in DNA damage pathways, such as *Tumor suppressor protein 53 (TP53)* or *P53-induced protein phosphatase 1 (PPM1D)*, and develop therapy related-malignancies [65-67]. However, most healthy individuals with ARCH will not develop AML. In fact, recent reports have shown

that ARCH in itself is unlikely to drive AML and that additional environmental factors, such as chronic inflammation, contribute to ARCH-related malignancies in murine models [68].

1.1.8 Myeloproliferative neoplasm

Myeloproliferative neoplasms (MPN) are a group of clonal hematopoietic disorders characterized by the overproduction of myeloid cells. The most common sub-types of MPN are chronic myeloid leukemia (CML), polycythemia vera (PV), essential thrombocythemia (ET), and primary myelofibrosis (PMF) [69]. CML is distinct from other MPNs, as it stems from a balanced genetic translocation $t(9;22)(q24;q11.2)$ involving a fusion of the *Abelson murine leukemia gene* (*ABL*) from chromosome 9q34 with a *breakpoint cluster region gene* (*BCR*) on chromosome 22q11.2 [70-72]. This chromosomal translocation is also known as the Philadelphia Chromosome (Ph^+) [73], which leads to the expression of the fusion onco-protein BCR-ABL. BCR-ABL is a constitutively active tyrosine kinase which promotes the survival of CML cells through several signaling pathways. CML is characterized by the overproduction of myeloid cells in the bone marrow, which often leads to anemia and splenomegaly [74]. The classical BCR-ABL-negative MPN subtypes include PV, ET, and primary myelofibrosis. The diagnosis differs based on which lineages are being affected. PV is characterized by excessive red blood cell production, ET is characterized by a predominance of excessive platelet production, and PMF is characterized by excessive bone marrow scarring and fibrosis [75]. MPN often progresses to acute myeloid leukemia (AML) through the acquisition of additional genetic alterations (reviewed in 1.2).

1.1.9 Myelodysplastic syndrome

Myelodysplastic syndrome (MDS) is a clonal hematopoietic disorder characterized by abnormal blood cell development and impaired differentiation of myeloid cells [69]. MDS can often manifest in multi-lineage cytopenia. MDS may progress slowly over the years with relatively stable immature blood cell counts. However, approximately 10-30% of MDS patients are at high risk of developing AML [76, 77]. Many MDS patients have mutations in genes involved in DNA methylation and chromatin modification, such as *DNMT3A*, *TET2*, and *IDH1/2*, along with *ASXL*, *TP53*, and mutations in components of the spliceosome [69].

1.2 Acute myeloid leukemia

1.2.1 Introduction to Acute myeloid leukemia

AML is a rapidly progressing hematopoietic malignancy, which is characterized by the accumulation of clonal myeloid progenitors within the BM. These malignant progenitors, also known as blasts, are impaired in their ability to differentiate into functional cells, which results in a multi-lineage cytopenia. AML has an extensive expansion potential, which leads to the failure of hematopoiesis in the bone marrow and infiltration of AML blasts to secondary hematopoietic organs and peripheral blood [78]. AML often occurs *de novo* without evolving from previous blood disorders, but it can also arise from MDS, MPN, or therapy-related genetic damage [79].

1.2.2 Epidemiology

AML accounts for only 1% of all new cancers diagnosed in the US. The median age of the disease is 68 years, and it increases with age. Only approximately 5% of cases are diagnosed among people younger than 20 years. The estimate of new cases of AML in 2022 in the US was

20,050, and the incidence of AML is 4.1 per 100,000 individuals per year. The estimated number of AML-related deaths in 2022 was 11,540 and represent 1.9% of all cancer-related deaths. AML is more common among men compared to women (5.1 vs 3.4 cases per 100,000). There are several factors associated with an increased risk of developing AML, including age, smoking, genetic disorders, high dose of irradiation or chemotherapy, occupational exposure to chemicals, and antecedent myeloproliferative disorders [80].

1.2.3 The genetic heterogeneity of AML

The mutations that drive AML change considerably with age. Whereas adult AML is thought to evolve through the stepwise acquisition of genetic changes driving tumor progression, pediatric leukemia shows a lower mutational burden. 70% of pediatric leukemias are driven by balanced translocations, which lead to the expression of fusion proteins and enhanced self-renewal signaling [81]. Adult AML is often driven by insertion-deletion (INDEL) or single nucleotide variant (SNV) mutations that occur over time. The Cancer Genome Atlas Research Network (TCGA) identified patterns of frequently mutated genes and classified them into nine functional groups: activated signaling, DNA methylation, chromatin modification, nucleophosmin (NPM1), myeloid transcription factors, transcription factor fusion, tumor suppressor, spliceosome complex and cohesion complex (**Table1.1**) [52]. Subsequent patient cohort studies in AML confirmed that 96% had genomic lesions that were identified through the TCGA study [82]. Many patients with AML harbor a combination of mutations from different functional groups, and these co-occurrences are thought to collaborate to promote AML development. Several murine models of AML have recapitulated human leukemogenesis and provided mechanistic insights into how mutations cooperate. For instance, loss of *Dnmt3a*, or cytosolic expression of the nucleophosmin

protein (Npm1c⁺) in murine HSCs, increase self-renewal potential through the overexpression of *Homeobox genes (HOX)* [83, 84]. Crossing these murine models with mice expressing gain-of-function mutations in FLT3 accelerates the progression of AML significantly, mirroring observations from AML patient cohorts [85]. Furthermore, with the help of NGS, mutations could be categorized in early events, also referred to as “founder mutations” (*DNMT3A, TET2, IDH1/2, etc.*), and in late drivers also referred to “cooperating mutations” (*NPM1, FLT3-ITD, NRAS, etc.*) leading to better understanding of the evolution of AML and its clonal architecture (**Figure 1.3**) [57].

Interestingly, sequencing of VAF in healthy individuals demonstrated a prevalence of those “founder mutations” in their HSCs, and it was observed that the occurrence of these mutations progressively increases with age. Specifically, approximately 5% to 10% of individuals over 70 years old and approximately 20% of individuals over 90 years old exhibit ARCH with AML-related mutations [58, 59, 86]. Those findings were crucial, as they demonstrate that collaborating secondary mutations are required for AML development.

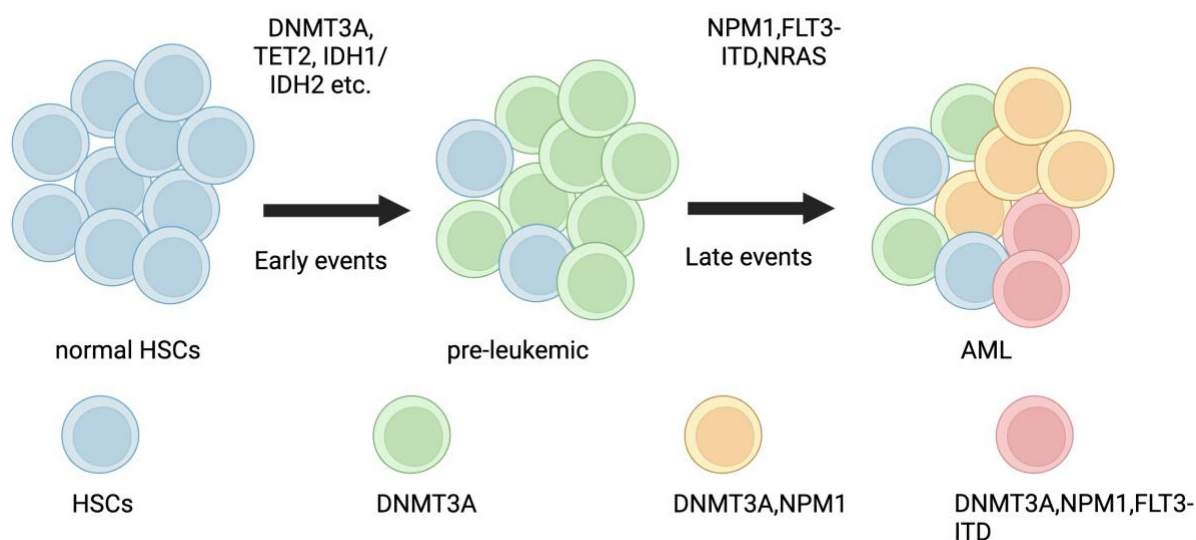


Figure 1. 3 AML development and clonal architecture, adapted from [87]. Created with BioRender.com.

Gene	Full name	Frequency in AML (%)	Gene function in AML	AML category
FLT3	FMS-like tyrosine kinase 3	26.60%	FLT3 is a cytokine receptor regulating cell growth and proliferation of HSCs.	Activated signaling
DNMT3A	DNA (cytosine-5)-methyltransferase 3A	23.90%	DNMT3A regulates HSC differentiation through silencing genes in HSC self-renewal.	DNA methylation
NPM1	Nucleophosmin 1	22.10%	NPM1 is a multifunctional shuttling protein, maintains HSC quiescence and self-renewal by regulating <i>HOX</i> genes.	NPM1
NRAS/KRAS	RAS viral oncogene homolog	15.10%	Proliferation and cell growth signaling.	Activated signaling
RUNX1	Runx family transcription factor 1	10.60%	TF involved in embryonic development of HSCs, RUNX1 drives differentiation of HSCs to MPPs.	Myeloid TFs
IDH2	Isocitrate dehydrogenase 2	10.40%	IDH2 is paralog of IDH1 and is a TCA-cycle enzymes that generate α KG to support the function of TET2.	DNA methylation
TET2	Ten-eleven translocase 2	9.30%	TET2 is an epigenetic-modifier that catalyzes the oxidation of 5-	DNA methylation

			methylycytosine (5mC) to 5-hydroxymethylcytosine (dhmC).	
IDH1	Isocitrate dehydrogenase 1	9.20%	IDH1 is a TCA-cycle enzymes that generate α KG to support TET2 function.	DNA methylation
TP53	Tumor protein 53	8.20%	TP53 is an essential tumor suppressor which guards cellular stress through DNA damage response.	Tumor suppressor
WT1	Wilms tumor 1	7.20%	WT is a tumor suppressor which is involved in HSC quiescence.	Tumor suppressor
CEBPA	CCAAT enhancer binding protein alpha	6.10%	CEBPA is a transcription factor, critical for myeloid cell differentiation and HSC maintenance.	Myeloid TFs
SRSF2	serine and arginine rich splicing factor 1	6.00%	SRSF2 belongs to the 3'RNA splicing machinery, and splices target genes involved in HSC activation.	Spliceosome
ASXL1	Additional Sex Combs Like 1	5.20%	ASXL1 belongs to the PRC1 complex. ASXL1 contributes to myeloid differentiation of HSCs through epigenetic silencing of <i>HOXA</i> clusters.	Chromatin Modifiers
PTPN11	Protein tyrosine phosphatase non-receptor type 2	4.90%	PTPN11 encodes a cytoplasmic tyrosine phosphatase. Gain of function mutations have been found to induce oncogenic RAS-ERK signaling in AML.	Activated signaling
STAG2	Stromal Antigen 2	4.30%	Member of the Cohesin complex. Transcriptional regulation of self-renewal genes.	Cohesin
RARA	Retinoic acid receptor alpha	3.60%	RARA is most often altered in fusion with PML in acute promyelocytic leukemia (APL). PML/ATRA fusion protein represses myeloid differentiation.	TF fusions
PML	promyelocytic leukemia protein	3.60%	RARA is most often altered in fusion with PML in acute promyelocytic leukemia (APL). PML/ATRA fusion protein represses myeloid differentiation.	TF fusions
MLLT10	MLLT10 histone lysine methyltransferase DOT1L cofactor	3.00%	MLLT10 is involved in CALM-AF10 and MLL-AF10 fusion. Aberrant self-renewal potential by upregulation of <i>HOXA</i> clusters.	Chromatin Modifiers
MYH11	Myosin heavy chain 11	2.10%	CBFB-MYH11 blocks myeloid differentiation and is predispose for AML initiation.	TF fusions
CBFB	Core-binding factor subunit beta	2.10%	CBFB is part of the Core-binding transcription factor complex. CBFs regulate self-renewal and myeloid differentiation.	TF fusions
KMT2A	Lysine Methyltransferase 2A	2.00%	KMT2A translocation increases self-renewal via upregulation of <i>HOX</i> genes.	Chromatin Modifiers

RUNX1	Runx family transcription factor 1	2.00%	RUNX1-RUNX1T is one of the CBF leukemias and regulates myeloid differentiation.	TF fusions
-------	------------------------------------	-------	---	------------

Table 1. 1 Top mutated genes and chromosomal rearrangements, data generated using cBioPortal using Beat AML, TCGA and TARGET data set. AML categories based on [88].

1.2.4 DNA methylation

DNA methylation is an important epigenetic mechanism to alter gene expression through the addition of methyl groups (CH₃) to CpG islands. Mutations related to DNA methylation are predominantly found in ARCH, MPN, and in AML [62]. Commonly mutated genes from this category are *DNMT3A*, which is mutated in 25% of all AML cases, *TET2*, which is mutated in 10%, and *isocitrate dehydrogenase genes 1 and 2 (IDH1/2)*, which are mutated in approximately 20% [88]. Interestingly, *DNMT3A* and *TET2* are characteristic of adult AML, since sequencing in pediatric cohorts of AML found that these mutations are completely absent in younger patients with AML [81, 89]. *DNMT3A* and *TET2* have distinct functions and roles in regulating methylation patterns in AML. *IDH1* and *IDH2* enzymes convert isocitrate to alpha-ketoglutarate in the citric acid cycle. Mutant *IDH1/2* enzymes lead to reduced production of α -KG and an accumulation of the oncometabolite 2-hydroxyglutarate (2-HG), which causes inhibition of TET proteins, including *TET2* [90]. Mutations in *DNMT3A* cause overall hypomethylation, while mutations in *TET2* and *IDH1/2* cause hypermethylation [91]. Despite the opposite effects on global methylation, advanced sequencing methods such as bisulfite- or pyrosequencing were extremely effective in identifying changes in methylation at specific CpG sites and the identification of downstream target genes. *Dnmt3a*-ko transgenic mouse models have been created to decipher its role in hematopoiesis [84]. Global DNA methylation analysis in *Dnmt3a*-ko HSCs found hypomethylation of genes regulating self-renewal, which were found to be frequently overexpressed in AML [84, 92, 93]. *Tet2*-ko transgenic mice showed a similar phenotype, resulting

in an increase in self-renewal potential and a delayed HSC differentiation with skewed development towards myeloid differentiation [91, 94-97]. Contrary to *Dnmt3a*-ko HSCs, which exhibit nearly limitless self-renewal *in vivo*, *Tet2*-ko HSCs surprisingly exhaust at a similar rate as wild-type HSCs in serial transplantation assays, despite an initial increase in self-renewal. Additionally, the loss of *Tet2* sensitizes HSCs to leukemic transformation in the presence of a common cooperating mutation (FLT3-ITD), different to the loss of *Dnmt3a*. *Tet2* mutations primarily result in a more pronounced skewing towards the myeloid lineage in committed HSCs rather than long-term HSCs [91]. This observation aligns with another study involving individuals with ARCH, which demonstrated that *DNMT3A* and *TET2* mutations have varying effects on the regulation of HSC differentiation [98].

1.2.5 Chromatin modifiers

Chromatin modifying proteins regulate the structure and function of chromatin, resulting in changes in gene expression. There are several modes of chromatin dysregulation in AML. For instance, translocations or mutations of the *mixed-lineage leukemia (MLL)* gene lead to aberrant H3K79 lysine methylation, resulting in transcriptional activation of target genes. MLL translocations may manifest in either acute lymphoid leukemia (ALL) or AML. Myeloid MLL translocations are found in approximately 5%-10% of AML and are most frequent in infant AML (38%) [81]. Partial tandem duplication of MLL (MLL-PTD) is found in 5%-7% of AML [99, 100]. MLL is also known as the *lysine methyltransferase 2A (KMT2A)* gene, which is a member of the SET domain-containing lysine methyltransferases.[101]. To date, there are more than 100 different fusion partners identified [102]. MLL fusion proteins lack the wild-type SET domain, and in some of the most common fusions, the SET domain is mainly replaced by members of the super

elongation complex (SEC), such as ALF transcription elongation factor 4 (AF4), MLLT3 super elongation complex subunit (AF9), MLLT1 super elongation complex subunit (ENL), and MLLT10 histone lysine methyltransferase DOT1L cofactor (AF10). MLL-transformed AML displays aberrant H3K79 methylation, leading to overexpression of stemness genes such as *HOX* clusters and *MEIS1* [103]. Until now, it is not fully understood what causes exactly the increased prevalence of MLL- rearrangements in pediatric AML in comparison to adult AML. Epidemiologic- and case-control studies of infant leukemia have found that exposure to insecticides and bioflavonoids, which can interfere with cell division, are potential risk factors [104, 105]. Genetic studies in monozygotic infant twins found occurrences of both twins developing leukemia within one year, suggesting that MLL rearrangements may occur prenatally [106]. It is not completely understood from which subtype of HSCs (fetal liver vs bone marrow HSC) pediatric leukemia develops.

Other recurrent mutations leading to chromatin modifications involve genes of the *polycomb repressor complex 2 (PRC2)*. *Enhancer of zeste 2 polycomb repressive complex 2 subunit (EZH2)* is an H3K27 methyltransferase that is part of the PRC2 complex, catalyzing transcriptional repression. Other mutated members of the PRC2 complex in AML involve *additional sex combs like transcriptional regulator 1 (ASXL1)*, *Jumonji AT-rich interactive domain 2 (JARID2)*, and *SUZ12 polycomb repressive complex 2 subunit (SUZ12)*, resulting in loss of function of the complex [107]. ASXL1 was found as one of the most commonly mutated genes in ARCH, MDS and other hematological malignancies [58, 61, 108]. Loss of function mutation of *Asxl1* in murine HSCs results in disordered *Hox* gene expression and gain in self-renewal [109].

1.2.6 NPM1 mutations

Nucleophosmin1 (NPM1) mutations are highly prevalent in AML, with a frequency of 30%. *NPM1* mutations affect mainly exon 12, causing changes in the nuclear export signal (NES) that lead to its aberrant cytoplasmic localization (NPM1c⁺) [110]. This type of mutation is linked to a specific subtype of AML, commonly referred to as NPM1-mutated AML or NPM1c AML. *NPM1* mutations are more common in adult AML and they are often found in co-occurrence with *DNMT3A* or *FLT3* mutations [111]. The *NPM1* gene encodes for a small ubiquitous multifunctional shuttling protein with predominant nucleolar localization. *NPM1* is a chaperone protein that regulates several biological functions such as cell cycle [112, 113], ribosomal biogenesis [114], heterochromatin formation, DNA damage response, rRNA 2'-O-methylation (2'-O-Me) [115], and phase separation in the nucleolus [116-118]. How exactly NPM1c⁺ mediates leukemogenesis is not fully understood. Co-localization experiments in NPM1c⁺ fibroblasts *in vitro* have found that NPM1c⁺ induces mis-localization of several proteins. Further mass-spectrometry analysis of endogenously tagged wild-type and NPM1-mutated AML cells found mis-localization of the myeloid transcription factor PU.1 [119]. Another interesting evidence of NPM1c⁺ mediated leukemogenesis was discovered through transcriptomic analysis in NPM1c⁺ and NPM1-wt AML cohorts. Microarray analysis conducted in human NPM1c⁺ mutant AML patients revealed that NPM1c⁺ AML led to the upregulation of numerous members of *HOX* gene family. Normally, *HOX* genes exhibit high expression levels in HSCs and their expression diminishes as cells undergo differentiation [120]. Interestingly, subsequent experiments employing *Npm1c*⁺ mutant mice demonstrated that correcting the nuclear localization of Npm1c⁺ promotes the differentiation of AML cells [121]. However, the specific mechanism through which NPM1c⁺ regulates *HOX* gene expression remains unclear. One proposed hypothesis suggests that

NPM1c⁺ interacts with nuclear factors necessary for the differentiation and downregulation of *HOX* genes, such as the myeloid transcription factor PU.1 [119, 122]. Additional supporting evidence from CRISPR dropout screenings confirmed the essential role of *HOX* genes in NPM1c⁺ AML cell lines [123-125]. Mouse models carrying the *Npm1c*⁺ mutation provided further evidence that *Npm1c*⁺ alone is not sufficient to initiate the development of leukemia [126]. The co-occurrence with *FLT3* and *DNMT3A* in patient cohorts implies a molecular synergy promoting AML development. Those mechanisms have been replicated in *Npm1/Flt3-ITD* combined mutant mice characterized by chemoresistance and a fast-growing phenotype [83, 85, 127].

1.2.7 Activated signaling

Aberrant signal transduction enhances the survival and proliferation of pre-leukemic HSCs, thereby promoting the onset of AML. Sequencing of AML patients revealed gain-of-function mutations in a variety of different signaling genes, such as *the Fms-like kinase 3 (FLT3)*, the *tyrosine kinase kit (KIT)*, members of the *proto-oncogene GTPase rat sarcoma virus (RAS)* family and the *protein tyrosine phosphatase non-receptor 11 (PTPN11)* gene. Collectively, these mutations are found in 59% of adult AML patients [88]. Alterations in *FLT3*, *RAS* family genes, and *KIT* are overall more common in children [81]. Activation of *FLT3* and *KIT* result in constant activation of the *RAS*-mediated *RAF/MEK/ERK* and *PI3K/AKT* signaling cascade. The *FLT3*-internal tandem duplication (*FLT3-ITD*) is prevalent in 30% of adult AML patients and usually co-occurs with mutations in *DNMT3A* and *NPM1* as described before. *FLT3-ITD* mutations often lead to the disruption of the functional juxta membrane domain of the tyrosine kinase *FLT3* resulting in a disrupted autoinhibition [128]. AML cohort studies have demonstrated that *FLT3*-

ITD is usually found as a later event during leukemogenesis. Transgenic *Flt3-ITD* mutant mouse models confirmed that *Flt3-ITD* alone does not fully transform HSCs into leukemia [129].

1.2.8 Tumor suppressor

Tumor suppressors play a critical role in preventing the development and progression of malignant cells. *TP53* mutations are found in ARCH, MPN and in approximately 5%-10% of adult AML patients. In therapy-related AML (t-AML), the prevalence of *TP53* mutations is higher, with approximately 30%-50% [130]. Most of the *TP53* mutations found in AML are missense mutations, usually arising within the DNA binding domain, and in some cases, deletion of chromosome 17 (17p). In both cases, *TP53* perturbations are associated with poor prognosis [131, 132]. *Wilms tumor gene 1 (WT1)* is another tumor suppressor, which is mutated in ~15% of AML cases. *WT1* was originally discovered as a potential biomarker in AML, as it is highly expressed in CD34⁺ AML cells but not on HSCs. *WT1* is structurally a zinc-finger protein and the mechanism of *WT1* mutations in leukemogenesis is not yet fully understood. Most of the *WT1* mutations are found to be LOF-mutation, and experimentally, it has been shown that mutant *WT1* fails to properly direct *TET2* to its target sites [133]. Recently, it has been found that *WT1* mutations are an independent marker of adverse clinical outcomes in intermediate-risk AML [134].

1.2.9 Transcription factor (TF) gene fusions

Overall, 20% of AML patients have TF gene fusions. Some of the most common transcription factor gene fusion include t(8;21)(q22;q22); *RUNX family transcription factor/RUNX1 partner transcriptional co-repressor 1 (RUNX1/RUNX1T1)*, and inv(16;16)/t(t16:16); *core-binding factor subunit beta/myosin heavy chain (CBFB/MYH11)* gene arrangements, which

are both known as core-binding factor complex AML (CBF-AML). The CBF-complex is a heterodimeric transcriptional complex involving the DNA-binding α subunit (RUNX1, RUNX2, or RUNX3) and the non-DNA-binding subunit β (CBF β) [135-138]. Normally, CBF β dimerizes with RUNX1 to increase its binding specificity for DNA. RUNX1/RUNX1T1 fusion protein dimerizes with CBF β and represses other transcription factors required for myeloid differentiation, such as CCAAT/enhancer-binding protein alpha (CEBPA) [139]. In the case of CBF β /MYH11, RUNX1 has a higher affinity to the fusion protein CBF β /MYH11 than CBF β protein, resulting in transcriptional deregulation and block in myeloid differentiation in HSCs [140]. Promyelocytic leukemia (APL) is a subtype of AML, which is characterized by a reciprocal translocation involving the promyelocytic leukemia gene PML on chromosome 15 and the retinoic acid receptor α (RAR α) on chromosome 17, thereby generating the PML-RAR α fusion oncoprotein [141-143]. PML-RAR α fusion leads to two major effects: the recruitment of transcriptional repressors (such as the histone deacetylases) to RAR α target genes, which results into a block in maturation at the promyelocytic stage of myeloid progenitors, and enhanced self-renewal activity [143-146].

The oncogenic PML-RAR α fusion can be targeted by all-trans retinoic acid (ATRA) and arsenic trioxide (ATO) via two mechanisms. ATRA induces a conformational change, resulting in the dissociation and degradation of the co-repressor complexes at the RAR α target genes [147-149]. ATO binds directly to specific cysteine residues on zinc fingers on the PML protein leading to PML-RARA sumoylation and proteasomal degradation [150]. Therefore, AML with RAR α fusion is treated differently than other AML subtypes (e.g., ATRA/ATO instead of chemotherapy), and carries a significantly higher probability of cure.

1.2.10 Myeloid transcription factor

RUNX1 and *CEBPA* mutations occur in 15%-20% of AML patients, arising sporadically in most cases, but a few patients (1.5%) harbor inherited *RUNX1* and *CEBPA* mutations [151]. *RUNX1* and *CEBPA* are key transcription factors regulating lymphoid and myeloid lineage commitment during hematopoiesis [152]. Studies in mice have shown that *Runx1* is upregulated during embryonic development but also during the lineage commitment of lymphoid cells and MEPs, whereas *Cebpa* expression is restricted to myelomonocytic cells during granulocyte differentiation [153]. *RUNX1* mutations are mechanistically distinct from *RUNX1* translocation and occur as dominant negative mutations perturbing or truncating the DNA-binding domain of *RUNX1* [154]. Comparative analysis of mutant- and rearranged *RUNX1* in cord blood and in induced pluripotent stem cells (iPSCs) has shown that mutant *RUNX1* leads to downregulation of *CEBPA*, resulting in a block of differentiation [154].

1.2.11 Spliceosome

Mutations in genes encoding proteins of the spliceosome complex (*SRSF2*, *U2AF1*, *SF3B1*, *ZRSR2*), show the highest frequency in MDS (50%) and AML with prior MDS or MPN (secondary AML) and t-AML [155-158]. *Serine and arginine rich splicing factor 2 (SRSF2)* is the most common mutated spliceosome gene with occurrence in 6% of AML cases [152, 156]. *SRSF2* contains a RNA binding domain that recognizes exonic splicing enhancers and a serine/arginine rich domain that recruits the *U2 small nuclear ribonucleoprotein auxiliary factor (U2AF)* complex and the *U1 spliceosomal RNA (snRNA)* to the 3' and 5' splice sites to initiate RNA splicing [159, 160]. Several groups have identified that alternative splicing provides an additional layer of gene dysregulation of AML-associated genes such as *EZH2* [161] [156]. Mutations in *IDH2* often co-

occur with *SRSF2*, and it has been shown that epigenetic changes caused by *IDH2* result in an increased stalling of RNA polymerase II, and increased mis-splicing in double mutant murine HSCs [162].

1.2.12 Cohesin complex

Mutations of the *cohesin subunit SA-2 (STAG2)* are found in 4% of AML and in 10%-15% of MDS. The cohesin complex is a multimeric protein complex, comprising STAG2, double-strand-break repair protein *rad21 homologue (RAD21)*, and *structural maintenance of chromosomes (SMC) proteins 1 A (SMC1A)- and 3 (SMC3) protein*, which encircles sister chromatids during replication [163]. Loss of *STAG2, RAD21, SMC1A and SMC3* was found to promote self-renewal and impair differentiation in human and murine HSCs through modulating the accessibility of chromatin, resulting in increased expression and binding of transcription factors such as *RUNX1, GATA binding protein 2 (GATA2)* and *ETS transcription factor (ERG)* [164, 165].

1.2.13 AML biology

AML is characterized by a set of common functional features, independent of the initiating genetic events. AML cells reside in their BM niche, which provides support for their cell growth via cytokines and nutrients and protection from chemotherapy. AML cells communicate directly via cell surface receptors and indirectly via cytokines with stroma cells, adipocytes, and differentiated hematopoietic cells present in the niche [166]. Like HSCs, AML cells exhibit a hierarchical organization, with leukemic stem cells (LSCs) positioned at the top, sustaining the disease. Notably, experimental evidence has shown that LSCs, in comparison to blasts, display distinct metabolic characteristics *in vivo*. Understanding how AML cells interact with their

surrounding environment and how AML cells exploit those factors is crucial for the development of novel therapeutics [33, 167].

1.2.14 The bone marrow niche in AML

AML cells primarily reside in the BM niche. Mirroring normal hematopoiesis, AML cells are organized into a functional hierarchy, with rare self-renewing LSCs that generate a more differentiated blast progeny. Several reports have demonstrated that LSCs are very rare and quiescent [78, 168]. It has been demonstrated that the BM niche provides a supportive environment for AML survival, cell growth and therapeutic resistance through direct cell interactions, cytokine signaling and nutritional support [169, 170]. Transplantation studies of human AML found that AML cells anchor in osteoblast-rich endosteal areas, where they suppress murine hematopoiesis and exhibit resistance to Cytarabine (Ara-C) treatment [171]. Those observations were replicated *in vitro* by culturing AML with mesenchymal stem cells (MSCs) under hypoxic conditions [172].

On one side, many reports revealed that growing AML cells in the BM induce changes in niche cell populations, including the loss of endosteal vessels, loss of the sympathetic innervation, and expansion of the osteoprogenitor pool [167, 169, 173, 174]. One report found that AML cells in endosteal regions have an enriched pro-inflammatory gene signature and expressed higher level of *tumor necrosis factor (TNF)* and the cytokine *CXCL2*, resulting in progressive niche remodeling [173, 175]. Murine models of pre-malignant -and aged HSCs showed that pro-inflammatory cytokine signaling was sufficient to impair MSCs, osteoblasts, and damage sympathetic innervations [169, 176, 177]. Similar observations were found in MDS patients, where MSCs showed higher production of pro-inflammatory cytokines and an increase in apoptosis [178]. On the other side, it has been shown, using cre-mediated conditional deletion, that direct alteration in

the BMN can lead to malignant transformation. Conditional deletion of *Dicer1* or *Sbds* in MSCs leads to a MDS-like phenotype in mice and secondary AML development [169, 179, 180]. The constitutive activation of *β -catenin* in osteoblasts induced the development of AML as well [169, 181, 182]. Further evidence for the niche as a predisposing factor comes from clinical observations during allogeneic HSC transplantations, in which healthy donor HSCs may transform into malignant clones in the new recipient [169, 183].

1.2.15 Metabolic adaptation in AML

Metabolic rewiring, a hallmark of cancer, refers to alterations in the metabolic pathways and processes within cells, leading to changes in energy production, nutrient utilization, and other metabolic activities [184]. AML cells acquire several metabolic adaptations, including an increase in oxidative phosphorylation, glycolysis, and the pentose-phosphate pathway [185-187]. Furthermore, several studies have demonstrated that normal HSCs, LSCs and AML blasts have distinct metabolic profiles [188]. For instance, experimental models involving depletion of key catabolic enzymes for glycolysis, including *lactate dehydrogenase A (LDHA)* and *pyruvate kinase muscle isoform M2 (PKM2)*, reduced leukemic development significantly, while depletion in HSCs affected function only under stress [189, 190]. Molecular imaging of glycolytic activity using a metabolic sensor monitoring NADH/NAD⁺ ratio (SoNar) has revealed that AML cells with high glycolytic activity home to hypoxic regions of the endosteal niche. Furthermore, AML cells overexpress the enzyme pyruvate dehydrogenase kinase 2 (PDK2), which restricts pyruvate entry into the tricarboxylic acid cycle (TCA), thereby shifting the metabolism to lactate and glycolysis [190, 191]. In addition to their glycolytic metabolic profile, AML cells demonstrate an increased metabolic activity and increased dependence on OXPHOS [170, 192, 193]. In comparison to HSCs

and AML blasts, quiescent LSCs are dependent on OXPHOS, and less on glycolysis, providing a therapeutic opportunity for targeting OXPHOS in LSCs [186, 194]. Several studies have documented other LSC-specific metabolic dependencies, including low levels of ROS, increased levels of glutathione, activated AMP-activated protein signaling, sensitivity to disruption of electron transport chain components, and increased activation of branched-chain amino acid metabolism [186, 194-197].

In addition to intrinsic metabolic adaptations, it has been shown that neighboring cells supply AML cells with metabolites through various mechanisms. Several studies have shown that the TCA cycle of AML cells is fueled predominantly by exogenous fatty acids [198-200]. More importantly, it has been shown that fatty acid oxidation is a feature of AML that has relapsed after therapy. In keeping with this finding, it has been shown that AML cell lines overexpress the fatty acid transporter *glycoprotein IV*, also known as *CD36*, to fuel their increased demand of fatty acids [201]. Lipids are mainly supplied by adipocytes and it has been demonstrated that AML cells stimulate adipocyte remodeling through *growth/differentiation factor-15 (GDF-15)* secretion [202-204]. Other groups have shown that AML cells fuel their nucleotide synthesis through glutamine and aspartate derived from MSCs, particularly within the framework of metabolic adaptation associated with chemotherapy [205].

1.2.16 Immune dysregulation in AML

The BM niche hosts a variety of immune cells that interact with AML cells at multiple levels [206]. T cells, NK cells, B cells, and plasma cells are highly relevant to AML biology. Several groups have described that lymphoid cells are overall reduced in the BM of AML patients in comparison to healthy controls and that the ratio between lymphoid populations is altered. AML

cells establish an immunosuppressive milieu characterized by elevated numbers of Foxp3⁺ regulatory T (Treg) cells, accompanied by diminished counts of fully functional T and natural killer (NK) cells. Furthermore, it has been demonstrated that AML blasts themselves exhibit reduced expression of major histocompatibility complex (MHC) molecules and an enhanced expression of inhibitory molecules, such as T-cell immunoglobulin and mucin-domain containing-3 (Tim-3), Galectin 1 (Gal-1), and Programmed death-ligand (PD-L1). This reduced expression extends to natural killer group 2D ligand (NKG2DL) and the activating/adhesion molecule DNAX-activating molecule (DNAM-1), ultimately resulting in impaired activation of natural killer (NK) cells [207-209]. AML cells release in the BM environment, ROS, indoleamine 2,3-dioxygenase-1 (IDO), arginase (ARG), and extracellular vesicles (EVs), which can inhibit the cytotoxic function of T and NK cells [208, 209]. Furthermore, studies in patients with AML have demonstrated that AML cells express IDO, which induces T cell tolerance by directly converting CD4⁺CD25⁻ T cells into Foxp3⁺Treg cells. Several groups have found that BM cytotoxic CD8⁺ T cells express transcriptional and phenotypic features of exhaustion, and display cellular features of senescence compared to peripheral blood CD8⁺ T cells [209-211]. NK cells constitute 2%-4% of the BM, and they possess cytotoxic abilities against leukemic cells. Conversely, AML cells develop several adaptations to escape NK cells, by either directly modulating the expression of cell surface receptors, for example, NKG2DL, or by secreting soluble immunosuppressive factors, such as TGF- β and IL-2R [209, 212]. NK cells of AML patients downregulate the cytotoxic receptor NKp46/CD335 and upregulate the inhibitory receptor NKG2A. Furthermore, phenotypic and functional defects can be induced in NK cells of healthy controls *in vitro* under transwell conditions with AML blasts through a primarily IL-10-dependent inhibitory effect [213]. An intriguing study using LSC xenografts in mice revealed that the downregulation of NKG2DL

was crucial for the successful engraftment of LSCs, highlighting its role in immune recognition in AML [214]. Furthermore, in the context of allogeneic stem cell transplantation, it has been shown that AML relapse after transplantation is linked to the downregulation of major MHC class II genes, while MHC class I genes are unaffected, demonstrating another immune escape strategy of AML. In a recent study, the the downregulation of MHC class II genes could be reversed by the administration of Interferon- γ , demonstrating potential therapeutic interventions to prevent relapse [215].

1.3 AML subtypes and diagnosis

AML is a genetically heterogeneous disease with variability in genotype between patients, but also between blasts and clones during disease progression. The variability between patients has contributed to the detailed classification of patients into subtypes based on genetic abnormalities for diagnosis and prognosis, inherited predisposition, and expression of molecular biomarkers to guide clinical management and treatment [69, 79]. Diagnosis of AML includes cell morphology and immunophenotype to distinguish AML cells from normal HSCs rapidly, as well as cytogenetic and molecular profiling to classify the AML subtype. Multiparameter flow cytometry and immunohistochemistry of the BM, or peripheral blood, allows the detection of AML blasts and estimates the percentage of blasts present. The World Health Organization (WHO) classifies AML based on morphologic, immunophenotypic, molecular, and cytogenetic data [216]. Additionally, the WHO defines AML with blast counts $>20\%$ to delineate it from MDS. Some AML types can be diagnosed with lower blast percentages, and those include for example AML subtypes with characteristic translocations such as *KMT2A*, *MECOM*, and *NUP98*, as they progress quicker and show clinical features of AML with higher blast counts [79] (**Table 1.2**). To

diagnose MDS-related AML, a blast count of >20% is required with an additional confirmation of a MDS related somatic mutation.

Using the 5th WHO edition, AML can be classified using two categories: AML, defined by genetic abnormalities, and AML, defined by differentiation. AML is classified based on differentiation only if genetic abnormalities are not present and criteria for other AML subtypes or myeloid neoplasm are not met. Differentiation-defined criteria are based on the previous French-American-British (FAB) classification system. The FAB classification classifies AML cells according to their morphological features, such as cell size, nuclear shape, nuclear-to-cytoplasmic ratio, and the presence of granules, into groups M0 through M7. Further cell surface markers are utilized for flow cytometry, such as CD33, CD13, CD117, CD41, CD61 and myeloperoxidase (MPO), which can be used to confirm AML maturation (**Table 1.3**). Genetic characterization of AML patients is used to stratify AML patients into three risk categories: favorable-, intermediate- or adverse risk categories, developed by recommendations of the European LeukemiaNET (ELN) [79]. The risk categories have been developed based on data from intensively treated patients and may help guide treatment decisions and predict prognosis. For instance, patients with mutated *NPM1* but without *FLT3-ITD* are classified as favorable whereas patients with mutated *FLT3-ITD* are grouped into intermediate risk, regardless of *NPM1* status. Patients with mutant *TP53* or *MLL*-rearrangements are categorized as adverse risk. While there have been many functional studies on mutations in other genes, such as *IDH1/IDH2* or *DNMT3A*, the current evidence is insufficient to assign them to a distinct ELN prognostic group.

More recently, multiparameter flow cytometry- or qPCR- based monitoring of residual disease (MRD), has been established for prognostic quantification of the remission status, which

is not yet included in the ELN guidelines. However, recent studies demonstrated that MRD status can be important to reclassify some patients with intermediate- AML risk categories [217-219].

Acute myeloid leukaemia with defining genetic abnormalities	Additional diagnostic criteria
Acute promyelocytic leukaemia with PML::RARA fusion	
Acute myeloid leukaemia with RUNX1::RUNX1T1 fusion	
Acute myeloid leukaemia with CBFβ::MYH11 fusion	
Acute myeloid leukaemia with DEK::NUP214 fusion	• ≥20% blasts
Acute myeloid leukaemia with RBM15::MRTFA fusion	• ≥20% blasts
Acute myeloid leukaemia with BCR::ABL1 fusion	• ≥20% blasts
Acute myeloid leukaemia with KMT2A rearrangement	
Acute myeloid leukaemia with MECOM rearrangement	
Acute myeloid leukaemia with NUP98 rearrangement	
Acute myeloid leukaemia with NPM1 mutation	
Acute myeloid leukaemia with CEBPA mutation	• ≥20% blasts
Acute myeloid leukaemia, myelodysplasia-related	• ≥20% blasts
	• specific cytogenetic and molecular abnormalities associated with MDS
Acute myeloid leukaemia with other defined genetic alterations	rare genetic fusions

Table 1. 2 5th edition WHO diagnosis criteria for AML types defined by genetic abnormalities, adapted from [216]

Type	Diagnostic criteria*
AML with minimal differentiation	• Blasts are negative (<3%) for MPO and SBB by cytochemistry
	• Expression of two or more myeloid-associated antigens, such as CD13, CD33, and CD117
AML without maturation	• ≥3% blasts positive for MPO (by immunophenotyping or cytochemistry) or SBB and negative for NSE by cytochemistry
	• Maturing cells of the granulocytic lineage constitute <10% of the nucleated bone marrow cells
	• Expression of two or more myeloid-associated antigens, such as MPO, CD13, CD33, and CD117
AML with maturation	• ≥3% blasts positive for MPO (by immunophenotyping or cytochemistry) or SBB by cytochemistry
	• Maturing cells of the granulocytic lineage constitute ≥10% of the nucleated bone marrow cells
	• Monocyte lineage cells constitute < 20% of bone marrow cells
	• Expression of two or more myeloid-associated antigens, such as MPO, CD13, CD33, and CD117
Acute basophilic leukemia	• Blasts & immature/mature basophils with metachromasia on toluidine blue staining
	• Blasts are negative for cytochemical MPO, SBB, and NSE
	• No expression of strong CD117 equivalent (to exclude mast cell leukemia)
Acute myelomonocytic leukaemia	• ≥20% monocytes and their precursors
	• ≥20% maturing granulocytic cells
	• ≥3% of blasts positive for MPO (by immunophenotyping or cytochemistry)
Acute monocytic leukaemia	• ≥80% monocytes and/or their precursors (monoblasts and/or promonocytes)
	• <20% maturing granulocytic cells
	• Blasts and promonocytes expressing at least two monocytic markers including CD11c, CD14, CD36 and CD64, or NSE positivity on cytochemistry
Acute erythroid leukaemia	• ≥30% immature erythroid cells (proerythroblasts)
	• Bone marrow with erythroid predominance, usually ≥80% of cellularity
Acute megakaryoblastic leukaemia	• Blasts express at least one or more of the platelet glycoproteins: CD41 (glycoprotein IIb), CD61 (glycoprotein IIIa), or CD42b (glycoprotein Ib)

Table 1. 3 5th edition WHO diagnosis criteria for AML types defined by differentiation, adapted from [216]

1.4 Treatment

The objective of the treatment is either to cure AML or delay its progression. Curative treatment is done by first achieving complete remission (CR) through initial therapy. CR is

considered attained when BM blasts are below 5%, and there are no circulating blasts or extramedullary AML. When CR is achieved, induction therapy is followed by consolidation therapy, which is usually several cycles of intermediate dose Ara-C treatment or targeted therapies depending on the molecular features of the disease [79]. The type of cytotoxic therapy that patients receive (high-intensity or low-intensity) depends on their age, associated comorbidities, and overall health. Unfortunately, there are also unfit patients who will receive only palliative care [220]. Although genetic classification can be useful in making prognostic predictions, not all genetic alterations can be targeted with available inhibitors. Patients who are sufficiently fit to qualify for curative treatment will receive high-intensity cytotoxic treatment, which usually consists of a combination of anthracycline and cytarabine (Ara-C). Patients who do not qualify for high-intensity induction therapy may benefit from alternative treatment regimens containing a low-dose cytotoxic treatment combined with targeted therapies. These regimens often contain either Ara-C or hypomethylating agents (HMA) such as azacytidine and decitabine..

1.4.1 High-dose cytotoxic induction therapy

The combination of Ara-C and anthracycline is also known as “7+3”, which was established in 1973 [221]. In this regimen, patients receive seven days of Ara-C and three days of anthracycline (idarubicin or daunorubicin). This type of induction therapy is commonly given to fit adults with AML. Ara-C belongs to the class of nucleoside analogues and is metabolically processed to its active form and incorporated in DNA during cell cycle. Integration of Ara-C in nascent DNA strands leads to a block in S-Phase during the cell cycle and apoptosis. Anthracyclines, which belong to the class of DNA intercalators, form a complex with topoisomerase-II, an enzyme that re-ligates dsDNA breaks. Anthracycline-DNA-topoisomerase II

complexes result in DSB and cell death [222, 223]. The different types of anthracyclines are daunorubicin, doxorubicin, epirubicin, idarubicin, mitoxantrone, and valrubicin [224]. Good- or intermediate-risk patients receive in addition to induction therapy a low dose of gemtuzumab ozogamycin, a humanized anti-CD33 IgG4 antibody, which is chemically modified with the toxic conjugate calicheamicin. CD33 is a cell-surface protein commonly expressed at the surface of AML blasts. Patients with FLT3-ITD mutation receive, in addition to induction chemotherapy, the FLT3-inhibitor midostaurin, which has been shown in clinical trials to improve the 4-year overall survival (OS) from 44.3% to 51.4% in patients 18-59 years of age [225, 226].

CPX-351 is a novel dual-drug liposomal formulation that contains Ara-C and daunorubicin in a 5:1 fixed molecular ratio. It was developed with the primary aim to stabilize the maximal drug synergy during IV administration [227]. In a randomized clinical trial in newly diagnosed AML patients with an adverse subtype or secondary AML, aged 60 to 75 years, treatment with CPX-351 improved the clinical response rate and OS compared with induction therapy [228, 229].

1.4.2 Low-dose cytotoxic therapy

Hypomethylating agents, such as azacitidine and decitabine, are nucleoside analogues that are metabolized and integrated into DNA and RNA like Ara-C. However, at lower doses, azacitidine and decitabine impair DNA methylation by inhibiting DNA methyltransferases, leading to a global loss of DNA methylation. HMAs are frequently combined with the anti-apoptotic protein B-Cell lymphoma 2 (BCL-2) inhibitor venetoclax. In clinical trials, combining venetoclax with HMAs improved the CR from 28.3% to 66.4%, and improved the median OS from 9.6 months to 14.7 months [230]. Not yet evaluated in randomized trials, similar results are

expected with decitabine in combination with venetoclax [231]. However, for patients failing venetoclax-based therapy, the overall prognosis remains very poor [232]. For patients unable to receive HMA, low-dose Ara-C in combination with venetoclax represents an alternative approach [233]. For newly diagnosed AML patients with IDH1 mutations, the IDH1 inhibitor ivosidenib plus azacitidine improved the CR (52.8% vs 17.6%) and median OS (24 vs 7.9%) compared with azacitidine alone [234]. The hedgehog inhibitor Glasdegib, which was promising in early-phase clinical trials, did not increase the CR rate in combination with chemotherapy [235].

1.4.3 Adverse effects of cytotoxic therapy

While the 5-year OS is 40%-50% in younger AML patients (<50 years), unfortunately, the 5-year OS of elderly patients (>65 years) is less than 10% [80, 236]. As patients age, the survival rate declines rapidly, which can be partially explained by the more frequent presence of adverse genetic profiles coupled with impaired organ function and a greater prevalence of comorbidities. Patients who undergo induction therapy suffer from significant side effects of cytotoxic therapy. Severe short-term side effects include cytopenias, gastro-intestinal toxicity, and infections. Furthermore, some patients experience long-term side effects that include organ damage, infertility, and the increased risk of developing secondary malignancies [236]. Given these challenges, the primary focus of the second chapter of this thesis seeks for combinatorial AML treatment strategies that effectively strike a balance between reducing cytotoxicity and preserving the curative effect.

1.4.4 Relapse and mechanisms of resistance

In addition to the problem of severe cytotoxicity, two-thirds of patients relapse after the initial response to chemotherapy. Relapse mostly occurs within the first 18 months after treatment,

and the 5-year OS for relapsed patients drops significantly to only 10%-20% [237, 238]. Unfortunately, the precise mechanisms behind AML relapse and resistance to therapy are not completely understood. Genome sequencing of AML patients, before and after relapse, provided a better understanding of the clonal evolution in AML and unveiled that relapse occurrences in AML are underpinned by distinct mechanisms. For example, Ding *et al.* showed that relapse can be driven by a secondary AML sub-clone, derived from the founder population, which acquires additional mutations during relapse [239]. Another group studied the origin of therapy-related AML and showed that older individuals may harbor HSCs with TP53 mutations at very low frequency (0.003-0.7), which gain a selective advantage for expansion following cytotoxic chemotherapy. Moreover, these researchers generated *Trp53*-heterozygous ko murine HSCs and observed a significant proliferation of these cells upon exposure to chemotherapy [240]. Single-cell RNA sequencing has shed further light on the changes in populations of AML cells, before and after chemotherapy, and found persistent quiescent AML stem cell profiles persisting during induction therapy [241, 242].

1.4.5 Introduction to nucleoside analogues

Nucleosides are the building blocks for DNA and RNA. Nucleoside analogues are chemically modified compounds that have been synthesized to mimic nucleotides and exploit the same metabolic pathways required for DNA and RNA synthesis [243]. Historically, the isolation of arabinose-containing nucleotides from marine organisms provided the basis of nucleoside analogues in anticancer treatment. Ara-C was approved by the FDA in 1969 as the first nucleoside analogue in the treatment of AML [243]. Ara-C is structurally similar to cytidine, but lacks the 2'-OH group on its sugar moiety, which makes it an arabinose sugar component. Mechanistically, all

nucleoside analogs share a similar cytotoxic mechanism of stalling replication by inhibiting DNA polymerase and DNA chain elongation [244]. Since the development of Ara-C, several additional nucleoside analogues have been developed for cancer treatment. For instance, the pyrimidine analogue gemcitabine is structurally similar to Ara-C, is distinguished by a fluorine group substituted at position 2' on the furanose ring. In addition, gemcitabine inhibits ribonucleotide reductase (RNR), the enzyme catalyzing the reduction of ribonucleotides. Gemcitabine is used in several solid cancers, such as pancreatic cancers, and it has been tested in leukemias and lymphomas [245-247]. The purine analogue fludarabine (Fludara) is used for the treatment of AML in a combination regime with Ara-C, G-CSF and Gemtuzumab Ozogamicin (FLAG-GO) in adverse risk groups [248]. Azacitidine and Decitabine are two other structurally related nucleoside analogues used in the treatment of AML; however, mechanistically, they act as demethylating agents [249-252]. All nucleoside analogues act as pro-drugs and require phosphorylation to be integrated into the 3'-end of the DNA chain. Nucleoside analogues enter the cell through nucleoside transporters. In humans, there are two main protein families of nucleoside transporters: the concentrative (CNTs) - and equilibrative nucleoside transporter (ENT) families. CNTs are active transporters, which utilize the energy from the sodium ion gradient to transport nucleosides against their concentration gradient, whereas ENTs are passive transporters that facilitate the bidirectional movement of nucleosides across the cell membranes. Nucleoside analogues are predominantly uptaken by the cell through equilibrative nucleoside transporter 1 (ENT1) also known as *SLC29A1*, and equilibrative nucleoside transporter 2 (ENT2) [253]. Once inside the cell, nucleoside analogues undergo a rate-limiting phosphorylation step by the enzyme deoxycytidine kinase (DCK). Subsequently, nucleoside monophosphate kinases and nucleoside diphosphate kinases phosphorylate nucleotides to their triphosphate state, which then can be incorporated into

DNA, leading to block in DNA synthesis resulting in replication stress and ultimately apoptosis [243, 254] (Figure 1.4).

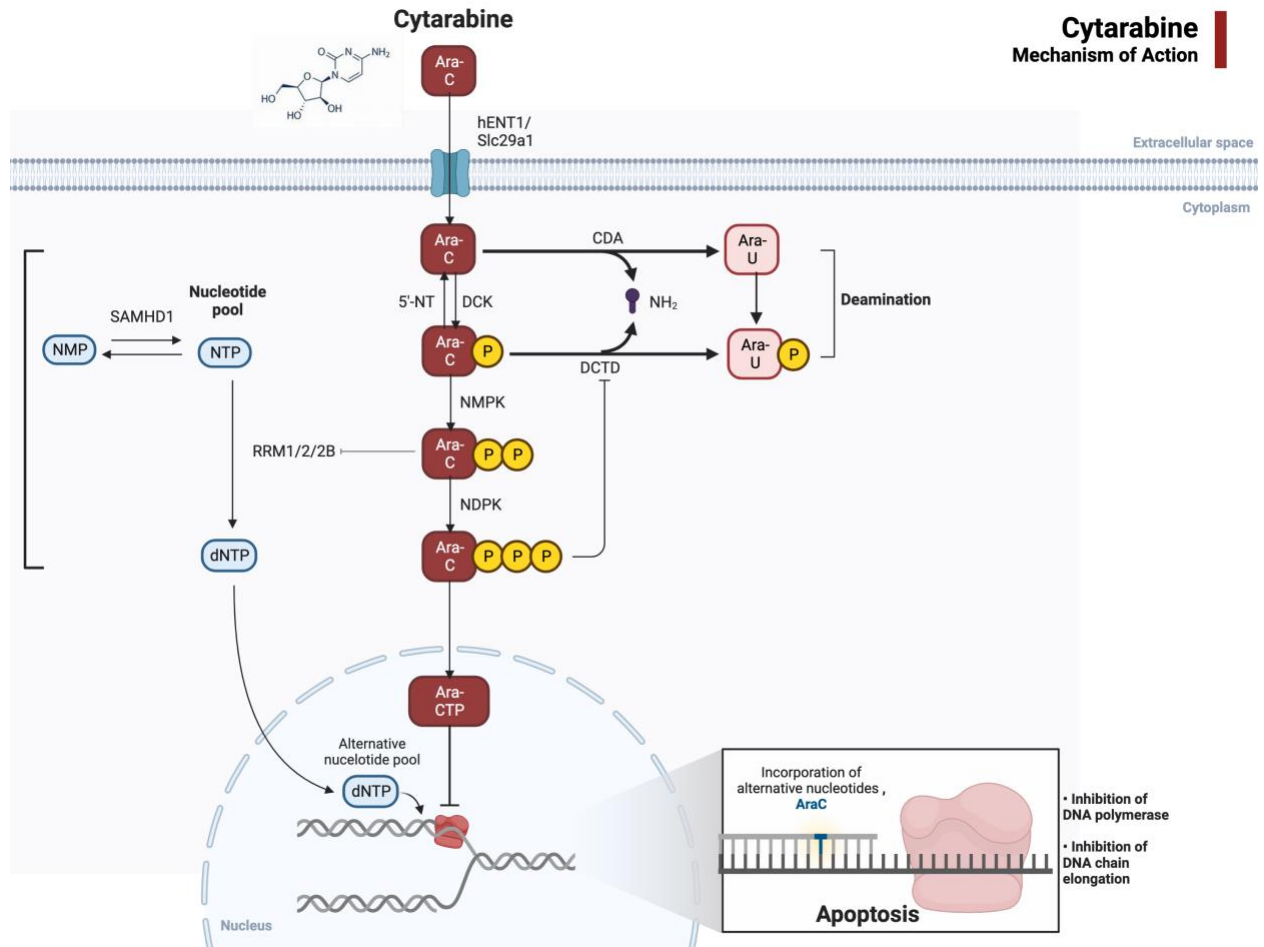


Figure 1. 4 Intracellular metabolism of Ara-C.

Ara-C is a prodrug and enters the cell through SLC29A1. Inside the cell, Ara-C is phosphorylated by DCK to Ara-CMP. This step is considered the rate limiting step in the activation of Ara-C. Ara-C is further phosphorylated to Ara-CTP, where it can be incorporated into the DNA, leading to inhibition of DNA polymerase and DNA chain elongation resulting into apoptosis. Adapted from “Gemcitabine”, by BioRender.com (2022). Retrieved from <https://app.biorender.com/biorender-templates>.

1.4.6 Intracellular nucleoside metabolism

Adequate nucleotide pools are required for numerous cellular processes such as DNA synthesis and DNA damage repair, and it has been shown experimentally that deficiency promotes genomic instability in the early stages of cancer development [255]. Nucleotide demand changes during cell proliferation and stages of cell cycle. The highest level of intracellular nucleotides is found during the transition of G1- to S-phase. Several enzymes are involved in the regulation of deoxyribonucleotide triphosphates (dNTP) pools by either increasing or reducing the pool size. Two distinct pathways contribute to the dNTP pool: 1) *de novo* dNTP synthesis in the cytoplasm and 2) *the salvage* pathway, which takes place in the cytoplasm and the mitochondria. For dNTP *de novo* synthesis, glucose, glutamine, and aspartate are the building blocks needed [256, 257]. The nucleotide salvage pathway utilizes free nucleotides, which are left from the degradation of cellular material. The rate-limiting step is the addition of the first phosphate by deoxynucleoside kinases. Thymidine kinase 1 (TK1) and DCK phosphorylate dNTPs in the cytosol and thymidine kinase 2 (TK2) and deoxyguanosine kinase (dGK), in mitochondria. DCK is relevant for the metabolism of pyrimidine and purine analogues and its activity is an important determinant of sensitivity to nucleoside analogue treatment [250, 258-260]. Experimentally, several studies have shown that genetic targeting or genetic silencing of DCK leads to Ara-C resistance. On the other side, overexpression of DCK in Ara-C resistant cell lines restored Ara-C sensitivity [261, 262]. The size of dNTP pools is further regulated through deamination, phosphorylation, and hydrolysis. The Sterile alpha motif and HD domain-containing protein 1 (SAMHD1) hydrolyses dNTPs into their constituent triphosphate and 2'-deoxynucleoside, acting as dNTP sensor for the maintenance of dNTP pools. Moreover, SAMHD1 was recently discovered to regulate the pool of Ara-CTP and the expression level of SAMHD1 in patients is correlated with improved OS and better Ara-C

response [263]. Genetic targeting of SAMHD1 led to improved Ara-C response in murine models of AML [263].

CRISPR-based genome-wide loss of function screening, combined with nucleoside analogue treatments such as Ara-C and 5-Aza-C, have identified that the main mechanism of Ara-C resistance is through loss of DCK and SLC29A1 (ENT1) [261, 262, 264, 265]. Ara-C and Ara-CMP can be inactivated by the cytidine deaminase (CDA) and the deoxycytidylate deaminase (DCTD), to Uracil Arabinoside (Ara-U) leading to an extremely short plasma half-life. CDA deregulation has been described in several reports as a risk factor for life-threatening toxicities with gemcitabine, capecitabine, and azacytidine [266, 267]. Furthermore, a small cohort study of AML patients demonstrated that patients with low expression of CDA had higher response rates to induction therapy, yet they were also at increased risk of developing lethal cytotoxicity after induction therapy [268].

1.5 Murine AML models

Extensive sequencing studies in AML cohorts have provided genomic landscapes of adult and pediatric AML, revealing many biological relationships. Beyond identifying genetic lesions, it is crucial to delineate molecular mechanisms on how these mutations cooperate and lead to AML onset. Murine models of AML represent an essential preclinical platform for answering crucial questions related to leukemogenesis, treatment, resistance, and novel drug target identification. Humans and mice share a genetic similarity of approximately 80%, and extensive studies in murine HSCs provided crucial knowledge of similarities and differences when interpreting mouse models of AML [269, 270]. In this thesis, I used MLL-AF9 and HoxA9/MEIS1-driven murine AML models. Both models are generated by retroviral transduction of murine GMPs isolated from BM

cells, followed by serial transplantation [192]. Both models replicate features of human AML, such as a defined AML hierarchy with the expression of different levels of differentiation- and stemness markers (e.g. Gr-1, Mac-1 and cKit), expansion and circulation of AML blasts in BM and peripheral blood, and partial response to Ara-C containing chemotherapy [271]. Previous studies have characterized retro-virally transduced mouse models of MLL-AF9 extensively. For instance, transformations of HSC and progenitor subtypes have demonstrated that AML can be transformed from different cells of origin. Retroviral transduction of MLL-AF9 and MLL-ENL fusion proteins revealed their transforming capacity through the upregulation of *Hox* genes [272]. *HoxA9* is a central regulator of HSCs, and overexpression studies have demonstrated that *HoxA9*, in combination with *Meis Homoeobox 1 (Meis1)*, lead to the rapid onset of AML through activation of signaling cascades [273-276]. Seminal studies using retroviral transduction of MLL-fusions in HSC and MPP sub-populations resulted in different latencies of AML. Transcriptomic- and epigenetic profiling in these AML cell models showed that distinct chromatin regions were altered, involving genes associated with self-renewal potential, highlighting the differences in cell of origin and potential pitfalls when comparing results [103] [277]. The overexpression of MLL-fusion constructs in isolated LSKs has been used extensively used as a preclinical platform and resulted in the discovery of *Disruptor of Telomeric silencing 1-like (DOT1L)*, *Bromodomain and Extra-Terminal domain family (BET)* and *Multiple Endocrine Neoplasia Type 1 (MENIN)* as therapeutic vulnerabilities in this genetic subtype [278-280].

As an alternative to the retroviral expression of MLL-fusion, MLL-driven models can be generated using genetically engineered mouse models (GEMMs). GEMMs are generated via homologous recombination and have been used to model fusion oncogenes, such as MLL-AF9 fusions, by creating inter-chromosomal rearrangement using Cre-loxP mediated recombination.

These models have been particularly useful in studying MLL-driven leukemogenesis in AML [281]. These models were taken a step further to model age-specific MLL-driven AML initiation by crossing *MLL-loxP* with *VAV-Cre* driver, a gene selectively expressed in HSCs and constitutively active from embryonic day 11 until adulthood [282, 283]. Using this approach, it was found that embryonic induction of MLL-driven AML had a significantly shorter latency compared to adult induction, providing an explanation for the increased prevalence of MLL translocations in infant AML. However, differences between experimental murine and human MLL-driven leukemia are also apparent. For instance, in one study, induction of MLL-driven inter-chromosomal translocations with ENL always resulted in AML, while in humans, MLL-driven rearrangements may also result in ALL [102]. More recently, CRISPR/Cas9-mediated gene editing has been used to induce inter-chromosomal rearrangements via dual single-guide RNAs targeting the breakpoint cluster region of MLL and AF9 in murine BM derived LSKs [284]. The key feature of all three models described above is their ability to engraft into fully immune-competent murine models when induced endogenously or in the context of transplantation.

1.6 CRISPR/Cas9-based genetic screening in AML

Clustered regularly interspaced short palindromic repeats (CRISPR/Cas) was discovered as bacterial adaptive immune system against viruses that recognizes and targets their DNA sequences, inducing DSB [285-287]. CRISPR was soon adapted for a wide range of applications, including functional genetic screening, a high-throughput approach to identify novel genes, pathways and mechanisms involved in given phenotypes in cell lines and model organisms *in vitro* and *in vivo*. Before the discovery and application of CRISPR/Cas9 in genetic screenings, large-scale gene perturbations were often carried out by RNA interference (RNAi) or short hairpin

(shRNA). However, siRNA and shRNA-genetic screening approaches are limited by off-target activity and variable knockdown efficiencies [288]. Alternative approaches for genetic screening involving CRISPR include CRISPR interference (CRISPRi) and CRISPR activation (CRISPRa), which use endonuclease dead Cas9 (dCas9) fused with distinct effectors. In CRISPRi, dCas9 is fused to Kruppel associated box (KRAB) domain, which represses gene expression when targeted to promotor regions. In CRISPRa, dCas9 is fused to the transcriptional activator VP64, enhancing gene expression [289-292].

Genome-wide CRISPR/Cas9-based genetic screening has been applied in AML *in vitro* and *in vivo* to systematically identify the functional effect of loss of every gene in a given library [293-296]. CRISPR/Cas9-based screening has had a significant impact in the field of AML research. A comprehensive search on PubMed, utilizing the search term 'CRISPR screening AML,' yielded over 100 articles published since 2016. These research endeavors have been primarily dedicated to identifying novel mechanisms within AML linked to cell survival, drug response, and cellular differentiation processes [123, 297, 298]. CRISPR/Cas9-based screening in AML is coupled with either murine models, human AML cell lines or primary AML cells [192, 299] [300]. Murine AML models are often derived from Cas9-transgenic knock-in mice with either constitutive or inducible expression of Cas9 [192]. Cas9 can be introduced into human AML cell lines and patient-derived xenograft (PDX) models either by lentiviral vectors or through non-viral vectors such as lipid nanoparticle or electroporation of CRISPR/Cas9:sgRNA ribonucleoprotein (RNP). Genome-wide sgRNA libraries are typically cloned into a lentiviral vector, containing up to 200,000 sgRNA sequences and targeting approximately 20,000 genes [301]. Successful examples of CRISPR/Cas9 based genome-wide screening in AML cells involve the discovery of mitochondrial processes mediating resistance to the BCL-2 inhibitor venetoclax [298], confirming

the link between metabolic targeting and venetoclax as a therapeutic opportunity for AML [302-305]. Furthermore, *MAPK and MTOR complex 1 (MTORC1)* were identified as contributing to resistance to FLT3 inhibitor Sorafenib in *FLT3-ITD* AML cells, providing novel therapeutic opportunities for patients resistant to FLT3 inhibitors [306]. Genome-wide CRISPR/Cas9 screening in combination with nucleoside analogues identified *DCK* as the main driver of sensitivity; however, other contributors of resistance were genes regulating cell cycle arrest [262, 265]. Genome-wide CRISPR screens in mice have particularly been useful for *in vivo* studies, identifying genetic vulnerabilities specifically relevant for cell-cell interaction, engraftment, and immune regulation [192].

1.7 Ubiquitin-proteasome system

The Ubiquitin-proteasome system (UPS) is an important quality control for protein stability and turnover and is fundamental to many biological processes. Ubiquitin (Ub) is a highly conserved regulatory protein, composed of 76 amino acids, which is covalently bound to a protein via a cascade of enzymatic reactions, including Ub-activating enzymes (E1), Ub-conjugating (E2) and Ub-ligating enzymes (E3) [307]. The human genome encodes only two E1 enzymes, Uba1 and Uba6 [308]. Humans have ~40 known conjugating-E2 enzymes, which assist more than 600 different E3 ligases to transfer Ub to the substrate [309]. E3-ligating enzymes are the most common and specific enzymes [310]. Ubiquitination is a three-step enzymatic reaction. Ub is first activated by E1 under ATP as a co-factor. Second, Ub is transferred from E1 to E2, which involves the formation of a thioester bond between the active site Cys residue and E1 and the C-terminal carboxyl group of Ub (E1~Ub). Third, E2 assists E3 in transferring the Ub to the substrate. Ubiquitination is reversible and can be removed through deubiquitinating enzymes (DUBs),

belonging to the family of Cys proteases. Approximately 100 DUBs are known that can be further divided into six families based on sequence and structure similarity [311]. Diverse DUBs have been discovered to participate in the regulation of p53. For instance, USP7 regulates the stability of p53 and Mdm2, USP2 regulates the stability of Mdm2, and USP10 modulates p53 stability and localization. On the other hand, OTUB1 diminishes p53 ubiquitination and activates p53 [312-314].

Protein ubiquitination is the second most common post-transcriptional modification (PTM) after phosphorylation [307]. There are three major types of ubiquitination: mono-, poly- or branched ubiquitination, which differentially regulate multiple cellular pathways [315]. Mono-ubiquitination refers to the attachment of 1 Ub to a lysine residue of the substrate and has been implicated in DNA damage response pathways. For instance, the mono-ubiquitination of FANCD2 and FANCI is crucial for the activation of the FA pathway and subsequent DNA repair processes, including homologous recombination and cell cycle regulation [316-318]. Polyubiquitination refers to the attachment of more than 2 Ub to the same lysine residue of the substrate. Ub can be linked to the substrate from 8 specific residues. K48-linked polyubiquitination was discovered as the first type of Ub linkage and signals degradation by the 26S proteasome [313]. Since then, a total of 8 Ub linkers have been identified (K6, K11, K27, K29, K33, K48, K63 and Met1) mediating several biological processes [307]. For example, branched polyubiquitination with K6 linkage is involved in the DNA damage response, whereas branched K11- chains promote cell-cycle dependent proteasomal degradation [319].

1.7.1 E3 Ub ligases

Around 600 known human E3 ligases mediate the degradation of specific substrates [307]. According to their catalytic structures, E3 ligases are grouped into three classes: the *really interesting new gene family (RING)* -type, the *homologous to the E6-AP carboxyl terminus (HECT)*-type and *ring between ring fingers (RBR)*-type [307]. Ring-type E3 ligases have a characteristic RING/U-box domain and catalyze Ub from E2 directly to the substrate in one step [320]. Ring-type ligases are the most common E3 ligases. For instance, a well-known E3 enzyme is the RING-type E3 enzyme MDM2 [321, 322].

HECT E3 and RBR E3 promote ubiquitination in a two-step sequential enzymatic reaction, whereby Ub is first transferred from E2 to the E3 through an intermediate cysteine onto the carboxy terminus of HECT E3s or the second RING of RBRs before the ligation to the lysine residue of the substrate. RBR E3 are the least common ligases, with only 14 characterized to date. There are 28 known HECT E3 ligases, which can further be sub-classified into three categories: Nedd4/Nedd4-like E3s with WW domain, HERC E3s containing an RLD domain, and other E3s without a WW or RLD domain [323]. Most of the HECT E3 ligases belong to the first and second group. Therapeutic targeting of HECT ligases is currently in development although, in comparison to other RING-type ligases, HECT-type E3 ligases appear to be more challenging to target. Using a phage display screening method, one group identified bicyclic peptides that bind specifically to the E2 binding site of the HECT domain of several E3 ligases such as: SMAD-specific E3 ubiquitin protein ligase 2 (SMURF2), Neural precursor cell expressed, developmentally down-regulated 4 (NEDD4), WW domain-containing E3 ubiquitin protein ligase 1 (WWP1) and Mcl-1 ubiquitin ligase E3 (MULE), resulting in the inhibition of their ligase activity [324]. The inhibitor Heclin was discovered as a HECT E3 ligase inhibitor, inhibiting a range of HECT-type E3 ligases [325].

Another group utilized specific Ub mutants, which were found by a phage screen to modulate HECT catalysis. The Ub mutants were able to bind the N-lobe exosite and the N-lobe surface involved in the interaction of E2, thereby promoting inhibition or activation dependent on the type of modification in the Ub mutant [323] [326].

1.8 Hypothesis and research objectives

The main problems in AML treatment remain the resistance to chemotherapy after the initial response and the high toxicity of therapy in patients. Older patients are frequently unable to tolerate intensive chemotherapy and are often ineligible for allogeneic transplantation. There is a **critical need for the identification of: 1) regulators of response to Ara-C, and 2) novel therapeutic targets that can be exploited to improve AML survival.**

I hypothesized that AML cells have non-mutated genetic vulnerabilities with “druggable” potential that can be discovered using genetic perturbation screens performed in functionally relevant contexts. Murine syngeneic models of the disease, albeit genetically simpler than human disease, lead to uniform *in vivo* and *in vitro* propagation that is essential for CRISPR/Cas9 screening. Using CRISPR/Cas9-based screening in syngeneic murine models of AML, I identified essential drivers of response to Ara-C (chapter 2) and immune escape (chapter 3). My specific hypotheses for each chapter were as follows:

Chapter 2: The E3 ubiquitin ligase HERC1 modulates the response to nucleoside analogs in AML cells both *in vitro* and *in vivo*; therefore, I investigated:

- a.) How *Herc1* influences the response of Ara-C *in vitro*.
- b.) What is the target of *Herc1* that influences the response to Ara-C in AML cells.
- c.) The pre-clinical relevance of targeting *Herc1* in AML *in vitro* and *in vivo*.

Chapter 3: MLL/AF9 Cas9⁺ AML cells are vulnerable to immune targeting *in vivo*. Therefore, I systematically mapped genetic vulnerabilities that are critical for AML survival *in vivo* by:

- a.) completing a focused based-dropout *in vivo* screen targeting different components of AML biology.
- b.) Identification of *Slc25a19* as a novel immune dependency *in vivo*.

**2 Chapter 2: The E3 ubiquitin ligase Herc1 modulates the response to nucleoside analogs
in acute myeloid leukemia**

Jankovic, M., Poon, W.L., Gonzales-Losada, C., Galicia Vazquez, G., Sharif-Askar, B., Ding, Y., D., Desombre, C., Iliac, A., Shi, J., Orthwein, A., Mercier, F.E.

(to be submitted for publication).

2.1 Preface to the manuscript

To better understand genetic factors influencing chemotherapy, I adapted genome-wide CRISPR-Cas9 screening technology *in vitro*, paired with experimental models of AML replicating human disease, to identify additional gene-drug interactions modulating Ara-C response. Aside from the deoxycytidine kinase *Dck*, which emerged as one of the top sensitizing genes, and the dNTPase enzyme *Samhd1*, which scored as one of the top genes providing resistance, thereby validating our CRISPR-based screening approach, I identified the E3 Ub ligase Herc1 as a novel modulator of Ara-C response. Herc1 is a member of the UPS, which is responsible for the degradation of nearly 80% of all proteins and plays a major role in biological homeostasis. Previous work on HERC1 has identified numerous important domains (HECT, RCC, WDR, BH3) which have been implicated in several biological processes such as apoptosis, oncogenic signaling, DNA damage. Little is known about the contribution of HERC1 in the response to nucleoside analogues and it may represent a potential biomarker in the context of AML.

The E3 ubiquitin ligase Herc1 modulates the response to nucleoside analogs in acute myeloid leukemia

Maja Jankovic^{1,2}, Wei Lam Poon^{1,2}, Cristobal Gonzales-Losada^{1,2}, Gabriela Galicia Vazquez¹, Bahram Sharif-Askari¹, Yi Ding³, Constance Desombre¹, Alexandru Iliac¹, Jiantao Shi³, Alexandre Orthwein^{1,2,4,5,#}, and Francois Mercier^{1,2,6,#}

¹ Lady Davis Institute for Medical Research, Segal Cancer Centre, Jewish General Hospital, Montréal, Canada; ² Division of Experimental Medicine, McGill University, Montreal, Canada; ³ State Key Laboratory of Molecular Biology, Shanghai Institute of Biochemistry and Cell Biology, University of Chinese Academy of Sciences, Shanghai, China ⁴ Gerald Bronfman Department of Oncology, McGill University, Montréal, Canada; ⁵ Department of Radiation Oncology, Winship Cancer Institute, Emory University, Atlanta, USA; ⁶ Department of Medicine, McGill University, Montréal, Canada; # co-corresponding authors

Running title: Herc1 in acute myeloid leukemia

Address correspondence to:

Francois Mercier, M.D.

Lady Davis Institute, Segal Cancer Centre

Jewish General Hospital

Montreal, Quebec, H3T 1E2 Canada

e-mail: francois.mercier@mcgill.ca

Alexandre Orthwein M.Sc., Ph.D.

Department of Radiation Oncology, Winship Cancer Center

Emory University

Atlanta, GA 30322 USA

e-mail: alexandre.orthwein@emory.edu

2.2 ABSTRACT

Acute myeloid leukemia (AML) is a hematological malignancy that emerges from hematopoietic precursors arrested at an early stage of development in the bone marrow. Nucleoside analogs, including cytarabine (Ara-C) and fludarabine (Fludara), are frequently used in front-line therapies to treat AML patients. Still, a significant proportion of AML cases becomes resistant or is refractory to these chemotherapeutic agents, representing a significant challenge in the clinic. Thus, understanding the genetic factors that modulate the response to nucleoside analogs in AML remains a critical unmet clinical need. Using CRISPR-based functional genomics, we identified the E3 ubiquitin ligase Herc1 as a key modulator of Ara-C response in both MLL/AF9 (MA) and HOXA9/MEIS1 (HM) murine AML models *in vitro*. Loss of Herc1 enhances nucleoside analog-induced cell death in both murine and human AML cell lines by compromising cell cycle progression. In-depth proteomic analysis identified the deoxycytidine kinase Dck as one of the top enriched proteins in Herc1-depleted murine AML cells and we confirmed that lack of Herc1 led to a significant increase in Dck protein levels at steady state in both MA and HM murine cells. Importantly, we showed that targeting of Herc1 enhanced the response of the murine MA AML model to Ara-C *in vivo*. Collectively, this study highlights the importance of Herc1 for the survival of AML cells and their response to nucleoside analogs, thereby establishing this E3 ubiquitin ligase as a potential therapeutic target for the treatment of AML.

Keywords: acute myeloid leukemia, nucleoside analogs, cytarabine, CRISPR, E3 ubiquitin ligase.

2.3 STATEMENT OF SIGNIFICANCE

We demonstrated the E3 ubiquitin ligase Herc1 as novel modulator of nucleoside analogs in murine AML models both *in vitro* and *in vivo*. Our study identified the deoxycytidine kinase Dck, the rate limiting step in the processing of nucleoside analogs, as one of the key targets of Herc1 in murine AML cells. Our data uncovers Herc1 as a potential prognostic factor and therapeutic target for human AML.

2.4 Introduction

Acute myeloid leukemia (AML) is a highly proliferative disease with great heterogeneity between patients both at the phenotypic and genomic levels [1, 2]. These differential features in AML cases contribute to the substantial challenges faced in the treatment of this pathology. Indeed, nearly half of adult AML cases relapse within three years from standard of care chemotherapy [3, 4], and these patients often fail to respond to conventional treatment with a dismal outcome. Thus, the overall five-year survival rates in adults diagnosed with AML is only at 28% [5], highlighting the critical and unmet clinical need of better understanding the chemo-response of AML cells.

Frontline induction chemotherapy for patients affected by AML, particularly those younger than 65 years of age, consists in the combination of a nucleoside analog, like cytarabine (Ara-C), with an anthracycline (e.g. idarubicin or daunorubicin) [1]. Problematically, many patients who relapse from this intensive chemotherapy regimen will no longer respond to Ara-C based salvage therapy. Mechanistically, Ara-C is a cytidine analog that interferes with DNA replication in cells that are fast growing, alike AML cells. Previous studies have identified key modulators of Ara-C response in AML, including the deoxycytidine kinase DCK [6, 7] and the deoxyribonucleoside triphosphate (dNTP) triphosphohydrolase SAMHD1 [8]. Both factors directly participate in the metabolic processing of nucleosides. To better understand genetic factors influencing chemotherapy, we adapted genome-wide CRISPR-Cas9 screening technology *in vitro*, paired with experimental models of AML replicating human disease, to identify additional gene-drug interactions modulating Ara-C response. Aside from the deoxycytidine kinase *Dck*, which emerged as one of the top sensitizing genes, and the dNTPase enzyme *Samhd1*, which scored as one of the top genes providing resistance, thereby validating our CRISPR-based screening approach, we

identified *Herc1* (Homologous to the E6AP carboxyl terminus (HECT) and regulator of chromosome condensation 1 (RCC1)-like domain-containing protein 1) as novel genetic resistant gene of Ara-C and other classes of nucleoside analogues in AML cells *in vitro*. We performed RNA sequencing and quantitative proteomic analysis in *Herc1*-deleted cell lines and discovered that *Herc1* regulates the steady-state protein levels of the deoxycytidine kinase Dck in murine AML cells. Finally, we showed that *Herc1*-depleted AML cells are hypersensitive to Ara-C treatment in the murine MA AML model *in vivo*. Altogether, this present study identified *Herc1* as novel regulator of Ara-C response in AML cells and links the ubiquitin-proteasome system to key enzymes relevant to nucleotide metabolism, in particular the deoxycytidine kinase Dck.

2.5 Materials and methods

2.5.1 Mice

Rosa26-CAG-Cas9/GFP knockin mice were used for constitutive Cas9 gene expression. All mouse strains were obtained from Jackson laboratories. Animal experiments were approved by the institutional review board of McGill University.

2.5.2 Generation of constitutive MLL/AF9-Cas9 (MA-Cas9) and HoxA9-Meis1-Cas9

(HM-Cas9) AML cell line

The KMT2A/MLLT3 (MLL/AF9) and HOXA9/MEIS1 retroviral leukemia models have been described previously [10, 11]. Lineage-Sca-1⁺C-kit⁺ hematopoietic progenitor cells (LSKs) from a male Cas9-GFP^{+/-} donor mice were sorted in RPMI-1640 media with 10% fetal bovine serum (fetal bovine serum, Wisent Bio Products and Hyclone) supplemented with cytokines mSCF (10 ng/mL, biolegend, Cat.#579706), mIL3 (5 ng/mL, biolegend, Cat.# 575506) and mIL6 (10

ng/mL, biolegend, Cat.# 575702) and 100 units/mL penicillin/streptomycin at 37 °C with 5% CO₂. LSKs were transduced with a MSCV-MLL/AF9-IRES-GFP (MA) or MSCV-HoxA9-IRES-Meis1 (HM) construct. After transduction, cells were passaged for 3-4 weeks until uninfected cells ceased proliferating overtime. After passaging the cells were injected intravenously into sublethally irradiated C57BL/6J recipients. After the primary recipients developed clinical signs of AML, the bone marrow leukemic cells were isolated and propagated in RPMI-1640 media with mSCF 10 ng/mL (biolegend, Cat.#579706), mIL3 5 ng/mL (Biolegend, Cat.#575506), 10% (fetal bovine serum, Wisent Bio Products and Hyclone) and 100 units/mL penicillin/streptomycin at 37 °C with 5% CO₂, to establish the lines used in this study [41].

2.5.3 Production of Lentivirus and transfection.

The HEK293T cell line was ordered from the American Type Culture Collection (ATCC). 3 x10⁶ HEK293T cells were seeded in 100 mm dish at a confluency at 70% in 10 mL of DMEM (Wisent bioproducts) + 10% FBS. Transfection was performed using FuGENE6 (Promega, Cat.#E5911) transfection reagent according to the manufactures protocol. 30 µL FuGENE6 in 500 µL DMEM was combined with 5 µg transfer plasmid, 1 µg envelope plasmid pCMV_VSVG (Addgene #8454) and 4 µg packaging plasmid pCMV_ΔR8.9 (Addgene, #12263). Plasmids were incubated for 30 min at room temperature, during that time DMEM media supplied with 10% FBS and 1% penicillin/streptomycin was changed on the HEK293T cells. After 30 min, the transfection mixture was added dropwise to HEK293T cells. Cells were incubated for 48 h and virus was collected every 8 h until 72 h post-transfection.

2.5.4 *In vitro* CRISPR screening

MA and HM cells were transduced with the murine GeCKO (Genome-Scale CRISPR Knock-Out) v2 genome-wide lentiviral libraries comprising 130 209 targeting sequences and 1000 sequences with no homology to the mouse genome as control (Addgene, Cat.# 1000000052). For the genome-wide CRISPR/Cas9 screen a total of 48 million cells MA-Cas9 and HM-Cas9 lines were infected with the GeCKO v2 library in the presence of 8 µg /mL polybrene (Sigma Aldrich # TR-1003) using freshly prepared virus at a MOI ~ 0.25. Immediately after transduction, 4 mL of fresh media was added to each well to dilute the polybrene. Twenty-four hours' post transduction cells were centrifuged at 500 g, 5 min at room temperature then resuspended in 100 mL of fresh media and transferred into T175 flasks into duplicates. At forty-eight hours' post transduction, cells were selected for 72h with puromycin (BioShop Canada) at final concentration of 10 µg/mL. Cells were passaged daily, and cell number was maintained at 500 x10⁵ cells/mL. Ara-C or Vehicle treatment started at day 7 with a sublethal dose of Ara-C (MA-Cas9 IC50 [40 nM] and HM-Cas9 [80 nM]). Cell lines were cultured *in vitro* for five more days at a confluency of 5 x10⁵ cells/mL. At each time point, cell pellets were collected for genomic DNA extraction using phenol/chloroform (Thermo Fisher, Cat.#15593031).

2.5.5 Library preparation

An Illumina PCR 1-step library protocol was used, to attach sequencing adaptors and index. PCR-amplification protocol was developed by the Genetic Perturbation Platform of the Broad Institute (available at: <https://portals.broadinstitute.org>). P5 primer mix NEON and P7 indexed primers were used. DNA from samples at following days was extracted and amplified: (1) three days *in vitro*, start of puromycin selection, (2) 7 days *in vitro* after transduction; before treatment

(3) 5 days *in vitro* after timepoint (2). From each condition 40 µg of DNA was amplified. PCR reactions were pooled into two sub-pools and analyzed on 0.8% agarose gel, expected bands were extracted at ~350 bp using QIAquick Gel Extraction Kit (Quiagen, Cat.#28704). Sequencing was performed on two lanes of a HiSeq 2000 flow cell (Illumina).

2.5.6 Analysis of genome wide CRISPR dropout screen

The read count files were generated from the CRISPR Fastq files, for each biological and technical replicate using the ‘count’ function of the MAGeCK algorithm [46]. To determine the technical performance of the screen, technical replicates were correlated using Pearson and Spearman, and read counts were combined. In the Ara-C genome-wide screen, the gene scores representing depletion or enrichment (normZ score) were estimated from the read count files using the drugZ algorithm [14]. Pathway enrichment analysis was performed by using String-db [47].

2.5.7 Validation of CRISPR screen using single sgRNAs

To generate *Herc1*-knock out cells sgRNA target sequences were designed using the Broad Institute Genetic Perturbation Platform (<https://portals.broadinstitute.org/gpp/public/gene/search>). sgRNA target sequences were subcloned into pKLV2-U6gRNA5(BbsI)-PGKpuro2AmCherry-W or pKLV2-U6gRNA5(BbsI)-PGKpuro2ABFP-W vectors as previously described [27]. 1×10^6 cells were plated in 6-well plates in 2 mL media as described above. 1 mL of freshly harvested virus (48 h) was added to cells with 8 µg /mL polybrene. Cells were spin-infected for 1 h at 1000g at 32 °C, then polybrene was diluted down with 4 mL of fresh media. Two days post-spin-infection, cells were selected with 10 µg /mL puromycin for five days. mCherry⁺ single cells were sorted into 96-Well plate and genotyping PCR was performed by designing primers targeting the genomic

target sites. Cells were transferred into 6-well plate after colonies began to grow and gene-KO was validated by PCR.

Table 2-1 sgRNAs human and mouse

Gene	species	sgRNA	sgRNA sequence
Samhd1	mouse	sgRNA-1	GGCTGCGAAGTTAAGTACCG
Samhd1	mouse	sgRNA-2	TCCCTGTAATCTCCACGTAG
Samhd1	mouse	sgRNA-3	CTTTGGGCCTCAGACAACCTG
Herc1	mouse	sgRNA-1	AGTACCTCAGAACGTTACCG
Herc1	mouse	sgRNA-2	ACCAACTAGAGGAATACCTG
Herc1	mouse	sgRNA-3	AGTGCATCAGTGCTTGACCG
Dck	mouse	sgRNA-1	CTATCTTCGAGCTACTCCCG
Dck	mouse	sgRNA-2	TGTATGAGAAACCTGAACGG
Dck	mouse	sgRNA-3	CATCGAGGGGAACATCGGTA
EGFP	mouse/ human	sgRNA-1	CAACTACAAGACCCGCGCCG
EGFP	mouse/ human	sgRNA-2	ATCCGCCACAACATCGAGGA
EGFP	mouse/ human	sgRNA-3	CAACGAGAAGCGCGATCACA
NTC-1	mouse/ human	sgRNA-1	GCGAGGTATTCGGCTCCGCG
NTC-3	mouse/ human	sgRNA-3	ATGTTGCAGTTCGGCTCGAT
NTC-4	mouse/ human	sgRNA-4	ACGTGTAAGGCGAACGCCTT
HERC1	human	sgRNA-1	GAAAGTGGTGCGGTACCGTG
HERC1	human	sgRNA-2	CAATACGTTTAGCAGACCAG
HERC1	human	sgRNA-3	AGTGCATCAGTGCTTGACCG
HERC1	human	sgRNA-4	GCCAGGGCAGATACCCAATG
HERC1	human	sgRNA-5	GTTCTATAGTAGCAATCCAG
HERC1	human	sgRNA-6	CAATTCTCGACGGTGCATGG

2.5.8 Plasmids.

The plasmids pKLV2-U6gRNA5(BbsI)-PGKpuro2AmCherry-W and pKLV2-U6gRNA5(BbsI)-PGKpuro2ABFP-W were a gift from Kosuke Yusa (Addgene plasmid # 67977 ; <http://n2t.net/addgene:67977> ; RRID:Addgene_67977; Addgene plasmid # 67974 ; <http://n2t.net/addgene:67974> ; RRID:Addgene_67974) [27]

2.5.9 Tracking of Indels by Decomposition (TIDE) assay

Genomic DNA (~1 × 10⁶ cells) was isolated using DNeasy Blood and Tissue kit (Qiagen, Cat.# 69504). PCR reactions were carried out with 100 ng genomic DNA in EasyTaq mix (Transgene biotech) according to manufacture instructions. PCR conditions were 1 min at 94°C (1×), followed by 30 s at 94°C, 15 s at 51°C (Herc1 sg1), 54°C (Herc1 sg2, sg3), 60°C (HERC1 sg4), and 1 min at 72°C (30×). The PCR products were purified using the Qiaquick PCR purification kit (Cat. #28104). Purified PCR products were submitted for sanger sequencing and TIDE analysis was performed using web platform tool: <https://tide.nki.nl> and by the Synthego Performance Analysis, ICE Analysis. 2019. v3.0. Synthego.

Table 2-2 Primer for TIDE analysis

Primer name	Fw 5'-3'	Rv 5'-3'	Annealing
mHerc1_sg 1_1 TIDE	CTCAGTGCACGC AATGTTCA	GCTTGGTAGGAACTT CCGCT	54 °C
mHerc1_sg 1_2 TIDE	GGGGTTCAAAAC TGCCCTTA	TCTCAGTTTGGCCCC TTTGT	54 °C
mHerc1_sg 2_1 TIDE	ATGGGCCACGG ACTAGATCA	CCACTTAAAAATTAC AAACCTGGGC	51 °C
mHerc1_sg 3_1 TIDE	GCGCTAAGAA AACGACTGC	ACCAAAGAAGACTCC CAAATCTCT	51 °C
hHERC1 sg4 TIDE	GTGGGCACAGA GGTTATCGT	GTGGGCACAGAGGT TATCGT	60 °C

2.5.10 Multicolor competition assays

Multicolor competition assays (MCA) were performed to verify the impact of gene KOs on fitness defects in the presence of Ara-C treatment. In these assays, targeted cells expressed both mCherry, while parental cell lines expressed EGFP. The cell lines were infected with either a Non-targeting control (sgCtrl) vector or a targeting sgRNA vector and allowed to expand for two days. After 48 hours, the cells were examined to determine the percentage of mCherry⁺ cells. Subsequently, the cells were plated in triplicates with a confluency of 2.5×10^4 cells/mL into 6-well plates. The cells were then treated with Ara-C at a concentration of 50nM for a minimum of 14 days. The competition of the cells was assessed using flow cytometry every 4 days using the BD LSRFortessa instrument.

2.5.11 Cell viability assays

A total of 5,000 cells were seeded into quadruplicates into a 96-well plate and subjected to serial dilutions (1:2) of Cytarabine (Selleckchem, Cat.#S1648), Gemcitabine (Selleckchem, Cat.#S1149), Fludarabine (Selleckchem, Cat.#S1491), and Doxorubicin (Selleckchem, Cat.#E2516), each in a volume of 200 μ L. After 72 hours, 100 μ L of cells were collected from each well, and CellTiter-Glo[®] reagent was introduced to every well. The luminescence signal was then measured using the FLUOstar OPTIMA[®] bioluminescent reader (BMG Labtech) after a 10-minute incubation period.

2.5.12 Apoptosis assay and cell cycle analysis

A total of 150,000 cells were seeded into 6-Well plates with 1 mL of cell culture media. Subsequently, they were treated with Ara-C at concentrations of 200nM (MA) and 400nM (HM) and 1 μ M (U937) for a duration of 24 and 48 (U937) hours. On the following day, the cells were collected and subjected to centrifugation at 500g for 5 minutes, followed by two washes with PBS. The cells were then stained in Annexin V binding buffer (Catalog No. 422201) with AnnexinV-APC (Biolegend, Cat.#64094) and DAPI, incubated for 15 minutes at room temperature in the dark, following the manufactures protocol. Cells were analyzed using the BD LSRFortessa instrument.

For intracellular Caspase-3 staining, a separate set of 500,000 MA cells were fixed using BD cytofix buffer for 15 minutes on ice. After centrifugation at 1000g for 5 minutes, the cells were washed twice with BD cytoperm buffer. The MA cells were then stained with Caspase-3 AF647 antibody (BD bioscience, Cat.#560626) for 30 minutes in the dark and washed with BD cytoperm buffer. The samples were analyzed using the BD LSRFortessa instrument.

To perform cell cycle analysis at different time points (6 hours, 12 hours, and 24 hours), 1×10^6 MA cells were seeded into 6-well plate and treated with 200nM Ara-C or H₂O as a vehicle control. After washing with PBS, the cells were permeabilized with 70% ethanol. Subsequently, the MA cells were washed twice with PBS and stained in 2x PI buffer (containing 40 μ g Propidium iodide, 0.4 mg RNase, and 0.4% TritonX-100) for 30 minutes at 37 degrees celsius. The samples were analyzed using the BDFortessa instrument.

2.5.13 HERC1 target identification

HERC1-Knockout cells (MA Clone E5) and Control cells (MA sgCtrl) were plated in 100 mm cell culture dish with a confluency of 0.5×10^6 cells/ml. Cells were cultured as described above and treated with 200 nM Ara-C for 6 hours. Cells were centrifuged at 500g for 5 min and aliquoted for RNA- and Protein extraction.

2.5.14 RNA sequencing

The isolation of total RNA was carried out using a combination of TRIzol (Invitrogen) and the RNeasy Mini Kit (Qiagen, #74106). Subsequently, cDNA libraries were prepared from the total RNA using the KAPA RNA HyperPrep Ribo Erase Kit and amplified for sequencing. The sequencing process was performed on the Nextseq500 platform. To prepare the sequences for analysis, they were trimmed for sequencing adapters and low-quality 3' bases using Trimmomatic version 0.35[42]. Alignment of the trimmed sequences to the reference mouse genome version GRCm38 was performed using STAR version 2.7.1a [43], utilizing gene annotation from Gencode version M25, based on Ensembl 100. Gene expressions were obtained from STAR, providing read counts and TPM (Transcripts Per Million) values. Additionally, RSEM[44] was employed to compute normalized gene and transcript-level expression, resulting in FPKM (Fragments Per Kilobase Million) and TPM values for the stranded RNA libraries.. DESeq2 version 1.30.1 was then employed to normalize gene read counts [45].

2.5.15 Tandem Mass Tag (TMT)-labeling and mass spectrometry

Cells were lysed using RIPA buffer (50mM Tris•HCl pH 7.6, 150mM NaCl, 1% NP-40, 1% sodium deoxycholate, 0.1% SDS) supplemented with protease inhibitor cOmplete™, Mini

Protease Inhibitor Cocktail, Roche, Cat.#11836153001) for 30 min on ice and subsequently sample were sonicated for 5 sec at 30% amplitude, 3 times.

Samples were treated with TMT-16plex reagents (ThermoFisher Scientific) according to the manufacturer's instructions. Labelled peptides were fractionated using Pierce™ High pH Reversed-Phase Peptide Fractionation Kit into 8 fractions. Each fraction was re-solubilized in 0.1% aqueous formic acid and 2 micrograms of each was loaded onto a Thermo Acclaim Pepmap (Thermo, 75uM ID X 2cm C18 3uM beads) precolumn and then onto an Acclaim Pepmap Easyspray (Thermo, 75uM X 15cm with 2uM C18 beads) analytical column separation using a Dionex Ultimate 3000 uHPLC at 250 nl/min with a gradient of 2-35% organic (0.1% formic acid in acetonitrile) over three hours running the default settings for MS3-level SPS TMT quantitation (McAlister et al, 2014 – Anal Chem. 2014 Jul 15;86(14):7150-8. Doi: 10.1021/ac502040v.), on an Orbitrap Fusion instrument (ThermoFisher Scientific) was operated in DDA-MS3 mode.

Briefly, MS1 scans were collected at 120,000 resolution, scanning from 375-1500 m/z, collecting ions for 50ms or until the AGC target of 4e5 was reached. Precursors with a charge state of 2-5 were included for MS2 analysis, which were isolated with an isolation window of 0.7 m/z. Ions were collected for up to 50ms or until an AGC target value of 1e4 was reached, and fragmented using CID at 35% energy; these were then read out on the linear ion trap in rapid mode. Subsequently, the top 10 (height) sequential precursor notches were selected from MS2 spectra for MS3 quantitative TMT reporter ion analysis, isolated with an m/z window of 2 m/z, and fragmented with HCD at 65% energy. Resulting fragments were read out in the Orbitrap at 60,000 resolution, with a maximum injection time of 105ms or until the AGC target value of 1e5 was reached.

2.5.16 Mass Spectrometry Raw Data Analysis.

To translate .raw files into protein identifications and TMT reporter ion intensities, Proteome Discoverer 2.2 (ThermoFisher Scientific) was used with the built-in TMT Reporter ion quantification workflows. Default settings were applied, with Trypsin as enzyme specificity. Spectra were matched against the mouse protein fasta database obtained from Uniprot(2022). Dynamic modifications were set as Oxidation (M), and Acetylation on protein N-termini. Cysteine carbamidomethyl was set as a static modification, together with the TMT tag on both peptide N-termini and K residues. All results were filtered to a 1% FDR.

2.5.17 Western Blotting

Cells were washed with cold PBS, and whole cell lysates were collected using freshly prepared LDS sample buffer containing proteinase inhibitor. Cell lysates were sonicated at 30% for 5 seconds for 3 rounds. Protein concentration was measured by nanodrop (A280). 1,4 uL of B-Mercaptoethanol (Sigma-Aldrich, Cat.#M3148) and 4x Laemmli Sample buffer (BioRad, Cat# 1610747), was added and samples were boiled at 70 degrees for 10 min.

20 ug and 100 ug of whole cell extracts were fractionated by SDS-PAGE (4–15% precast polyacrylamide gel) for 15 min 120V and 60 min 60V, and transferred to a polyvinylidene difluoride (PVDF, Cat.#1620177, BioRad) membrane overnight, 30V. After incubation with 5% non-fat milk and 3% Bovine Serum Albumin in TBST (10 mM Tris, pH 8.0, 150 mM NaCl, 1% Tween 20 (Cat.P1379,Sigma-Aldrich)) for 60 min, the membrane was washed once with TBST and incubated with antibodies against dCK (Thermofisher, Cat.# PA5-27787, 1:1000), α -tubulin (Cell signaling, 11H10, Cat.#21255,), vinculin (cell signaling, Cat.# 13901) at 4 °C for overnight. Membranes were washed three times for 7 min and incubated with a 1:2000 dilution of horseradish

peroxidase-conjugated anti-rabbit (cell signaling, Cat.#7074S) antibodies for 2 h. Blots were washed with TBST three times for 7 min and developed with the ECL prime system (Amersham Biosciences , Cat.#RPN2236) according to the manufacturer's protocols.

2.5.18 RT qPCR

MA cells were grown in supplemented RPMI media as it is described above. RNA was extracted with Rneasy kit (Qiagen, Cat.#74106), cell pellets were eluted in H₂O, and RNA concentration and absorbance ratios (A₂₆₀/280 and A₂₆₀/230) were measured using spectrophotometer Nanodrop 2000. 1000 ng of RNA was added for reverse transcription using iScript™ cDNA synthesis kit (Biorad, Cat.#1708890) and reaction was run following manufactures instructions. cDNA was diluted 1:10 and following RT qPCR was performed using Luna® Universal qPCR Master Mix with 2 ul of cDNA product. SYBR® mode setting on the Applied Biosystems 7500 Fast instruments was selected and RT PCR was performed following Luna® Universal qPCR Master Mix Protocol (NEB, Cat.#M3003). To confirm product specificity, melting curve analysis was performed after each amplification. Following primer sequences were used for RT qPCR amplification: *Dck* forward (5'- CCTCTGAGGATTGGGAAGTGG-3'), reverse (5'- CACCGCTCTTCTGAGACGTT-3'), *Gapdh* forward (5'- GCACAGTCAAGGCCGAGAAT-3'), reverse (5'- GCCTTCTCCATGGTGGTGAA-3'), *B2m* forward (5'- ACGTAACACAGTTCACCCG-3'), reverse (5'- CAGTCTCAGTGGGGGTGAAT-3').

2.5.19 MA-Cas9 *In vivo* experiments.

24 h prior transplantation sgHerc1-knockout MA-cells were mixed with sgCtrl MA-cells. Into each recipient 1,000,000 MA-Cas9 cells were transplanted into sub-lethally irradiated (4,5 Gy) C57BL/6J mice. 14-16 days post transplantation peripheral blood analysis was performed to estimate onset of leukemia. Mice with >5% detectable amount of leukemic GFP⁺ cells, were treated with 100 mg/ml of Ara-C (U-19920A) for 5 constitutive days.

2.5.20 Statistical analysis.

Quantitative experiments measuring the half maximal inhibitory effect (IC₅₀), apoptosis, cell cycle and Edu experiments are graphed with mean +/- SEM with data from at least three independent experiments, as described in the figure legend. All data sets were tested for normal distribution by Shapiro-Wilk Test. Statistical significance was determined using the test indicated in the legend. All statistical analyses were performed in Prism v9 (Graphpad Software).

2.6 Results

2.6.1 CRISPR screening identifies Herc1 as a modulator of Ara-C in AML cells

To better understand the factors that modulate Ara-C response in AML cells, we employed two different murine AML mouse lines that recapitulate the main clinical features observed in AML patients *in vivo* [9, 10]: the MA cell line where overexpression of the fusion protein MLL/AF9 (KMT2A/MLLT3) in sorted murine multipotent progenitors drives AML development [10], and the HM cell line, which involves the overexpression of the transcription factors Hoxa9 and Meis1 in murine lineage-negative progenitors [11]. We performed CRISPR-based genome-wide screening in both murine AML cell lines by transducing them with the GeCKO v2 sgRNA

library [12] and maintaining them in the presence of puromycin for 4 days to allow selection and proper genome editing [13] (**Fig. 2.1A**). Both MA and HM transduced cell lines were subsequently treated with either Ara-C IC₅₀ or with vehicle (H₂O) for 5 days before being processed for next-generation sequencing (NGS) analysis. DrugZ algorithm was used to monitor the relative abundance of a given sgRNA and identify genes whose knockout confer either resistance (red) or sensitivity (green) to Ara-C ($-2 < \text{NormZ-score} < 2$; [14]). In both cell lines, the deoxycytidine kinase *Dck* emerged as one of the top resistant genes while the dNTPase enzyme *Samhd1* scored as one of the top sensitizers (**Fig. 2.1B**), validating our CRISPR-based screening approach. To take into consideration the high heterogeneity between AML patients, we focused our attention on hits that were commonly identified in both MA and HM cell lines (**Fig. 2.1C**). Importantly, only 11 genes were providing resistance to Ara-C in both cell lines upon knockout (left panel, **Fig. 2.1C**), while 39 genes were common sensitizers in murine AML cells (right panel, **Fig. 2.1C**). KEGG analysis of these common sensitizers identified p53 signaling ($p=0.0089$), AMPK signaling ($p=0.0229$), and cell cycle ($p=0.0243$) as top enriched pathways (**Fig. 2.1D**). To gain further insight into these hits, we examined their expression profile in a panel of 188 human blood cancer cell lines. As expected, the transcriptional regulators *IKZF1* and *POU2AF1* were amongst the most expressed hits in this panel (**Fig. 2.1E**). Interestingly, the E3 ubiquitin (Ub) ligase *HERC1* scored third in this classification, suggesting a potential role in the pathobiology of AML. *Herc1* ranked 6 in MA cells (NormZ-score -3,88) and ranked 18 in HM cells (NormZ-score -4,02) (**Fig. 2.1C, not shown**). Since *HERC1* possesses an enzymatic activity, we focused our attention on this potential “druggable” target. Using a CRISPR-based competition assay [15], where our constitutively Cas9-expressing MA cell line was transduced with a vector that co-expresses both a sgRNA and mCherry (**Fig. 2.1F**), we monitored the relative abundance of transduced (mCherry⁺) and

untransduced cells (mCherry⁻) in control (vehicle) and Ara-C treated conditions (IC₅₀) via flow cytometry. We incorporated in this experimental design sgRNAs that targeted *Samhd1*, *Dck* and *non-targeting sgRNAs* as controls. As expected, targeting *Dck* in MA cells provided resistance to Ara-C (**Fig. 2.1G, red**), while knocking out *Samhd1* hypersensitizes MA cells to this chemotherapeutic agent (**Fig. 2.1G, green**). Interestingly, deletion of *Herc1* provides a similar phenotype to *Samhd1* deletion (**Fig. 2.1G, blue**), suggesting a potential role for this E3 Ub ligase in the modulation of Ara-C response *in vitro*.

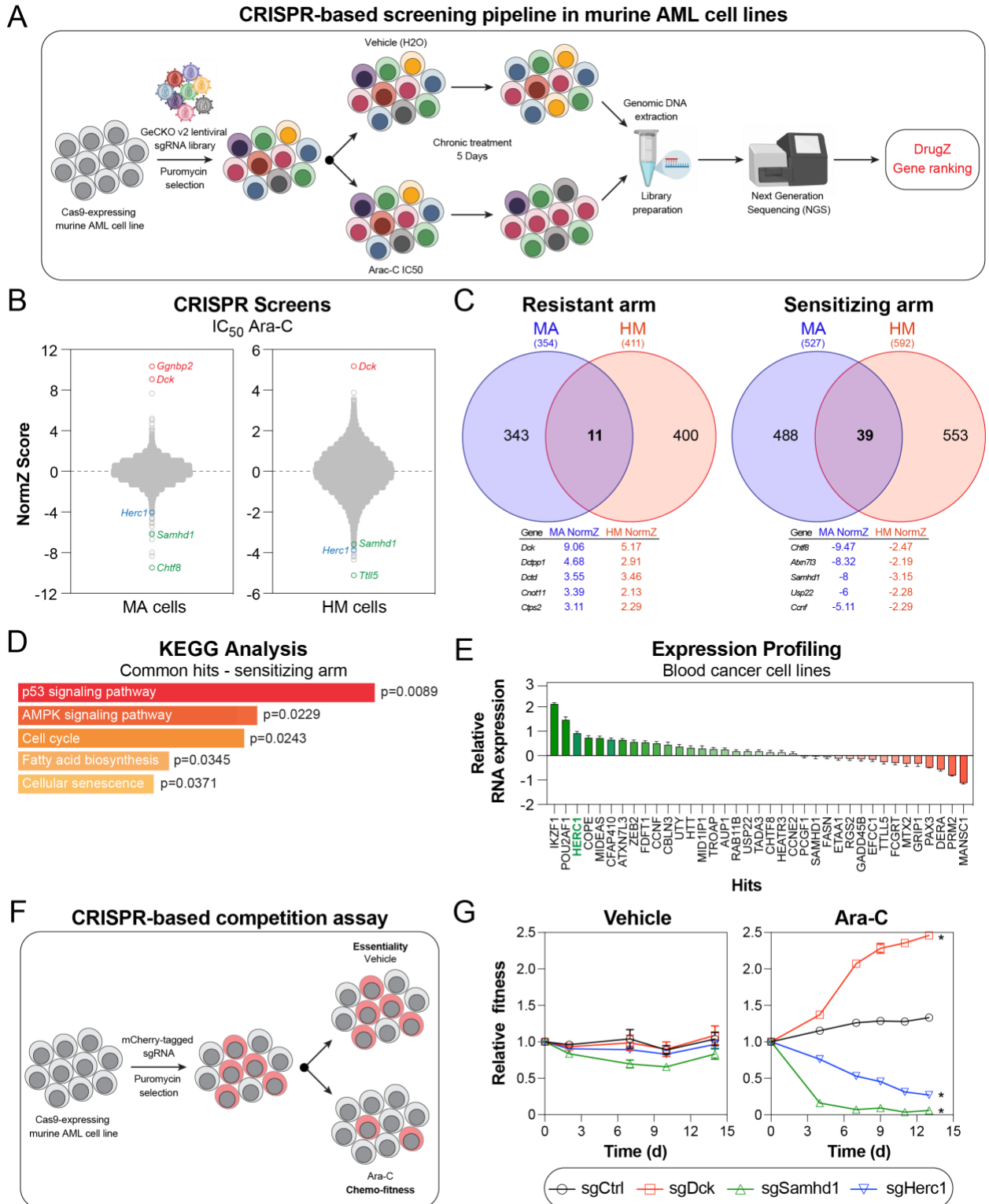


Figure 2. 1 CRISPR screen identifies HERC1 as modulator of Ara-C.

- (A) Schematic of our CRISPR/Cas9-based screening pipeline developed in murine AML cells.
- (B) Representation of CRISPR/Cas9 based dropout screen performed in MA and HM cells in the presence of Ara-C (IC₅₀).
- (C) Representation of overlapping genes which are providing sensitivity and resistance to Ara-C ($-2 < \text{NormZ-score} < 2$).
- (D) Pathway enrichment analysis of sensitizing genes using KEGG database.
- (E) Expression analysis of the 39 overlapping sensitizers in the hematopoietic and lymphoid tissues from the CCLE database (n=24).
- (F) Schematic of CRISPR-based competition assay.
- (G) Competitive growth assay \pm Ara-C (50 nM) or H₂O (Vehicle) in MA cells. Data are represented as the ratio of mCherry⁺ normalized to day 0 (three independent transductions). Significance was determined by two-way ANOVA followed by a Dunnett's test. *P \leq 0.05.

2.6.2 Loss of Herc1 increases the sensitivity of murine AML cell to nucleoside analogs *in vitro*

To further characterize the role of Herc1 in the modulation of nucleoside analogs (**Fig. 2.2A**), we generated Herc1 knock-out clones (#1 and #2) from murine MA cells (**Figs.S2.1A-B**), and we monitored their response to Ara-C using the cell titer glow (CTG) assay. We observed that loss of Herc1 led to a ~2-fold decrease in the IC₅₀ of MA cells to Ara-C (**Figs.2.2B-C**). We extended our analysis to another pyrimidine analog, gemcitabine (Gem, **Fig.2.2A**), which is used as frontline therapy in pancreatic cancers and has been proposed as salvation therapy for the treatment of relapsed AML patients [16, 17]. Strikingly, we noticed a similar trend in Herc1-

depleted MA cells exposed to Gem compared to control cells, with a ~2.4-fold decrease in their IC₅₀ to Gem (**Figs.2.2D-E**). Similarly, Herc1 knock-out MA cells were hypersensitized to the purine analog Fludarabine (Flu, **Fig.2.2A**), with a ~7-fold and ~3.5-fold decrease in the IC₅₀ to Flu for clone #1 and clone #2, respectively (**Fig.2.2F**). Importantly, we did not observe any significant difference in the response of Herc1-depleted MA cells to doxorubicin (Doxo) compared to control cells (**Fig.S2.1C**), suggesting that Herc1 specifically modulates the response of MA cells to nucleoside analogs. Next, we extended our approach to the HM cell line where we targeted Herc1 with two distinct sgRNAs (sg1 and sg2) (**Figs.S2.1A, S2.1D**). As previously observed, targeting Herc1 hypersensitized HM cells to Ara-C compared to control cells, resulting in a ~1.5-fold decrease in the IC₅₀ to Ara-C for both sgRNAs against Herc1 (**Figs.2.2G-H**). Altogether, our data indicate that targeting Herc1 improves the sensitivity of murine AML models to nucleoside analogs *in vitro*.

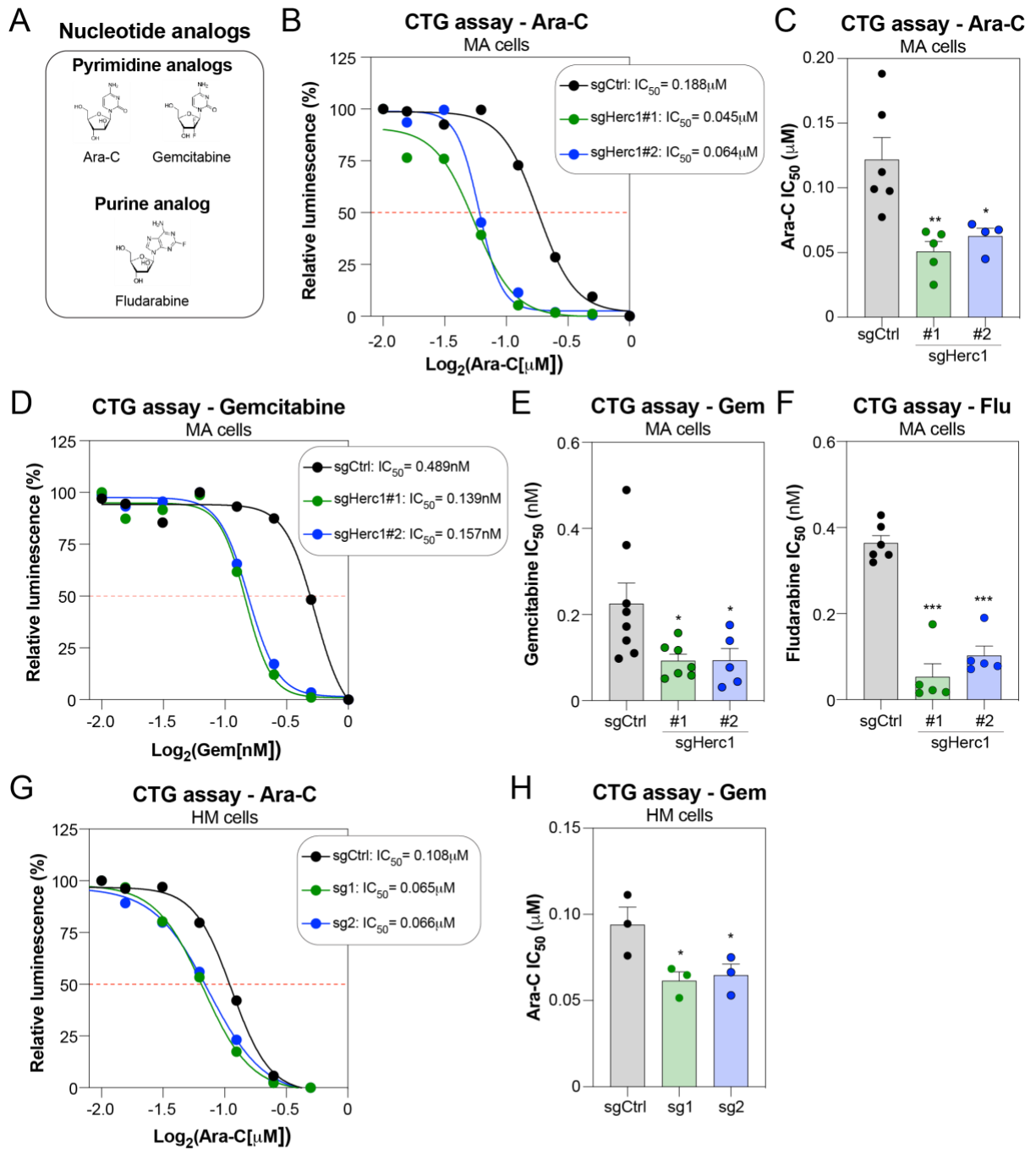


Figure 2. 2 Loss of Herc1 increases the sensitivity of murine AML cell to nucleoside analogs *in vitro*.

- (A) Representation of nucleoside analogs used for cell viability assays.
- (B) MA cells were seeded in quadruplicates into 96-well plates and treated with varying concentrations of Ara-C. The number of viable cells was measured after 72 h using the CellTiter-Glo Luminescent Cell Viability Assay. One of independent experiments is shown.
- (C) IC₅₀ concentrations of Ara-C in MA cells (n=6). Values are means \pm SEM. Significance was determined using one-way ANOVA followed by Dunnett's multiple comparisons test. *P \leq 0.05.
- (D) MA cells were seeded in quadruplicates into 96-well plates and treated with varying concentrations of Gemcitabine. The number of viable cells was measured after 72 h using the CellTiter-Glo Luminescent Cell Viability Assay. One of independent experiments is shown.
- (E) IC₅₀ concentrations of Gemcitabine in MA cells (n=8). Values are means \pm SEM. Significance was determined using one-way ANOVA followed by Dunnett's multiple comparisons test. *P \leq 0.05.
- (F) IC₅₀ concentrations of Fludarabine in MA cells (n=6). Values are means \pm SEM. Significance was determined using one-way ANOVA followed by Dunnett's multiple comparisons test. *P \leq 0.05.
- (G) HM cells were seeded in quadruplicates into 96-well plates and treated with varying concentrations of Ara-C. The number of viable cells was measured after 72 h using the CellTiter-Glo Luminescent Cell Viability Assay. One of independent experiments is shown.
- (H) IC₅₀ concentrations of Ara-C in HM (n=3). Values are means \pm SEM. Significance was determined using one-way ANOVA followed by Dunnett's multiple comparisons test. *P \leq 0.05.

2.6.3 Targeting the E3 Ub ligase Herc1 exacerbates Ara-C-induced apoptosis in AML cells

We further investigated the contribution of Herc1 in the modulation of Ara-C response by monitoring cell death using the presence of cells with fractional DNA content, designated as sub-G1 population [18]. This analysis revealed that targeting Herc1 led to a significant induction of sub-G1 population upon treatment of MA cells with Ara-C (200nM, **Fig.2.3A**). Of note, we observed no significant impact on Herc1-depleted MA cells at steady state (**Fig.2.3A**), highlighting the specific contribution of Herc1 in the response to nucleoside analogs. Flow cytometry analysis of murine MA cells by annexin V and DAPI staining confirmed the significant increase in the proportion of Herc1-depleted cells in apoptosis compared to control cells (**Figs.2.3B-C**). We made similar observations in HM cells, where we noticed a ~3-fold increase in the proportion of apoptotic cells that were depleted from Herc1 and exposed to Ara-C treatment, compared to non-targeting controls (sgCtrl) (**Fig.2.3D**). More importantly, annexin V/DAPI profiling of the U937 pro-monocytic human myeloid leukemia cell line revealed that loss of HERC1 resulted in a ~1.5-fold increase in the proportion of apoptotic cells following exposure to Ara-C (**Fig.2.3E**). Upon phosphorylation of Ara-C by the deoxycytidine kinase DCK, it competes directly with dCTP for incorporation into newly synthesized DNA, thereby causing a delay in replication fork progression and interfering with cellular proliferation. To better understand the role of Herc1 in the response of AML cells to Ara-C, we analyzed the progression of MA cells through the cell cycle in presence or absence of Ara-C. As previously observed [19], Ara-C treatment induced a marked decrease in the proportion of cells in G1 phase and a concomitant increase in the proportion of cells in S phase at 6h and 12h post-exposure (**Fig.2.3F**). Strikingly, loss of Herc1 increased the proportion of cells in G1 phase at early time point (6h) but had limited impact on the cell cycle distribution of MA

cells after 12h of treatment with Ara-C (**Fig.2.3F**), suggesting that Herc1 may be important in the early stage of Ara-C response.

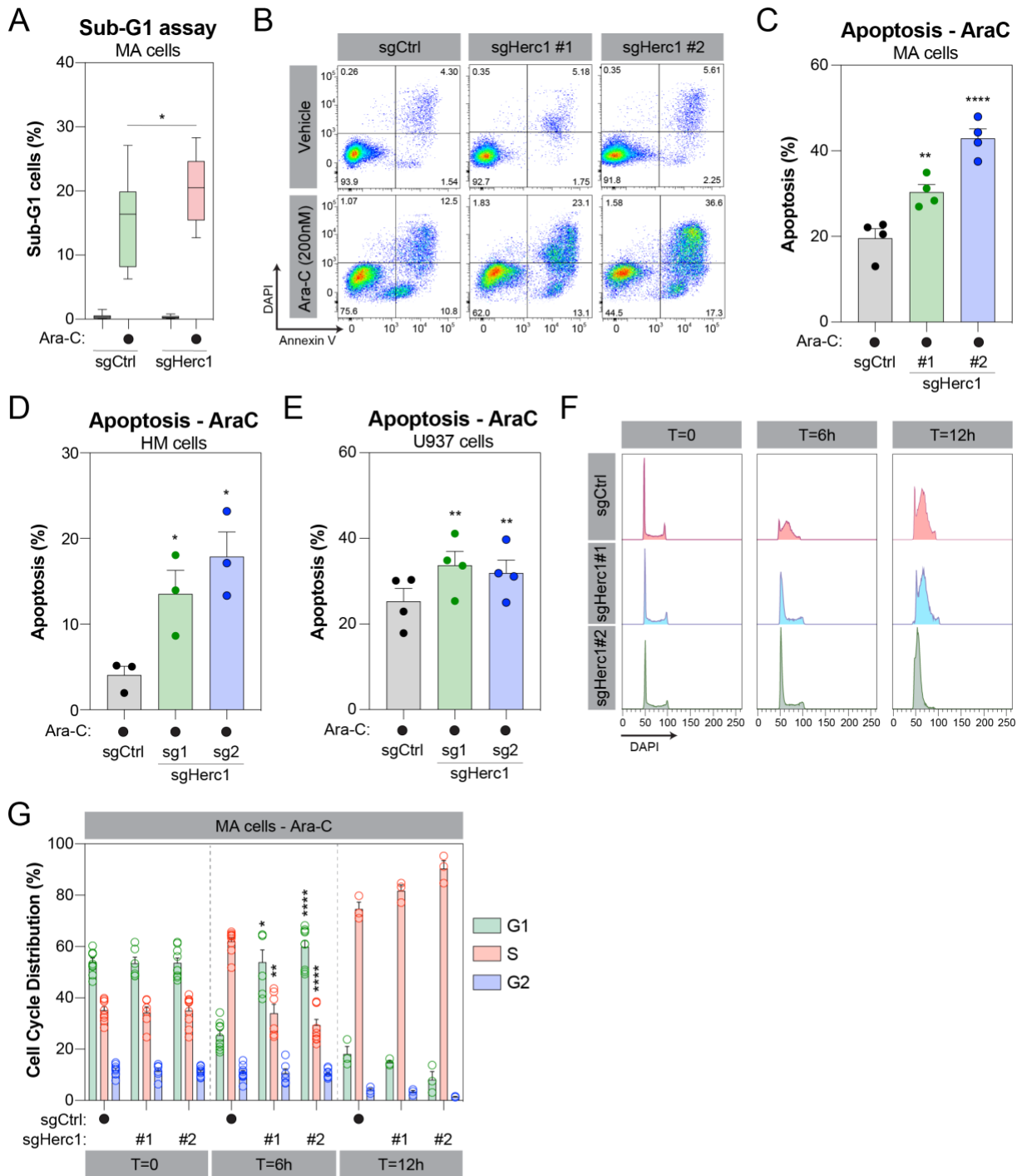


Figure 2. 3 Targeting the E3 Ub ligase Herc1 exacerbates Ara-C-induced apoptosis in AML cells.

(A) MA cells were plated for 24h in triplicates into 6-well plates and treated with \pm Ara-C (200 nM) or H₂O (Vehicle). Values are means \pm SEM, (n=3). Significance was determined by two-way ANOVA analysis followed by Holm-Šídák's multiple comparisons test. *P \leq 0.05.

(B) Representative flow cytometry analysis of MA cells treated with with \pm Ara-C (200 nM) or H₂O (Vehicle) for 24 hours and stained with annexin-V/DAPI.

(C) Representation of the annexin-V/DAPI analysis displayed in panel B for MA cells). Values are means \pm SEM, (n=4). Significance was determined using one-way ANOVA followed by Holm-Šídák's multiple comparisons test. **P \leq .005;**** P \leq 0.0001.

(D) Representation of the annexin-V/DAPI analysis displayed in panel B for HM cells. Values are means \pm SEM, (n = 3). Significance was determined using one-way ANOVA followed by Holm-Šídák's multiple comparisons test. *P \leq 0.05.

(E) Representation of the annexin-V/DAPI analysis displayed in panel B for U937 cells. Values are means \pm SEM, (n=4). Significance was determined using one-way ANOVA followed by Holm-Šídák's multiple comparisons test. *P \leq 0.05.

(F) Representative flow cytometry analysis of MA cells treated with \pm Ara-C (200 nM) or H₂O (Vehicle) for 0 hours, 6 hours and 12 hours stained with PI or DAPI for cell cycle analysis.

(G) Representation of the cell cycle analysis displayed in panel B for MA cells with \pm Ara-C (200 nM) or H₂O (Vehicle) for 0 hours and 6 hours (n=3 independent experiments with 3 technical replicates) and for 12 hours (n=1 independent experiment, 3 technical replicates). Significance was determined using mixed-effects analysis followed by Holm-Šídák's multiple comparisons test. *P \leq 0.05; **P $<$ 0.01; ****P $<$ 0.0001.

2.6.4 Herc1 controls Dck protein levels in murine AML cells

HERC1 is the largest member of the HERC family (4861 amino acids in *Homo sapiens* and 4859 amino acids in *Mus musculus*), structurally characterized by a Homologous to the E6AP Carboxyl Terminus (HECT) domain at its C-terminus and by a single SPRY (spl A and Ryanodine Receptor), WD40 (G protein β subunit like repeats), two RCC1-like domains (RLDs) as well as a putative BH3 domain (**Fig.2.4A**). HERC1 acts as a E3 ubiquitin ligase through its HECT domain [20], thereby promoting the ubiquitination and degradation of many cellular proteins related to DNA damage repair, cell proliferation and migration [21-26]. To gain better insight into how Herc1 impact Ara-C response in murine AML cells, we used a mass-spectrometry (MS)-based proteomic approach and quantified substrates that were stabilized upon Herc1 loss in MA cells. In total, we detected 3511 proteins that were differentially abundant between sgHerc1- and sgCtrl MA cells, including 96 that were significantly up- or down-regulated in Herc1-depleted cells ($p > 0.05$; **Fig.4B**, **Table 2.3**). Pathway enrichment analysis identified nucleotide metabolism, including pyrimidine salvage reactions (e.g., Dck, Uck2) and purine catabolism (e.g., Gda, Gpx1) as significantly enriched in this subset of proteins (**Fig.2.4C**). To ensure that these changes at the protein level are not resulting from transcriptional dysregulation, we performed a systematic RNA-seq analysis of both Herc1-depleted and control MA cells. Of note, 143 out of the 3511 targets identified by proteomics could not be quantified by RNA-seq. A limited portion of targets (10/106) were significantly up- or down-regulated at the RNA level ($\log_2FC_{\pm 1.5}$, $p < 0.05$; **Fig.2.4D**), including Staf1, Staf3, S100a8 and S100a9. To prioritize targets based on their relevance to Ara-C response, we focused our attention on the 40 MS targets that were significantly enriched in Herc1-depleted MA cells but did not result from major transcriptional changes in our RNA-seq analysis. To identify any relevant target for Ara-C response, we intersected them with our

CRISPR-based genome-wide screens data and identified 10 targets that scored significantly in at least one murine AML cell line (NormZ-score \pm 1.5, **Fig.2.4E**).

If Herc1 regulates the protein levels of a given target, we hypothesized that targeting this substrate by CRISPR should mimic Herc1 depletion and provide resistance to Ara-C. Interestingly, Dck emerged as the only substrate identified by MS that provided resistance to Ara-C in both MA and HM cells (**Fig.2.4E**). To validate our MS findings, we monitored Dck levels in Herc1-depleted MA and HM clones by western blot. Strikingly, lack of Herc1 resulted in a significant increase in the steady state protein levels of Dck in both MA and HM cells (**Figs.2.4F-G**). Importantly, these changes did not correlate with any significant alteration of *Dck* RNA levels as measured by qPCR in MA cells (**Fig.2.4H**). Altogether, these data suggest that Herc1 modulates Ara-C response by controlling Dck protein levels at steady state in murine AML cells.

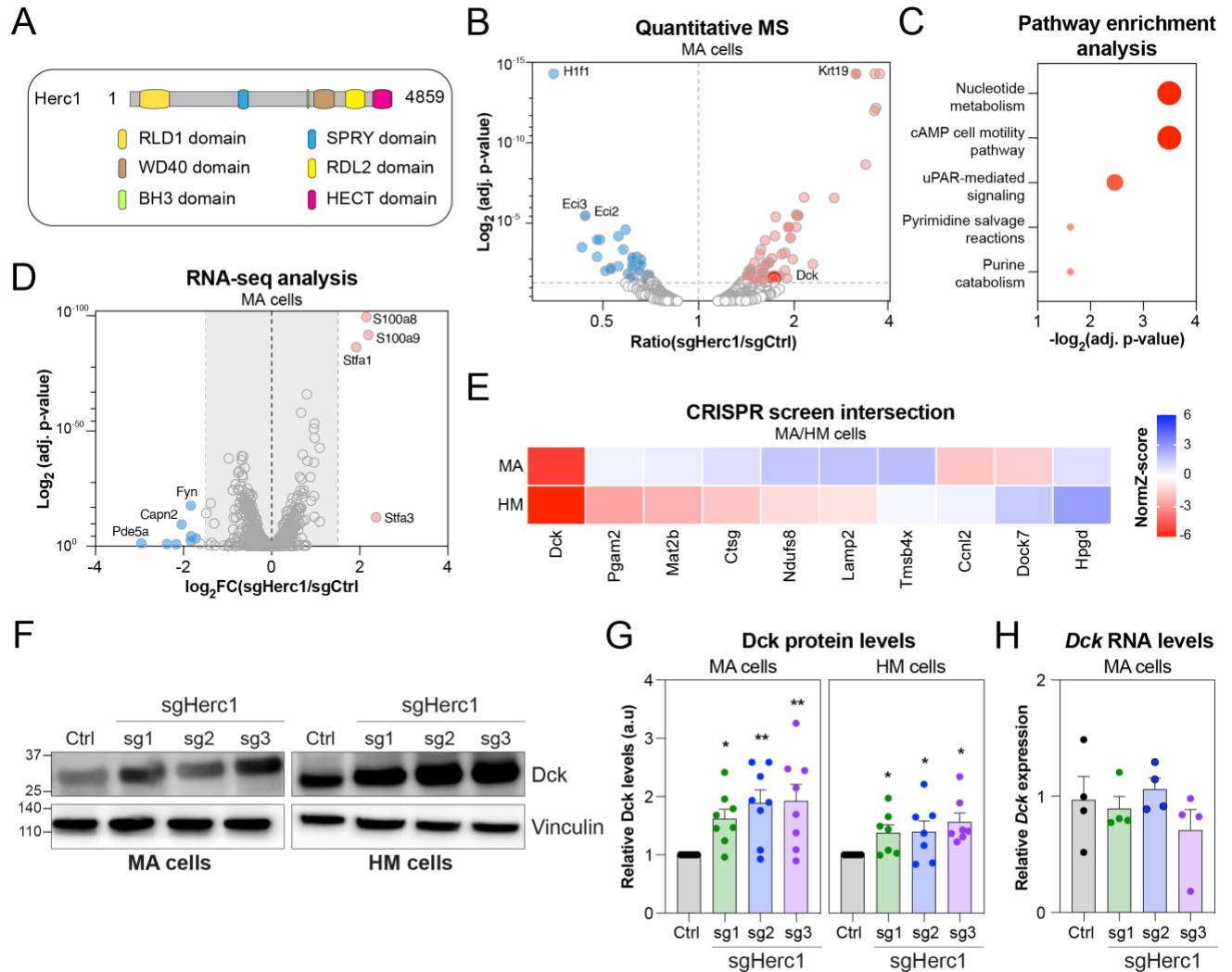


Figure 2. 4 Herc1 controls Dck protein levels in murine AML.

(A) Representation of the functional domains of HERC1 protein.

(B) Volcano plot showing protein abundance in sgHerc1-MA cells vs sgCtrl-MA cells. P-values are calculated using the t-test and corrected for multiple hypothesis testing with Benjamin-Hochberg method. Dashed line represents $p = 0.05$.

(C) Pathway enrichment analysis of on 106 proteins that are significantly abundant in sgHerc1-MA cells.

(D) Volcano plot showing differential expressed genes in sgHerc1-MA cells vs sgCtrl-MA cells. Dashed line represents \log_2FC of ± 1.5 .

(E) Integration of transcriptomic and proteomic data with CRISPR/Cas9 screen to identify potential targets of Herc1. Potential candidates which passed the following criteria of (1) greater protein abundance (> 1.5 -fold) (shown in B) and 2) no corresponding change in mRNA transcript abundance (<1.5 -fold) (shown in D).

(F) Assessment of Dck in Herc1-gene edited cells. Representative western blot of whole cell lysates shows Dck protein level in MA and HM-sgCtrl and sgHerc1-KO cells using 3 different sgRNAs. (G) Quantification of Dck Western blot as shown in F. Proteins are represented in arbitrary units (s.u.) normalized to sgCtrl. Values are means \pm SEM, $n = 8$ (MA) and $n=7$ (HM) independent replicates. Significance was determined using Wilcoxon signed-rank test. $*P\leq 0.05$; $**P<0.01$. (H) Quantitative PCR shows the mRNA levels of Dck in MA cells. Values are means \pm SEM, ($n=4$). Significance was determined using one-way ANOVA followed by Dunnett's multiple comparisons test. $*P\leq 0.05$; $**P<0.01$.

2.6.5 Targeting Herc1 modulates Ara-C response *in vivo*

To evaluate the pre-clinical relevance of our findings, we targeted Cas9-expressing MA cells with either sgCtrl coupled to BFP or sgHerc1 coupled to mCherry and mixed them in a 1:1 ratio before transplanting them into syngeneic sublethally irradiated C57BL6.J mice (**Fig.2.5A**). Peripheral blood (PB) was collected upon injection to monitor the initial mixed population (**Fig.2.5B**). MA cells were allowed to engraft for 14 days and analysed by PB extraction

before mice were treated with Ara-C for 6 days (**Fig.2.5A**). Mice were subsequently sacrificed, and bone marrow (BM) were harvested for flow cytometry analysis (**Fig.2.5B**). The presence of mCherry-positive MA cells was monitored in the PB after injection (d₁₄) and in the BM after Ara-C treatment (d₂₁). Interestingly, we observed a significant decrease in the percentage of mCherry-positive cells expressing sgHerc1 (**Fig.5C**). While the expected normalized ratio of mCherry-positive cells between d₂₁ and d₁₄ should be ~1, we observed a median ratio of 0.37 (**Fig.2.5C**), suggesting that Herc1-depleted MA cells are hypersensitive to Ara-C treatment *in vivo*. Importantly, cells sorted for BFP or mCherry expression before injection or after *in vivo* Ara-C treatment, preserved their differential Dck protein levels (**Fig.2.5D**). Altogether, our data point toward a model where Herc1 modulates Ara-C response in murine AML cells both *in vitro* and *in vivo*, by controlling Dck proteins steady state levels (**Fig.2.5E**).

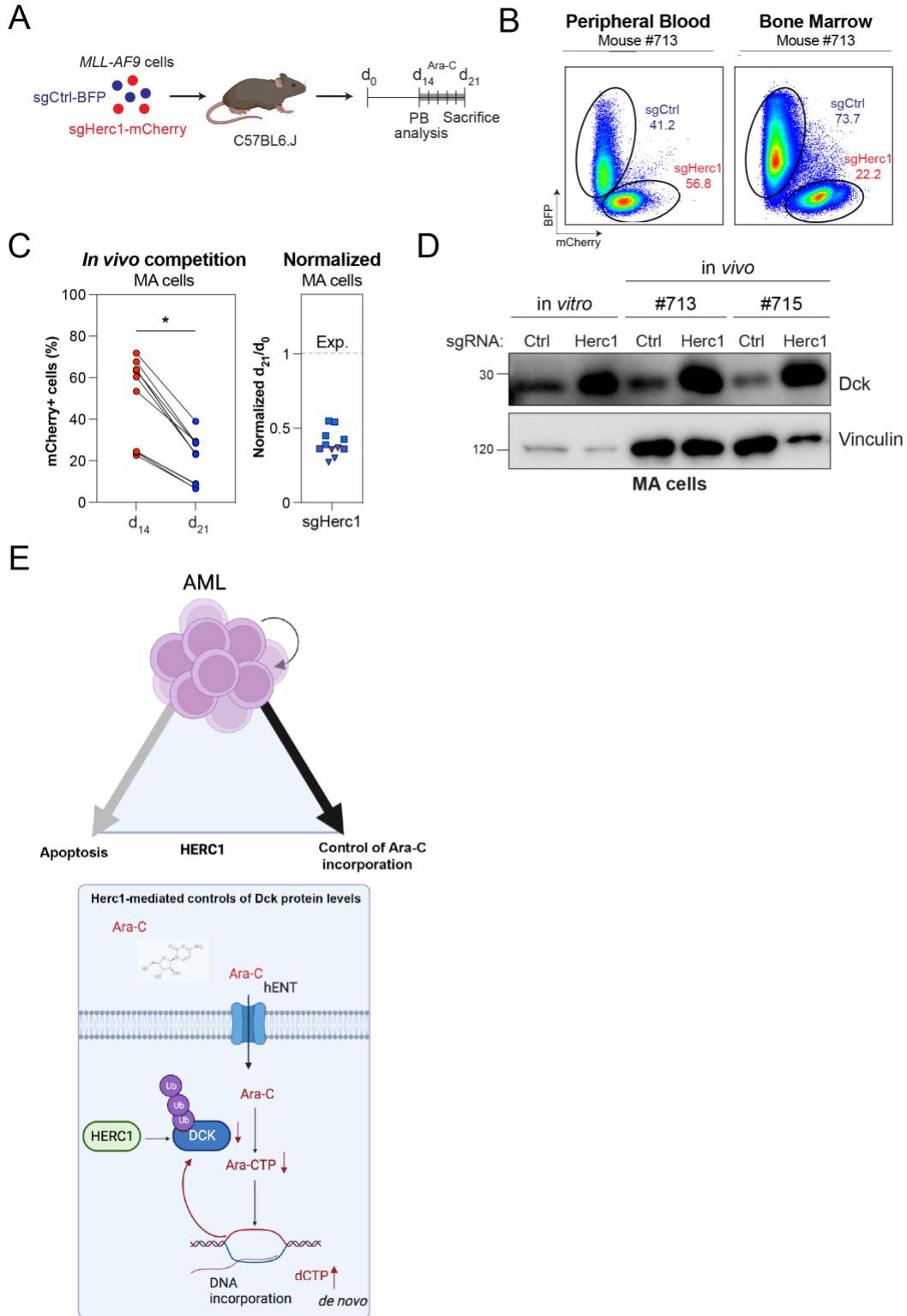


Figure 2. 5 Loss of Herc1 *in vivo* sensitizes AML to Ara-C.

(A) Schematic of *in vivo* competition experiment. sgHerc1-mCherry cells and sgCtrl-BFP cells were combined in 1:1 ratio prior transplantation. Mix of 1×10^6 cells was transplanted in sub-lethally irradiated C57BL6.J mice. MA cells were analyzed at indicated timepoints: *in vitro* (d0), PB- pre Ara-C treatment (d14), BM- post Ara-C (100mg/kg) treatment (d21).

(B) Representation of flow cytometry analysis of PB and BM before and after Ara-C treatment, as described in (A).

(C) Representation of *in vivo* competition experiment displayed in (B) for MA cells. Values represent 1 mouse ($n = 2$, independent experiments). Significance was determined using paired t-test. $*P \leq 0.0001$. MA cells were normalized to day 14 (PB), 2 independent experiments are indicated by the symbol shape.

(D) Assessment of DCK in Herc1-gene edited cells *in vitro*, and 2 mice. BFP⁺ and mCherry⁺ cells were sorted prior western blot analysis.

(E) Model of Herc1-mediated DCK regulation. Created with BioRender.com.

2.7 Discussion

CRISPR functional genomics in murine AML cells

Comprehensive CRISPR-based functional genomics screens have been powerful in identifying novel *in vitro* and *in vivo* genetic vulnerabilities in AML cells with therapeutic potential [27-32] In this study, we employed an *in vitro* CRISPR screen approach to identify genes that regulate murine AML cells susceptibility to Ara-C cytotoxicity. Systematic approaches have been previously employed to map the landscape of modulators to Ara-C [6, 7, 33], which identified loss of deoxycytidine kinase DCK as a major mechanism of resistance towards Ara-C treatment. Similar findings were observed in our CRISPR-based approach, where targeting of *Dck* provided

resistance to Ara-C in both MA and HM AML cell lines *in vitro*. Previous work has also shown that loss of SAMHD1 activity potentiates the cytotoxicity of Ara-C in AML cells [8], which was confirmed in our CRISPR screens, thereby validating our approach in murine AML cells.

Aside from these well-established modulators of Ara-C response in AML cells, our screen identified several members of the SAGA deubiquitylating module (SAGA-DUBm) as regulators of Ara-C cytotoxicity, including ATXN7L3 and USP22. Previous study revealed that inactivating the SAGA-DUBm sensitized AML cells to double-negative T cells-mediated cytotoxicity [34] suggesting a potential role for the SAGA-DUBm as resistance marker for different regimens used in the treatment of AML patients. More generally, these findings highlighted the importance of ubiquitylated/de-ubiquitylated events in the pathobiology of AML and its response to different stress conditions [35]. Here, we found that depleting the E3 ubiquitin ligase HERC1 increased susceptibility of both murine and human AML cells to Ara-C-induced apoptosis. More importantly, we showed that Herc1-depleted MA cells are hypersensitive to Ara-C treatment *in vivo*. Therefore, inhibiting HERC1 may enhance Ara-C response in AML patients and could potentially reduce the adverse toxicity associated with this harsh chemotherapeutic regimen, particularly in elder patients. A number of FDA-approved drugs that modulate ubiquitination has shown to improve patient outcome in a series of hematological malignancies, including multiple myeloma and mantle cell lymphoma. Adding proteasome inhibitors to salvage chemotherapy has been suggested for AML patients (age 60 to 75 years) [36] and should be further explored to improve the response to Ara-C and limit the development of resistance to this chemotherapeutic regimen.

Our approach further highlights the central role of nucleotide metabolism in predicting the outcome of Ara-C treatment in AML cells. Gene expression of DCK has been shown to be an indicator of chemotherapy response in AML treated with Ara-C [37] and alternatively spliced

forms of DCK have been linked to the development of resistance in AML patients [38-40]. Our study delineated additional level of regulation of murine Dck, namely at the post-translational levels by modulating the steady state protein levels of this critical enzyme by the E3 ubiquitin ligase Herc1. Our data suggest a highly complex network of regulatory processes controlling Dck levels and activity, thereby influencing the response of AML cells to Ara-C.

Our work demonstrates the power of CRISPR-based genome-wide screens to identify novel genetic vulnerabilities in AML cells and the importance of ubiquitin-proteasome system in modulating the response of AML cells to Ara-C both *in vitro* and *in vivo*.

2.8 DISCLOSURE OF CONFLICTS OF INTEREST

The authors declare that they have no conflict of interest

2.9 AUTHORSHIP CONTRIBUTIONS

Contribution: M.J. designed and completed most of the experiments presented in the manuscript, analyzed all data, and helped in writing the manuscript under the supervision of F.M. A.O. W.P. performed the genome-wide screen and helped preparing the libraries for NGS. M.J. analyzed the genome-wide screen. C.G.L. assisted in western blot experiments and cell viability assays. G.G.V. C.D., A.I., under the supervision of M.J. helped in the generation of the reagents for the experiments presented in this study. B.S. assistant with *in vivo* experiments and mouse colony management. D.Y. helped with analysis of RNA-seq data under the supervision of J.S. MJ, AO and FM conceived the study, designed the research, provided supervision, and wrote the manuscript with input from all the other authors.

2.10 Acknowledgments

We are grateful for assistance from the Genomics Platform at Institute for Research in Immunology and Cancer (IRIC) for RNA sequencing analysis, Université de Montréal, Montréal, Canada. Mass spectrometry analysis was performed by the Proteomics and Molecular Analysis Platform at the Research Institute of the McGill University Health Centre (RI-MUHC), Montreal, Canada. M.J. is a recipient of a Cole Foundation doctoral scholarship and Lady Davis Institute/TD Bank Studentship Award. Work in the FM laboratory was supported by a Transition Grant from the Cole Foundation and an internal Operating Fund from the Sir Mortimer B. Davis Foundation of the Jewish General Hospital.

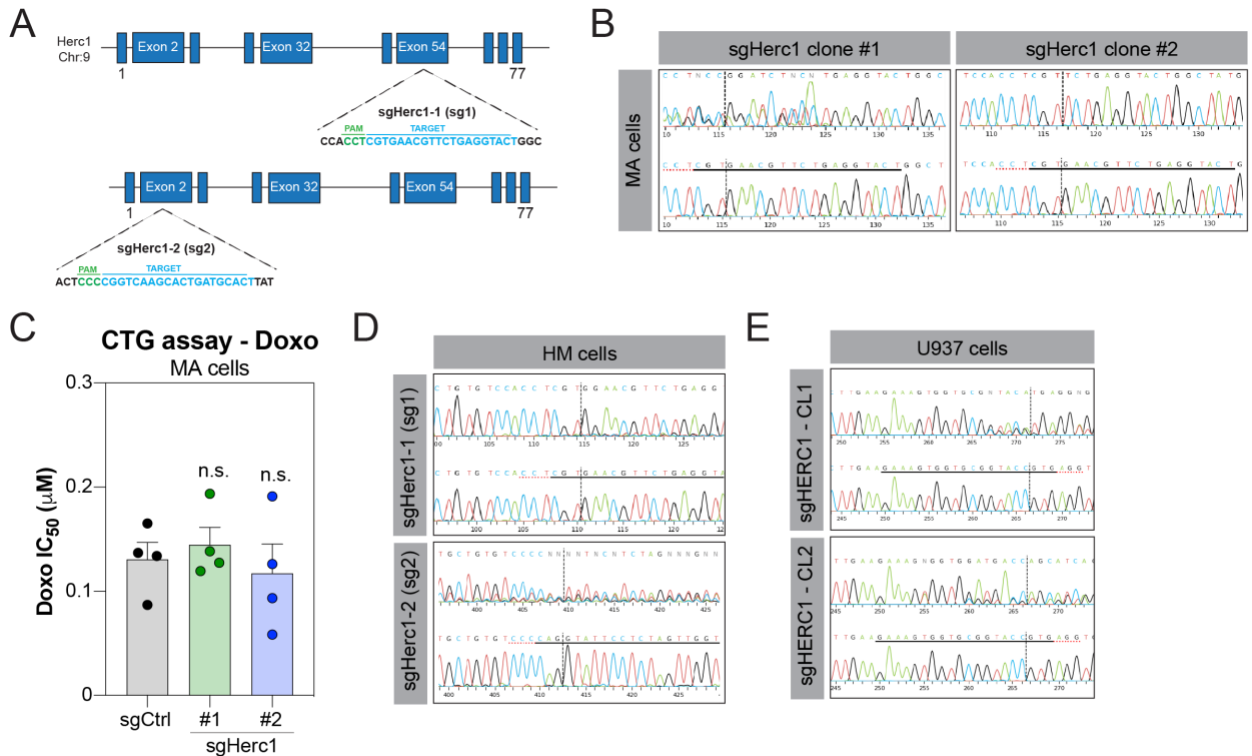
2.11 References

1. Dohner, H., et al., *Diagnosis and management of AML in adults: 2022 recommendations from an international expert panel on behalf of the ELN*. *Blood*, 2022. **140**(12): p. 1345-1377.
2. TCGA, *Genomic and Epigenomic Landscapes of Adult De Novo Acute Myeloid Leukemia*. *New England Journal of Medicine*, 2013. **368**(22): p. 2059-2074.
3. Ganzel, C., et al., *Very poor long-term survival in past and more recent studies for relapsed AML patients: The ECOG-ACRIN experience*. *Am J Hematol*, 2018. **93**(8): p. 1074-1081.
4. Yilmaz, M., et al., *Late relapse in acute myeloid leukemia (AML): clonal evolution or therapy-related leukemia?* *Blood Cancer Journal*, 2019. **9**(2): p. 7.
5. SEER. *Surveillance, Epidemiology, and End Results (SEER) Program (www.seer.cancer.gov) SEER*Stat Database: Incidence - SEER Research Data, 8 Registries, Nov 2021 Sub (1975-2020) - Linked To County Attributes - Time Dependent (1990-2020) Income/Rurality, 1969-2020 Counties, National Cancer Institute, DCCPS, Surveillance Research Program, released April 2023, based on the November 2022 submission*. 2021.
6. Rathe, S.K., et al., *Using RNA-seq and targeted nucleases to identify mechanisms of drug resistance in acute myeloid leukemia*. *Sci Rep*, 2014. **4**: p. 6048.
7. Ling, V.Y., et al., *Targeting cell cycle and apoptosis to overcome chemotherapy resistance in acute myeloid leukemia*. *Leukemia*, 2022.
8. Schneider, C., et al., *SAMHD1 is a biomarker for cytarabine response and a therapeutic target in acute myeloid leukemia*. *Nat Med*, 2017. **23**(2): p. 250-255.
9. Zuber, J., et al., *Mouse models of human AML accurately predict chemotherapy response*. *Genes and Development*, 2009.
10. Krivtsov, A.V., et al., *Transformation from committed progenitor to leukaemia stem cell initiated by MLL-AF9*. *Nature*, 2006. **442**(7104): p. 818-22.
11. Kroon, E., et al., *Hoxa9 transforms primary bone marrow cells through specific collaboration with Meis1a but not Pbx1b*. *EMBO Journal*, 1998.
12. Shalem, O., et al., *GeCKO v2. pooled libraries*. *Science*, 2014.
13. Shalem, O., et al., *Genome-scale CRISPR-Cas9 knockout screening in human cells*. *Science*, 2014.
14. Colic, M., et al., *Identifying chemogenetic interactions from CRISPR screens with drugZ*. *Genome Medicine*, 2019.
15. Girish, V. and J.M. Sheltzer, *A CRISPR Competition Assay to Identify Cancer Genetic Dependencies*. *Bio Protoc*, 2020. **10**(14): p. e3682.
16. Rao, A.V., et al., *Phase I evaluation of gemcitabine, mitoxantrone, and their effect on plasma disposition of fludarabine in patients with relapsed or refractory acute myeloid leukemia*. *Leuk Lymphoma*, 2008. **49**(8): p. 1523-9.
17. Nakano, Y., et al., *Gemcitabine chemoresistance and molecular markers associated with gemcitabine transport and metabolism in human pancreatic cancer cells*. *Br J Cancer*, 2007. **96**(3): p. 457-63.

18. Plesca, D., S. Mazumder, and A. Almasan, *DNA damage response and apoptosis*. *Methods Enzymol*, 2008. **446**: p. 107-22.
19. Tomic, B., et al., *Cytarabine-induced differentiation of AML cells depends on Chk1 activation and shares the mechanism with inhibitors of DHODH and pyrimidine synthesis*. *Sci Rep*, 2022. **12**(1): p. 11344.
20. Garcia-Gonzalo, F.R., et al., *Interaction between HERC1 and M2-type pyruvate kinase*. 2003.
21. Ali, M.S., et al., *The Downregulation of Both Giant HERCs, HERC1 and HERC2, Is an Unambiguous Feature of Chronic Myeloid Leukemia, and HERC1 Levels Are Associated with Leukemic Cell Differentiation*. *J Clin Med*, 2022. **11**(2).
22. Schneider, T., et al., *The E3 ubiquitin ligase HERC1 controls the ERK signaling pathway targeting C-RAF for degradation*. *Oncotarget*, 2018. **9**(59): p. 31531-31548.
23. Pedrazza, L., et al., *HERC1 deficiency causes osteopenia through transcriptional program dysregulation during bone remodeling*. *Cell Death Dis*, 2023. **14**(1): p. 17.
24. Zavodszky, E., et al., *Identification of a quality-control factor that monitors failures during proteasome assembly*. *Science*, 2021. **373**(6558): p. 998-1004.
25. Holloway, A., et al., *Resistance to UV-induced apoptosis by β -HPV5 E6 involves targeting of activated BAK for proteolysis by recruitment of the HERC1 ubiquitin ligase*. *International Journal of Cancer*, 2015.
26. Chong-Kopera, H., et al., *TSC1 stabilizes TSC2 by inhibiting the interaction between TSC2 and the HERC1 ubiquitin ligase*. *Journal of Biological Chemistry*, 2006.
27. Tzelepis, K., et al., *A CRISPR Dropout Screen Identifies Genetic Vulnerabilities and Therapeutic Targets in Acute Myeloid Leukemia*. *Cell Rep*, 2016. **17**(4): p. 1193-1205.
28. Manguso, R.T., et al., *In vivo CRISPR screening identifies Ptpn2 as a cancer immunotherapy target*. *Nature*, 2017. **547**(7664): p. 413-418.
29. Lin, K.H., et al., *Systematic Dissection of the Metabolic-Apoptotic Interface in AML Reveals Heme Biosynthesis to Be a Regulator of Drug Sensitivity*. *Cell Metab*, 2019. **29**(5): p. 1217-1231.e7.
30. Chen, X., et al., *Targeting Mitochondrial Structure Sensitizes Acute Myeloid Leukemia to Venetoclax Treatment*. *Cancer Discov*, 2019. **9**(7): p. 890-909.
31. Lin, S., et al., *An In Vivo CRISPR Screening Platform for Prioritizing Therapeutic Targets in AML*. *Cancer Discov*, 2022. **12**(2): p. 432-449.
32. Vujovic, A., et al., *In Vivo Screening Unveils Pervasive RNA-Binding Protein Dependencies in Leukemic Stem Cells and Identifies ELAVL1 as a Therapeutic Target*. *Blood Cancer Discov*, 2023. **4**(3): p. 180-207.
33. Kurata, M., et al., *Using genome-wide CRISPR library screening with library resistant DCK to find new sources of Ara-C drug resistance in AML*. *Scientific Reports*, 2016. **6**(1): p. 36199.
34. Soares, F., et al., *CRISPR screen identifies genes that sensitize AML cells to double-negative T-cell therapy*. *Blood*, 2021. **137**(16): p. 2171-2181.
35. Lei, H., et al., *Deubiquitinases in hematological malignancies*. *Biomarker Research*, 2021. **9**(1): p. 66.
36. Attar, E.C., et al., *Bortezomib added to daunorubicin and cytarabine during induction therapy and to intermediate-dose cytarabine for consolidation in patients with previously untreated acute myeloid leukemia age 60 to 75 years: CALGB (Alliance) study 10502*. *J Clin Oncol*, 2013. **31**(7): p. 923-9.

37. Wu, B., et al., *Deoxycytidine Kinase (DCK) Mutations in Human Acute Myeloid Leukemia Resistant to Cytarabine*. *Acta Haematol*, 2021. **144**(5): p. 534-541.
38. Veuger, M.J., et al., *High incidence of alternatively spliced forms of deoxycytidine kinase in patients with resistant acute myeloid leukemia*. *Blood*, 2000. **96**(4): p. 1517-24.
39. Veuger, M.J., et al., *Deoxycytidine kinase expression and activity in patients with resistant versus sensitive acute myeloid leukemia*. *Eur J Haematol*, 2002. **69**(3): p. 171-8.
40. Veuger, M.J., et al., *Functional role of alternatively spliced deoxycytidine kinase in sensitivity to cytarabine of acute myeloid leukemic cells*. *Blood*, 2002. **99**(4): p. 1373-80.
41. Mercier, F.E., et al., *In vivo genome-wide CRISPR screening in murine acute myeloid leukemia uncovers microenvironmental dependencies*. *Blood Adv*, 2022. **6**(17): p. 5072-5084.
42. Bolger, A.M., M. Lohse, and B. Usadel, *Trimmomatic: a flexible trimmer for Illumina sequence data*. *Bioinformatics*, 2014. **30**(15): p. 2114-20.
43. Dobin, A., et al., *STAR: ultrafast universal RNA-seq aligner*. *Bioinformatics*, 2013. **29**(1): p. 15-21.
44. Li, B. and C.N. Dewey, *RSEM: accurate transcript quantification from RNA-Seq data with or without a reference genome*. *BMC Bioinformatics*, 2011. **12**: p. 323.
45. Love, M.I., W. Huber, and S. Anders, *Moderated estimation of fold change and dispersion for RNA-seq data with DESeq2*. *Genome Biol*, 2014. **15**(12): p. 550.
46. Li, W., et al., *MAGeCK enables robust identification of essential genes from genome-scale CRISPR/Cas9 knockout screens*. *Genome Biol*, 2014. **15**(12): p. 554.
47. Szklarczyk, D., et al., *STRING v10: protein-protein interaction networks, integrated over the tree of life*. *Nucleic Acids Res*, 2015. **43**(Database issue): p. D447-52.

2.12 Supplementary data



Supplementary Figure 2. 1 Gene editing of Herc1.

(A) Schematic representation of CRISPR/Cas9 genetic targeting of murine HERC1.

(B) Chromatogram of CRISPR/Cas9-mediated mutations in MA cells. The PCR amplified DNA fragments containing the HERC1-sgRNA target sites from each MA clone was analyzed by sanger sequencing. Intact wildtype sequence is shown on the bottom of the panel.

(C) IC₅₀ concentrations of Doxorubicin of 4 independent repeated experiments in MA with either sgHerc1#1 and sgHerc1#2. Significance was determined by one-way ANOVA followed by a Dunnett's test.

(D) Chromatogram of CRISPR/Cas9-mediated mutations in HM cells. The PCR amplified DNA fragments containing the HERC1-sgRNA target sites from each HM cells was analyzed by sanger sequencing. Intact wildtype sequence is shown on the bottom of the panel.

(E) Chromatogram of CRISPR/Cas9-mediated mutations in U937 cells. The PCR amplified DNA fragments containing the HERC1-sgRNA target sites from each U937 clone was analyzed by sanger sequencing. Intact wildtype sequence is shown on the bottom of the panel.

Table 2-3 MS significant hits

Accession	Description	Abundance Clone/Control	p_{adj}
P05784	Keratin, type I cytoskeletal 18 OS=Mus musculus OX=10090 GN=Krt18 PE=1 SV=5	3.126009693	4.98286E-15
Q9QWL7	Keratin, type I cytoskeletal 17 OS=Mus musculus OX=10090 GN=Krt17 PE=1 SV=3	3.126009693	4.98286E-15
P35175	Stefin-1 OS=Mus musculus OX=10090 GN=Stfa1 PE=3 SV=1	3.585081585	4.98286E-15
P19001	Keratin, type I cytoskeletal 19 OS=Mus musculus OX=10090 GN=Krt19 PE=1 SV=1	3.126009693	4.98286E-15
P43275	Histone H1.1 OS=Mus musculus OX=10090 GN=H1-1 PE=1 SV=2	0.354945055	4.98286E-15
P35173	Stefin-3 OS=Mus musculus OX=10090 GN=Stfa3 PE=3 SV=1	3.723744292	4.98286E-15
Q00623	Apolipoprotein A-I OS=Mus musculus OX=10090 GN=Apoa1 PE=1 SV=2	3.615979381	6.7768E-13
P27005	Protein S100-A8 OS=Mus musculus OX=10090 GN=S100a8 PE=1 SV=3	3.576496674	1.03266E-12
P31725	Protein S100-A9 OS=Mus musculus OX=10090 GN=S100a9 PE=1 SV=3	3.361788618	2.23813E-09

Q61096	Myeloblastin OS=Mus musculus OX=10090 GN=Prtn3 PE=1 SV=2	2.152209493	2.48085E-07
Q8VED5	Keratin, type II cytoskeletal 79 OS=Mus musculus OX=10090 GN=Krt79 PE=1 SV=2	2.674347158	2.67538E-07
Q3UV17	Keratin, type II cytoskeletal 2 oral OS=Mus musculus OX=10090 GN=Krt76 PE=1 SV=1	2.025925926	2.98067E-06
P08730	Keratin, type I cytoskeletal 13 OS=Mus musculus OX=10090 GN=Krt13 PE=1 SV=2	2.049382716	3.39817E-06
P02088	Hemoglobin subunit beta-1 OS=Mus musculus OX=10090 GN=Hbb-b1 PE=1 SV=2	2.062590975	3.39817E-06
Q78JN3	Enoyl-CoA delta isomerase 3, peroxisomal OS=Mus musculus OX=10090 GN=Eci3 PE=1 SV=1	0.435916003	3.39817E-06
P02089	Hemoglobin subunit beta-2 OS=Mus musculus OX=10090 GN=Hbb-b2 PE=1 SV=2	2.062590975	3.39817E-06
Q9WUR2	Enoyl-CoA delta isomerase 2 OS=Mus musculus OX=10090 GN=Eci2 PE=1 SV=2	0.435916003	3.39817E-06
Q9D1A2	Cytosolic non-specific dipeptidase OS=Mus musculus OX=10090 GN=Cndp2 PE=1 SV=1	1.746537396	3.98304E-06
P02104	Hemoglobin subunit epsilon-Y2 OS=Mus musculus OX=10090 GN=Hbb-y PE=1 SV=2	2.029411765	1.7621E-05
Q922U2	Keratin, type II cytoskeletal 5 OS=Mus musculus OX=10090 GN=Krt5 PE=1 SV=1	1.91813602	1.7621E-05
Q9Z331	Keratin, type II cytoskeletal 6B OS=Mus musculus OX=10090 GN=Krt6b PE=1 SV=3	1.91813602	1.7621E-05
P50446	Keratin, type II cytoskeletal 6A OS=Mus musculus OX=10090 GN=Krt6a PE=1 SV=3	1.91813602	1.7621E-05
Q8BGZ7	Keratin, type II cytoskeletal 75 OS=Mus musculus OX=10090 GN=Krt75 PE=1 SV=1	1.91813602	1.7621E-05
P34022	Ran-specific GTPase-activating protein OS=Mus musculus OX=10090 GN=Ranbp1 PE=1 SV=2	0.594036697	2.55694E-05

Q9JJK7	Tropomodulin-2 OS=Mus musculus OX=10090 GN=Tmod2 PE=1 SV=2	1.741267788	6.151E-05
Q91VE6	MKI67 FHA domain-interacting nucleolar phosphoprotein OS=Mus musculus OX=10090 GN=Nifk PE=1 SV=1	0.562208398	6.47931E-05
Q2XU92	Long-chain-fatty-acid--CoA ligase ACSBG2 OS=Mus musculus OX=10090 GN=Acsbg2 PE=1 SV=1	1.949286846	8.33276E-05
P01027	Complement C3 OS=Mus musculus OX=10090 GN=C3 PE=1 SV=3	1.949286846	8.33276E-05
O35658	Complement component 1 Q subcomponent-binding protein, mitochondrial OS=Mus musculus OX=10090 GN=C1qbp PE=1 SV=1	0.488856937	0.000105402
Q3UA16	Kinetochore protein Spc25 OS=Mus musculus OX=10090 GN=Spc25 PE=2 SV=1	0.480274443	0.000106262
P24527	Leukotriene A-4 hydrolase OS=Mus musculus OX=10090 GN=Lta4h PE=1 SV=4	1.617105263	0.000115876
Q3UYH7	Beta-adrenergic receptor kinase 2 OS=Mus musculus OX=10090 GN=Adrbk2 PE=1 SV=2	0.43151171	0.000312185
Q9Z2W1	Serine/threonine-protein kinase 25 OS=Mus musculus OX=10090 GN=Stk25 PE=1 SV=2	0.577476715	0.00043315
P50543	Protein S100-A11 OS=Mus musculus OX=10090 GN=S100a11 PE=1 SV=1	1.571819425	0.000442325
Q8R1A4	Dedicator of cytokinesis protein 7 OS=Mus musculus OX=10090 GN=Dock7 PE=1 SV=3	1.873935264	0.000708529
Q99388	Component of Sp100-rs OS=Mus musculus OX=10090 GN=Csprs PE=2 SV=1	1.827089337	0.000859391
P28650	Adenylosuccinate synthetase isozyme 1 OS=Mus musculus OX=10090 GN=Adss1 PE=1 SV=2	1.563233377	0.000897273
P19467	Mucin-13 OS=Mus musculus OX=10090 GN=Muc13 PE=2 SV=1	0.482142857	0.001231633

Q9WVA4	Transgelin-2 OS=Mus musculus OX=10090 GN=Tagln2 PE=1 SV=4	0.640689089	0.001254343
Q9R226	KH domain-containing, RNA- binding, signal transduction- associated protein 3 OS=Mus musculus OX=10090 GN=Khdrbs3 PE=1 SV=1	0.616270146	0.0013588
P0CW03	Lymphocyte antigen 6C2 OS=Mus musculus OX=10090 GN=Ly6c2 PE=1 SV=1	1.698762036	0.001565969
Q8CG03	cGMP-specific 3',5'-cyclic phosphodiesterase OS=Mus musculus OX=10090 GN=Pde5a PE=1 SV=2	1.984195402	0.001722808
Q9R0L6	Pericentriolar material 1 protein OS=Mus musculus OX=10090 GN=Pcm1 PE=1 SV=2	0.618515563	0.001835723
P56959	RNA-binding protein FUS OS=Mus musculus OX=10090 GN=Fus PE=1 SV=1	0.658657829	0.001865237
O35892	Nuclear autoantigen Sp-100 OS=Mus musculus OX=10090 GN=Sp100 PE=1 SV=2	1.658503401	0.002755064
Q9QUH0	Glutaredoxin-1 OS=Mus musculus OX=10090 GN=GlrX PE=1 SV=3	1.665254237	0.002793883
P28293	Cathepsin G OS=Mus musculus OX=10090 GN=Ctsg PE=1 SV=2	1.496296296	0.002923671
P11103	Poly [ADP-ribose] polymerase 1 OS=Mus musculus OX=10090 GN=Parp1 PE=1 SV=3	0.654300169	0.003154439
Q91W10	Metal cation symporter ZIP8 OS=Mus musculus OX=10090 GN=Slc39a8 PE=1 SV=1	2.289473684	0.00356105
Q8BMK4	Cytoskeleton-associated protein 4 OS=Mus musculus OX=10090 GN=Ckap4 PE=1 SV=2	1.631105398	0.00356105
Q9D6F9	Tubulin beta-4A chain OS=Mus musculus OX=10090 GN=Tubb4a PE=1 SV=3	0.658974359	0.003825756
Q64314	Hematopoietic progenitor cell antigen CD34 OS=Mus musculus OX=10090 GN=Cd34 PE=1 SV=1	0.624084622	0.003955687
Q99LB6	Methionine adenosyltransferase 2 subunit beta OS=Mus musculus	1.622542595	0.004617877

	OX=10090 GN=Mat2b PE=1 SV=1		
O35215	D-dopachrome decarboxylase OS=Mus musculus OX=10090 GN=Ddt PE=1 SV=3	0.564516129	0.004902845
Q9JLQ0	CD2-associated protein OS=Mus musculus OX=10090 GN=Cd2ap PE=1 SV=3	0.526083762	0.006150428
Q8JZN7	Mitochondrial Rho GTPase 2 OS=Mus musculus OX=10090 GN=Rhot2 PE=1 SV=1	0.616326531	0.006233744
P11352	Glutathione peroxidase 1 OS=Mus musculus OX=10090 GN=Gpx1 PE=1 SV=2	1.586513995	0.006965235
P63328	Serine/threonine-protein phosphatase 2B catalytic subunit alpha isoform OS=Mus musculus OX=10090 GN=Ppp3ca PE=1 SV=1	0.529279279	0.006965235
P99029	Peroxiredoxin-5, mitochondrial OS=Mus musculus OX=10090 GN=Prdx5 PE=1 SV=2	1.456037515	0.007090133
Q8VBV7	COP9 signalosome complex subunit 8 OS=Mus musculus OX=10090 GN=Cops8 PE=1 SV=1	0.530148786	0.007090133
Q8BSK8	Ribosomal protein S6 kinase beta-1 OS=Mus musculus OX=10090 GN=Rps6kb1 PE=1 SV=2	1.874074074	0.008743493
Q62348	Translin OS=Mus musculus OX=10090 GN=Tsn PE=1 SV=1	0.649765991	0.009389354
P11835	Integrin beta-2 OS=Mus musculus OX=10090 GN=Itgb2 PE=1 SV=2	1.440533981	0.009389354
Q9DBJ1	Phosphoglycerate mutase 1 OS=Mus musculus OX=10090 GN=Pgam1 PE=1 SV=3	1.443337484	0.009389354
Q99PM9	Uridine-cytidine kinase 2 OS=Mus musculus OX=10090 GN=Uck2 PE=1 SV=1	0.514509804	0.009389354
P97315	Cysteine and glycine-rich protein 1 OS=Mus musculus OX=10090 GN=Csrp1 PE=1 SV=3	0.646544182	0.009389354
Q9Z0J0	NPC intracellular cholesterol transporter 2 OS=Mus musculus OX=10090 GN=Npc2 PE=1 SV=1	1.459324155	0.010156437

P57016	Ladinin-1 OS=Mus musculus OX=10090 GN=Lad1 PE=1 SV=1	1.594813614	0.012444449
Q3U0P1	Partner and localizer of BRCA2 OS=Mus musculus OX=10090 GN=Palb2 PE=1 SV=2	1.594813614	0.012444449
P05555	Integrin alpha-M OS=Mus musculus OX=10090 GN=Itgam PE=1 SV=2	1.551813472	0.014332747
Q9D1E6	Tubulin-folding cofactor B OS=Mus musculus OX=10090 GN=Tbcb PE=1 SV=2	0.60242915	0.014332747
Q9R111	Guanine deaminase OS=Mus musculus OX=10090 GN=Gda PE=1 SV=1	1.437192118	0.015748963
Q9CPQ1	Cytochrome c oxidase subunit 6C OS=Mus musculus OX=10090 GN=Cox6c PE=1 SV=3	0.695510204	0.016395016
P15864	Histone H1.2 OS=Mus musculus OX=10090 GN=H1-2 PE=1 SV=2	0.691983122	0.016665791
P20065	Thymosin beta-4 OS=Mus musculus OX=10090 GN=Tmsb4x PE=1 SV=1	1.41547619	0.01705744
P27046	Alpha-mannosidase 2 OS=Mus musculus OX=10090 GN=Man2a1 PE=1 SV=2	1.803834808	0.018398412
Q8VC88	Grancalcin OS=Mus musculus OX=10090 GN=Gca PE=1 SV=1	1.650750341	0.019830363
P17047	Lysosome-associated membrane glycoprotein 2 OS=Mus musculus OX=10090 GN=Lamp2 PE=1 SV=2	1.425245098	0.019830363
Q9QZD9	Eukaryotic translation initiation factor 3 subunit I OS=Mus musculus OX=10090 GN=Eif3i PE=1 SV=1	0.69579288	0.021972105
Q8K363	ATP-dependent RNA helicase DDX18 OS=Mus musculus OX=10090 GN=Ddx18 PE=1 SV=1	0.698548249	0.021972105
Q8VCC1	15-hydroxyprostaglandin dehydrogenase [NAD(+)] OS=Mus musculus OX=10090 GN=Hpgd PE=1 SV=1	1.433002481	0.0228071
P62737	Actin, aortic smooth muscle OS=Mus musculus OX=10090 GN=Acta2 PE=1 SV=1	0.612903226	0.02463852

P68134	Actin, alpha skeletal muscle OS=Mus musculus OX=10090 GN=Acta1 PE=1 SV=1	0.612903226	0.02463852
P68033	Actin, alpha cardiac muscle 1 OS=Mus musculus OX=10090 GN=Actc1 PE=1 SV=1	0.612903226	0.02463852
P63268	Actin, gamma-enteric smooth muscle OS=Mus musculus OX=10090 GN=Actg2 PE=1 SV=1	0.612903226	0.02463852
P04104	Keratin, type II cytoskeletal 1 OS=Mus musculus OX=10090 GN=Krt1 PE=1 SV=4	1.768613975	0.02463852
Q9D8T2	Gasdermin-D OS=Mus musculus OX=10090 GN=Gsdmd PE=1 SV=1	1.43236715	0.024646926
Q3UP87	Neutrophil elastase OS=Mus musculus OX=10090 GN=Elane PE=1 SV=1	1.520253165	0.025611211
P43346	Deoxycytidine kinase OS=Mus musculus OX=10090 GN=Dck PE=1 SV=1	1.726666667	0.026018971
Q9JJA7	Cyclin-L2 OS=Mus musculus OX=10090 GN=Ccnl2 PE=1 SV=1	1.90070922	0.027125294
Q6NZF1	Zinc finger CCCH domain- containing protein 11A OS=Mus musculus OX=10090 GN=Zc3h11a PE=1 SV=1	0.690713101	0.027943931
Q8K3J1	NADH dehydrogenase [ubiquinone] iron-sulfur protein 8, mitochondrial OS=Mus musculus OX=10090 GN=Ndufs8 PE=1 SV=1	1.583218707	0.029021227
Q9JHP7	Protein O-glucosyltransferase 2 OS=Mus musculus OX=10090 GN=Poglut2 PE=1 SV=1	1.73054755	0.031724628
Q3V0K9	Plastin-1 OS=Mus musculus OX=10090 GN=Pls1 PE=1 SV=1	1.600969305	0.031724628
P18181	CD48 antigen OS=Mus musculus OX=10090 GN=Cd48 PE=1 SV=1	0.678782756	0.033129408
Q9CXW3	Calcyclin-binding protein OS=Mus musculus OX=10090 GN=Cacybp PE=1 SV=1	0.712673611	0.036101366
P62900	60S ribosomal protein L31 OS=Mus musculus OX=10090 GN=Rpl31 PE=1 SV=1	0.705679862	0.036101366

Q8CFE2	Histone PARylation factor 1 OS=Mus musculus OX=10090 GN=Hpf1 PE=1 SV=1	0.689501779	0.036914992
P01942	Hemoglobin subunit alpha OS=Mus musculus OX=10090 GN=Hba PE=1 SV=2	1.477987421	0.037920174
P06467	Hemoglobin subunit zeta OS=Mus musculus OX=10090 GN=Hbz PE=2 SV=2	1.477987421	0.037920174
Q6ZWU9	40S ribosomal protein S27 OS=Mus musculus OX=10090 GN=Rps27 PE=1 SV=3	0.686886708	0.039862647
P61358	60S ribosomal protein L27 OS=Mus musculus OX=10090 GN=Rpl27 PE=1 SV=2	0.694380293	0.042319706
O70250	Phosphoglycerate mutase 2 OS=Mus musculus OX=10090 GN=Pgam2 PE=1 SV=3	1.369119421	0.042319706
P56960	Exosome component 10 OS=Mus musculus OX=10090 GN=Exosc10 PE=1 SV=2	0.628184713	0.042319706
P62281	40S ribosomal protein S11 OS=Mus musculus OX=10090 GN=Rps11 PE=1 SV=3	0.720136519	0.048439825
P11680	Properdin OS=Mus musculus OX=10090 GN=Cfp PE=1 SV=2	1.54047619	0.049965984

Table 2-4 Overlap proteomics and RNA seq

Protein	Proteomics Abundance Clone/Control >1.5	Proteomics padj	log2FC RNA seq	RNA seq padj
Stfa3	3.723744292	4.98286E-15	2.37030126	2.22514E-13
Stfa1	3.585081585	4.98286E-15	1.91701683	4.13432E-87
S100a8	3.576496674	1.03266E-12	2.14742938	3.2863E-100
S100a9	3.361788618	2.23813E-09	2.19464717	2.20727E-92
Krt17	3.126009693	4.98286E-15	-0.4510165	NA
Slc39a8	2.289473684	0.00356105	-1.4836489	4.42423E-15
Prtn3	2.152209493	2.48085E-07	0.43007618	4.59595E-10
Hbb-y	2.029411765	1.7621E-05	-2.3754867	0.100169435
Pde5a	1.984195402	0.001722808	-2.9596188	0.062396282
C3	1.949286846	8.33276E-05	0.36045347	6.34827E-07

Krt5	1.91813602	1.7621E-05	-0.0803426	NA
Ccnl2	1.90070922	0.027125294	-0.2293521	0.015740408
Rps6kb1	1.874074074	0.008743493	-0.0682318	0.495664609
Dock7	1.873935264	0.000708529	0.11486396	NA
Man2a1	1.803834808	0.018398412	0.18443558	0.023173193
Gba	1.798898072	0.130007166	0.20570522	0.07702783
Ppp1r21	1.752336449	0.189816042	0.35487218	0.000489785
Cndp2	1.746537396	3.98304E-06	1.09201372	1.78038E-43
Pdlim7	1.74248927	0.089671662	0.01146032	0.985938865
Poglut2	1.73054755	0.031724628	0.75637044	3.29364E-12
Dck	1.726666667	0.026018971	0.1998507	0.028088768
Ly6c2	1.698762036	0.001565969	0.80893988	9.83292E-38
Mrgbp	1.6904474	0.234364446	-0.0643789	0.726598678
Ociad2	1.675753228	0.272934014	0.68428615	0.000256372
Inf2	1.673942701	0.293309932	0.07864283	0.714721266
Glrx	1.665254237	0.002793883	0.48353851	4.92251E-06
Ndc1	1.664981037	0.173415194	0.14896751	0.031047346
Capn2	1.664391354	0.147011762	-2.0462998	3.26438E-10
Cebpe	1.663421419	0.179841898	0.44608115	2.62731E-07
Sp100	1.658503401	0.002755064	1.09064004	2.34019E-11
Gca	1.650750341	0.019830363	0.2516482	9.19356E-05
Arsb	1.640522876	0.151207466	0.70862865	4.04616E-22
Zadh2	1.638888889	0.297542208	0.96998997	6.07018E-54
Commd1	1.636010363	0.162488128	0.16230047	0.478048812
Ckap4	1.631105398	0.00356105	0.96273794	1.68932E-22
Mat2b	1.622542595	0.004617877	0.40831943	7.15915E-10
Strn	1.617801047	0.310574739	-0.038746	0.808321309
Lta4h	1.617105263	0.000115876	0.70386997	1.62695E-40
Surf4	1.615384615	0.152229631	0.34263605	2.57767E-14
Snx32	1.606232295	0.293461048	0.08778857	0.915285544
Pls1	1.600969305	0.031724628	-1.8301833	4.10323E-05
Pycr1	1.600247525	0.124692777	0.42367169	0.000508481
Syk	1.599184783	0.341138891	0.33686149	4.93103E-08
Palb2	1.594813614	0.012444449	0.01983644	0.879389215
Scai	1.59469697	0.355779204	-0.2031735	0.323102935
Gpx1	1.586513995	0.006965235	0.37906145	4.3578E-07
Ndufs8	1.583218707	0.029021227	0.09485944	0.540063621
Cpt2	1.58089172	0.382615673	-0.0376503	0.879110709
Vkorc111	1.572916667	0.162488128	0.00168893	0.984364839

S100a11	1.571819425	0.000442325	0.39942511	4.35184E-07
Endod1	1.564720812	0.151207466	0.37186439	2.1373E-09
Adssl1	1.563233377	0.000897273	0.56404626	1.4036E-13
Ctdp1	1.5626703	0.151207466	0.89653915	1.61748E-20
Itgam	1.551813472	0.014332747	0.53061215	4.67876E-09
Cfp	1.54047619	0.049965984	0.36906917	4.70356E-05
Ldlrap1	1.529784537	0.151207466	0.36517884	5.7459E-05
Cmssl	1.525622255	0.24144917	-0.200892	0.145999244
Amdhd2	1.521970706	0.522826184	0.39827814	0.00112131
Exoc2	1.520754717	0.233294445	0.07659257	0.563297522
Elane	1.520253165	0.025611211	0.62425929	3.38677E-17
Arfgef1	1.518806744	0.514219123	0.2815975	2.1527E-05
Fgfr1op2	1.513108614	0.344776919	0.09694282	0.192989334

3 Chapter 3: Importance of the mitochondrial transporter SLC25a19 in AML

Preface to the manuscript

While there is a need to improve the cytotoxic treatment of AML in general, there is also urgent need to identify alternative AML vulnerabilities. Like HSCs, AML reside in the BM microenvironment. Experimental evidence points towards a role of the microenvironment in regulating AML survival through cell homing, metabolic reprogramming, and immune evasion [192, 327] [175, 328]. While numerous studies have adapted large-scale CRISPR screens *in vitro*, and more recently *in vivo*, comparative CRISPR-based screens evaluating loss of immunity have so far not been performed in AML. To better understand genetic factors influencing AML survival, I developed a focused CRISPR/Cas9 library covering several categories of AML vulnerabilities (i.e., metabolic, cell-adhesion, immune). I performed *in vivo* CRISPR screening using the murine syngeneic MLL/AF9 AML model transplanted in parallel into immune-competent C57/Bl6 mice and immune deficient NSG mice. Using this approach, I identified the mitochondrial thiamine transporter *Slc25a19* as novel dependency in immune competent mice. *Slc25a19* is in the inner membrane of mitochondria and transports thiamine pyrophosphate (TPP) inside, where it is needed as cofactor in the TCA cycle. The identification of *Slc25a19* highlights a novel link between thiamine metabolism and the immune response.

***In vivo* CRISPR/Cas9 systematic mapping uncovers *SLC25a19* as
potential immune regulator in murine leukemia.**

Manuscript in progress

Maja Jankovic^{1,2}, Wei Lam Poon^{1,2}, Yi Ding³, Constance Desombre¹, Jiantao Shi³, Alexandre Orthwein^{1,2,4,5}, and Francois Mercier^{1,2,6}

Affiliations of Authors: ¹ Lady Davis Institute for Medical Research, Segal Cancer Centre, Jewish General Hospital, Montréal, Canada; ² Division of Experimental Medicine, McGill University, Montreal, Canada; ³ State Key Laboratory of Molecular Biology, Shanghai Institute of Biochemistry and Cell Biology, University of Chinese Academy of Sciences, Shanghai, China
⁴ Gerald Bronfman Department of Oncology, McGill University, Montréal, Canada; ⁵ Department of Radiation Oncology, Winship Cancer Institute, Emory University, Atlanta, USA; ⁶ Department of Medicine, McGill University, Montréal, Canada;

co-corresponding authors

Running title: Slc25a19 in acute myeloid leukemia

Address correspondence to:

Francois Mercier, M.D.

Lady Davis Institute, Segal Cancer Centre

Jewish General Hospital

Montreal, Quebec, H3T 1E2 Canada

e-mail: francois.mercier@mcgill.ca

3.1 Abstract

Acute myeloid leukemia (AML) is a hematological malignancy characterized by aberrant self-renewal and a block in the differentiation of myeloid progenitors. AML originates from the bone marrow microenvironment (BME) and is genetically and cellularly heterogeneous, which makes it extremely difficult to target. Advancements in immunotherapies in AML have been relatively slow compared to various cancers due to intrinsic features of AML, such as low mutational burden and the lack of specific cell surface makers. The role of the immune system in the progression of AML needs to be better understood, particularly regarding novel targeted therapies. To pinpoint the critical dependencies of AML cells *in vivo*, we curated a focused CRISPR/Cas9 screen to target specific *in vivo* dependencies in the syngeneic MLL-AF9 AML mouse model under varying levels of immunity. We found five new potential genetic candidates (*Slc25a19*, *Ankrd52*, *Csf3r*, *Copg1*, *Cflar*) which have not been described in AML in the context of immune vulnerability. *Slc25a19*, a mitochondrial thiamine transporter, was the only metabolic candidate highly essential in immune-competent mice. These data suggest that metabolic adaptations may be important for AML growth in an immune proficient environment.

3.2 Introduction

Acute myeloid leukemia (AML) is a hematological malignancy characterized by the rapid accumulation of clonal myeloid progenitors. The curative treatment for AML consists of a combination of cytarabine (Ara-C) and anthracycline [1]. Sequencing technologies have reshaped our understanding of the disease and have led to the generation of novel targeted therapies, including the FLT3 tyrosine kinase inhibitor (TKIs), IDH1 and IDH2 inhibitors, BCL-2 inhibitor venetoclax [2-6]. Despite the introduction of novel targeted therapies, the 5-year overall survival rate remains low at 30% [7]. While immunological treatments have succeeded in various solid cancers, their efficacy in AML has been somewhat modest, as ongoing trials suggest [8]. However, there is a glimmer of hope from preclinical research, which has unveiled the potential of the "don't eat me" signal—the CD47/SIRP α axis. This axis has entered clinical trials for AML treatment [9-14]. Nonetheless, a critical gap exists in comprehending the specific immune regulatory mechanisms unique to AML *in vivo* and devising more potent strategies for targeting the disease.

To effectively eliminate leukemic cells, it is crucial to gain a deeper understanding of the distinct characteristics exhibited by AML that are not influenced by mutations. AML cells reside in the bone marrow and are organized hierarchically with the leukemic stem cells (LSC) at the apex, sustaining the disease [15, 16]. Within the bone marrow, LSCs respond to the cues of the bone marrow microenvironment, in which they often manipulate their environment to nurture their growth and protect them from chemotherapy [17]. These adaptive mechanisms include abnormal metabolic rewiring [18], nutrient salvage [19, 20], cytokine signalling [21], and immune evasion [11], all of which contribute to sustaining the growth and survival of LSCs.

A powerful approach for identifying essential genes regulating immune-specific processes of AML is through CRISPR/Cas9 genetic screening. CRISPR/Cas9 genetic screenings have been powerful in identifying crucial genes for AML growth *in vitro*. More recently, our group has developed a systematic CRISPR/Cas9 screening pipeline for identifying essential genes *in vivo* and found essential genes related to oxidative phosphorylation (OXPHOS), the microenvironment, and immune regulation [22]. In this study, our objective was to curate a CRISPR/Cas9-based library designed to target specific groups of genes associated with *in vivo* processes in AML. We conducted a CRISPR/Cas9 screen in a murine model of AML driven by the MLL-AF9 (KMT2A-MLLT3) fusion gene, both in the presence and absence of the immune response. Through this screening, we successfully identified five previously unknown genes involved in the immune response in AML. Notably, we discovered the mitochondrial transporter Slc25a19, which establishes a connection between mitochondrial metabolism and immune regulation in the context of AML. This finding highlights the potential significance of this gene in modulating the immune response in AML and suggests a novel avenue for further research and potential therapeutic interventions.

3.3 Materials and methods

3.3.1 Mice

Rosa26-CAG-Cas9/GFP knockin mice were used for constitutive Cas9 gene expression (stock no. 024858). Immunodeficient NOD-scid IL2Rgnull-3/GM/SF (NSGS) mice used for genetic screening were obtained from the Jackson Laboratory (stock no. 013062). Animal experiments were approved by the institutional review board of McGill University.

3.3.2 Generation of constitutive MLL/AF9-Cas9 (MA-Cas9) and HoxA9-Meis1-Cas9 (HM-Cas9) AML cell line

The KMT2A/MLLT3 (MLL/AF9) and HOXA9/MEIS1 retroviral leukemia models have been described previously [23, 24]. Lineage-Sca-1⁺C-kit⁺ hematopoietic progenitor cells (LSKs) from a male Cas9-GFP^{+/-} donor mice were sorted in RPMI-1640 media with 10% fetal bovine serum (fetal bovine serum, Wisent Bio Products and Hyclone) supplemented with cytokines mSCF (10 ng/mL, biolegend, Cat.#579706), mIL3 (5 ng/mL, biolegend, Cat.# 575506) and mIL6 (10 ng/mL, biolegend, Cat.# 575702) and 100 units/mL penicillin/streptomycin at 37 °C with 5% CO₂. LSKs were transduced with a MSCV-MLL/AF9-IRES-GFP (MA) or MSCV-HoxA9-IRES-Meis1 (HM) construct. After transduction, cells were passaged for 3-4 weeks until uninfected cells ceased proliferating overtime. After passaging the cells were injected intravenously into sublethally irradiated C57BL/6J recipients. After the primary recipients developed clinical signs of AML, the bone marrow leukemic cells were isolated and propagated in RPMI-1640 media with mSCF 10 ng/mL (biolegend, Cat.#579706), mIL3 5 ng/mL (Biolegend, Cat.#575506), 10% (fetal bovine serum, Wisent Bio Products and Hyclone) and 100 units/mL penicillin/streptomycin at 37 °C with 5% CO₂, to establish the lines used in this study [22].

3.3.3 sgRNA library generation for focused CRISPR screen

To design the focused CRISPR libraries, we targeted protein-coding transcripts using the GPP sgRNA Design tool [25, 26]. We selected 10 sgRNAs per gene, and this resulted in a murine library containing 1260 sgRNAs. Furthermore, we selected 900 control sgRNAs that do not target the genome (sgCtrls) [27]. The sgRNA oligo design for the array synthesis was followed as described

in [28]. Briefly, each sgNRA 20-mer was flanked by primer sequences and BsmBI sites for subsequent PCR cloning into lentiGuide-Puro vector [27]. Controls and sgRNAs were designed with different set of PCR primers and retrieved from master pool using their unique primer pair.

Primer Set; Forward Primer, 5'-3'; Reverse Primer, 5'-3' In vivo library 1;
CCGTCATTCTACGCGGGATGTTAT, TATCGTCTTGCGGCAGTATGCGAT
sgControls; CCACTCTCGTTTAGTCGGAATCAG, CGATTATGGCACTAGAATGCGGCT

PCR retrieval was performed using 45 μ L Accuprime Pfx supermix (ThermoFisher, Cat#123440400.5 μ L Oligo pool (20 ng), 1 μ L of primer mix at a final concentration of 0.5 μ M and 5 μ L water. The PCR cycling condition was as follows. Hot start: 95°C for 5 min; PCR reaction: 95°C (15 s), 55°C (15 s), 72°C (15 s) cycles with 15 s per step for 15 cycles; final extension: 72°C for 2 min. PCR product was gel extracted (Qiagen, Cat.#28704) and quantified using UV-Vis Spectrophotometer (Nanodrop2000). To clone PCR products into the lentiviral sgRNA expression vector LentiGuide-puro, the following Golden Gate reaction mixture was used. PCR Amplicon of sgRNA insert 4.3 ng, linearized LentiGuide-puro plasmid 150 ng, Esp3I 10 U (ThermoFisher, Cat.#ER0451), T7 DNA ligase 3,000 U (New England Biolabs, Cat.#M0318S), ATP 10 mM, total reaction volume was 20 μ L. Esp3I is a type of BsmBI that works best at a temperature of 37°C. The process was carried out using the following conditions. For the Golden Gate ligation process, the reaction mixture was pre-incubated at 37°C for 2 hours without T7 ligase. After this initial incubation, T7 ligase was added and the mixture was incubated at a cycle of 20°C for 20 minutes and 37°C for 5 minutes, repeating this cycle 10 times. The ligation product was ethanol precipitated and ~30 ng was electroporated (Biorad) into 20 μ L of ElectroMAX Stbl4 competent bacteria per manufacturer's instructions (ThermoFisher, Cat.#11635018). The electroporated bacterial was

recovered in 500 μ L of SPC media at 30°C for 90 min. A small amount of the bacterial culture was plated on 10 cm LB-agarose plates with ampicillin in serial dilutions to estimate transformation efficiency. The rest of the bacterial culture was plated out on 24 cm square LB-agarose plates with ampicillin and incubated at 30 °C for ~40 h. Colonies were washed off the plate and transferred to 100 mL of pre-warmed liquid LB media containing ampicillin. After 2 h of growth at 30 °C with shaking, plasmids were extracted as maxi-preps (Qiagen, Cat.#12162).

3.3.4 Virus production

HEK293T cells were cultured in Dulbecco's Modified Eagle medium (DMEM; Wisent). 3,000,000 HEK293T cells were seeded in 100 mm dish at a confluency at 70% in 10 mL of DMEM + 10% FBS. Transfection was performed using FuGENE6 (Promega, Cat.#E5911) transfection reagent according to the manufacturer's protocol. Briefly, the in vivo library and the non-targeting control plasmids were pooled into a 2:1 ratio. 30 μ L FuGENE6 in 500 μ L DMEM was combined with 5 μ L transfer plasmid, 1 μ L pCMV_VSVG (Addgene #8454), pCMV_ Δ R8.9 (Addgene #12263). Plasmids were combined with FuGENE6 and incubated for 30 min at room temperature, during that time media was changed on the HEK293T cells. After 30 min, the transfection mixture was added dropwise to HEK293T cells. Cells were incubated for 48 h and virus was collected every 8 h until 72 h post-transfection.

3.3.5 Concentration of Lentivirus

Virus supernatant was filtered through a 0.45 μ M filter. To concentrate virus following reagents were added: 96 mL of virus, 26 mL of PEG (50%), 9,24 mL of NaCl (5M), 22,8 mL PBS, to a

final volume of 153,6 mL. Mixture was agitated at 4°C for 90 min and afterwards centrifuged at 4000 g at 4°C for 10 min. Supernatant was removed and virus was stored at -80°C.

3.3.6 Determination of lentiviral titer

MA-Cas9 cells were transduced in 96-well plates with 100 µL 2-fold serial dilution of virus with 10,000 cells per well in the presence of 8 µg/µL polybrene. The plate was centrifuged at 1000 g for 1 h at 32 °C and was then transferred to a 37 °C incubator for 4–6 h. 48 h post-transduction, 10 µg/µL puromycin was added and cells were selected for 72 h and viability was assessed using The CellTiter-Glo® (Promega, Cat.#G7570). Viral dose resulting of 25 % transduction efficiency, was used for subsequent library screening at MOI=0.25.

3.3.7 *In vitro* and *in vivo* CRISPR screening

1,000,000 MA-Cas9 cells were plated into 6-well plate. 20×10^6 MA-Cas9 cells were transduced in replicates at a low MOI (0.25) in the presence of 8 µg/mL polybrene. Cells were centrifuged at 1000 g for 1 h at 32°C and then transferred to a 37 °C incubator for 4–6 h. Polybrene was diluted by adding 4 mL of supplemented RPMI media to the cells. The next day cells were combined into four T25 flasks and split daily 1:2 to monitor growth. Cell confluency was kept at 250-500,000 cells/ mL. 48 h post spin-oculation puromycin was added to the media at a final concentration of 10 µg/mL and incubated for 3 days. MA-Cas9 cells were cultured *in vitro* for 10 days at a confluency of 250-500,000 cells/ mL. On day 10 replicates were pooled and 20,000,000 cells were transplanted via tail vein injection into each sub-lethally irradiated (4.5 Gy) mouse. The mice were sacrificed after 18 days *in vivo* and each bone marrow was analyzed by flow cytometry for the percentage of GFP⁺ cells. *In vitro* culture was maintained without biological replicates for 18 days.

At each time point, cell pellets were collected for genomic DNA extraction using phenol/chloroform (Thermo Fisher Cat#15593031).

3.3.8 Library preparation and sequencing.

An Illumina PCR 1-step library protocol was used, to attach sequencing adaptors and index. PCR-amplification protocol was developed by the Genetic Perturbation Platform of the Broad Institute (available https://portals.broadinstitute.org/gpp/public/dir/download?dirpath=protocols/production&filename=sgRNA_shRNA_ORF_PCR_for_sequencing_20200619_public.zip) at

P5 primer mix NEON and P7 indexed primers were used. DNA from samples at following days was extracted and amplified: (1) three days *in vitro*, start of puromycin selection, (2) 10 days *in vitro* after transduction; (3) 14 days *in vivo* after timepoint (2). From each condition 13.2 ug of DNA was amplified, 1 ng/ul of Plasmid was used as baseline sgRNA representation. PCR reactions were pooled into two sub-pools and analyzed on 0.8% agarose gel, expected bands were extracted at ~350 bp using QIAquick Gel Extraction Kit (Quiagen Cat#28704). Sequencing was performed on two lanes of a HiSeq 2000 flow cell (Illumina).

3.3.9 Analysis of pooled CRISPR screen

The read count files were generated from the CRISPR Fastq files, for each biological and technical replicate using the 'count' function of the MAGeCK algorithm [28]. To determine the technical performance of the screen, technical replicates were correlated. Pearson and Spearman, and read counts were combined. In the *in vivo* screen, the gene scores were estimated from the read count

files using the ‘mle’ function from the MAGeCK package. Genes were determined as “essential” with a FDR < 0.01. Pathway enrichment analysis was performed by using String-db [30].

3.3.10 Cloning of single sgRNAs

To generate *GFP-* and *Slc25a19*-knock out cells sgRNA target sequences were designed using the Broad Institute Genetic Perturbation Platform (<https://portals.broadinstitute.org/gpp/public/gene/search>). sgRNA target sequences were subcloned into pKLV2-U6gRNA5(BbsI)-PGKpuro2AmCherry-W or pKLV2-U6gRNA5(BbsI)-PGKpuro2ABFP-W vectors as previously described [123]. 1×10^6 cells were plated in 6-well plates in 2 mL media as described above. 1 mL of freshly harvested virus (48 h) was added to cells with 8 μ g /mL polybrene. Cells were spin-infected for 1 h at 1000g at 32 °C, then polybrene was diluted down with 4 mL of fresh media.

Oligo	Sequence (5' ->3')
Slc25a19 sgRNA 1 Fw primer pair 1	CCGGAAGCAAGCTCCTCTATG
Slc25a19 sgRNA 1 Rv primer pair 1	TGCCTGAACAGGAACAGCTAA
Slc25a19 sgRNA 2 Fw primer pair 1	CCCCAGCAGGAACACATAA
Slc25a19 sgRNA 2 Rv primer pair 1	GATGCATTTGGGCGGAAACC
sgSLC25a19 #1	AGAACTGCAGGCCCGCGTAG
sgSLC25a19 #2	ACGGACCATGTATAAGACCG

3.3.11 Multicolor competition assay

Multicolor competition assays (MCA) were performed to verify the impact of gene knockouts on fitness defects in *in vivo*. In these assays, targeted cells expressed both mCherry, and BFP. The cell lines were infected with either sgGFP-mCherry vector or a sgSlc25a19-BFP vector and allowed to expand for seven days. 24h prior transplantation sgSlc25a19-knockout-BFP MA-cells were mixed with sgGFP-knockout-mCherry MA-cells. Into each recipient 1,000,000 MA-

Cas9 cells were transplanted into sub-lethally irradiated C57BL/6J (4,5 Gy) and NSG (2,0 Gy) mice. 14-16 days later mice were sacrificed, and bone marrow was extracted.

3.3.12 Statistical analysis

Statistical analysis was performed using Prism version 9.00 for Mac, GraphPad Software (California, USA). Significant differences ($p < 0.05$) between BL6 and NSG mice were determined by multiple paired t-tests (two-tailed). All statistical analysis was performed in GraphPad Prism and have been documented in the figure legends. In order to assess normality, the data was subjected to both the Shapiro-Wilk and Kolmogorov-Smirnov tests.

3.4 Results

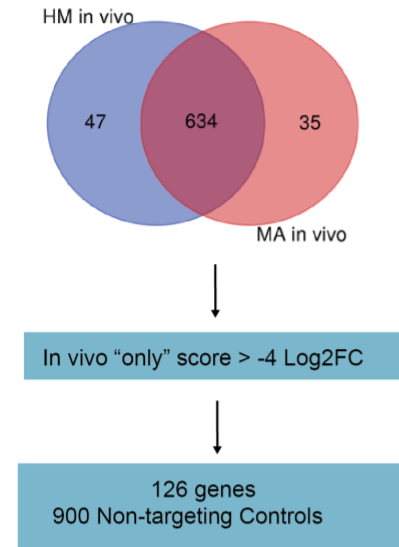
3.4.1 Focused based-dropout screen targets different components of AML biology.

In vivo-specific genetic drivers were selected from our previous study [22], then rescreened in immune-competent C57BL/6J (BL6) and immune-compromised NSG mice. Specifically, for every gene in the previously reported screen, we retrieved the Log_2FC depletion values of the *in vivo* and *in vitro* arms, then selected candidates with a greater depletion *in vivo* ($\text{Log}_2\text{FC}_{\text{vivo}} - \text{Log}_2\text{FC}_{\text{vitro}} < -4$). (**Figure 3.1 A**). This analysis identified 126 *in vivo*-dependent genes enriched in various biological pathways, such as immune regulation, cell adhesion, glycosylation, and metabolism (**Figure 3.1 C**). Additionally, we included essential genes for AML, which we expected to drop out in both experimental conditions (*Myb*, *Runx2*, *Cbfb*). We curated the focused *in vivo* library from a single master oligo pool generated by array synthesis using parallel oligonucleotide retrieval [28] (**Figure 3.1 B**). We designed 10 targeting single-guide RNAs (sgRNA) for each gene and added 900 additional negative controls to generate a focused library

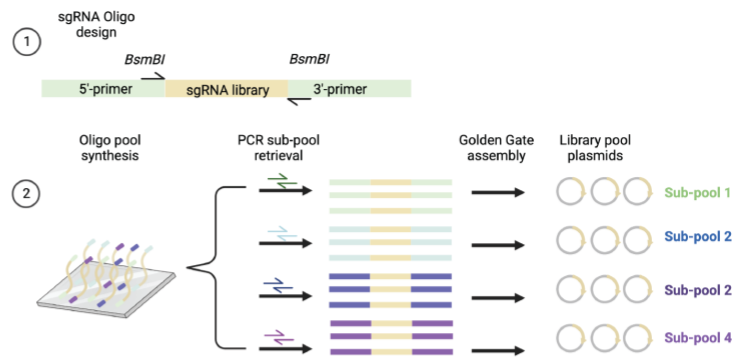
containing 2160 sgRNAs (**Figure 3.1 B, C**). We screened this library using the murine AML cell line MLL/AF9, which was generated in hematopoietic progenitors isolated from Rosa26^{CAG-CAS9-GFP} knock-in mice [22]. AML cells were transduced with an MOI of 0.25 *ex vivo* before transplantation into sublethal irradiated C57BL6/J (BL6) and NSG mice. We expanded the cells 10 days *in vitro* and transplanted 1.5×10^7 cells per mouse. Bone marrow-derived cells were collected 18 days post-transplantation for gDNA extraction and next-generation sequencing (NGS) (**Figure 3.1 D**). We examined the bone marrow by flow cytometry before processing for NGS and found both groups of mice highly leukemic (>90%) (**Supplementary Figure 3.1 A, B**). We used MAGeCK to score each gene tested in our focused library, and the median value of each sgRNA was used to represent the score of the gene [31]. Consistent with expectations, the non-targeting control gRNAs displayed no systematic enrichment or depletion. Conversely, among the initially selected sgRNAs, we observed a drop out of more than 90% (with a cutoff $\text{Log}_2\text{FC} > -1.5$) in all tested sgRNAs, validating our previous results [22] (**Figure 3.1 E**).

A

Mercier et al., 2022
Top dependencies in vivo



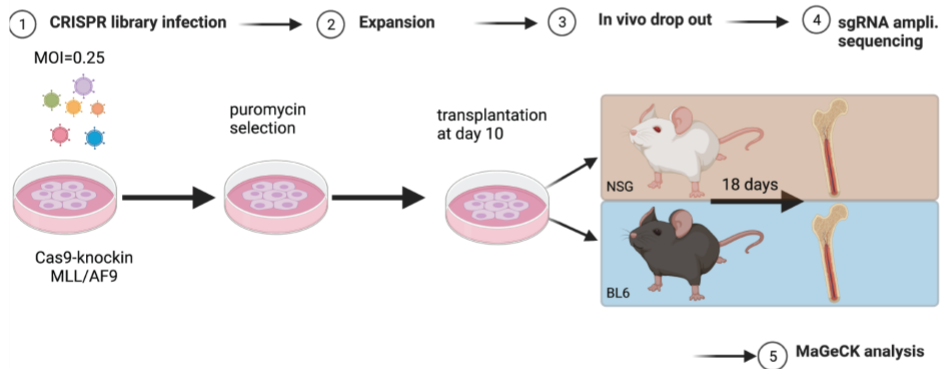
B



C

Library construction			
Gene family	#gene	#guides/gene	#guides
In vivo hits (Mercier et al., 2022)	126	10	1260
Metabolism		10	
Cell adhesion and glycosylation		10	
Myeloid differentiation		10	
AML essential genes		10	
Non-Targeting sgRNA Controls	900	10	900
Total			2160

D



E

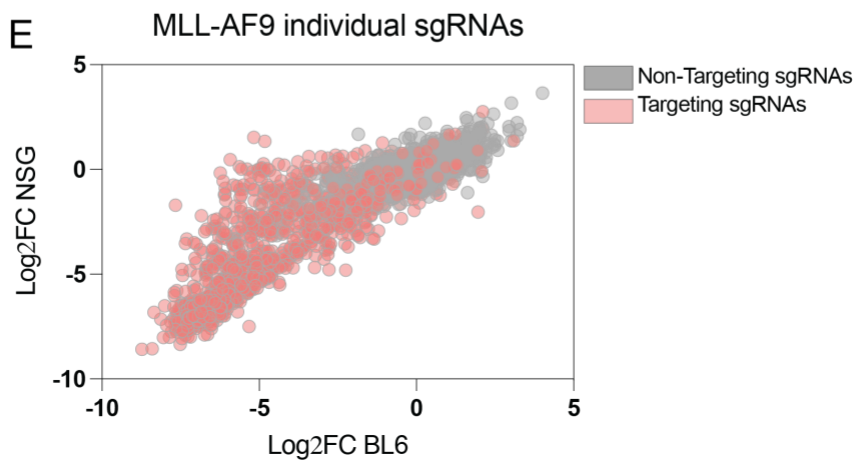


Figure 3.1 Generation of focused *in vivo* library.

(A) Representation of Selection criteria of genetic candidates for *in vivo* screening. The „*in vivo* genes” were selected based on their Log₂FC depletion values; only genes with a greater depletion *in vivo* ($\text{Log}_2\text{FC}_{\text{vivo}} - \text{Log}_2\text{FC}_{\text{vitro}} < -4$) were selected. Additionally, 900 non-targeting controls were added to the library. 126 genes were retrieved from our previous study [22].

(B) Schematics of sgRNA oligo design. Pre-designed sgRNA 20-mers are flanked by 5'- and 3'- PCR primers and BsmBI sites. Library oligos with different flanking primer sequences were synthesized on a chip together as a single master pool. Specific primer pairs were used to amplify and retrieve subsets of oligos from the master pool. Sub-pool amplicons were digested with BsmBI and cloned into Lentiguide-puro via Golden Gate ligation. Schematics adapted from [28] and created with biorender.com.

(C) Overview of gene families in CRISPR library. Each gene was targeted with ten sgRNAs.

(D) *In vivo* screen pipeline. MA-Cas9 cells were infected. At day 3, cells were selected with puromycin and expanded until day 10. On day 10, cells were pooled and transplanted into B57BL/6 or NSG mice. Mice were sacrificed after 18 days *in vivo*, and gDNA was extracted from bone marrow. gDNA was isolated, and PCR was performed for library preparation and NGS. Created with BioRender.com.

(E) Log₂fold-change representation of each targeting and non-targeting sgRNA in MA- cells. Log₂fold-change was determined for each sgRNA relative to day 0 (plasmid).

3.4.2 CRISPR screening identifies *Slc25a19* as an immune regulator in AML.

We performed a STRING analysis to understand further how the genes relate to each other. From 126 genes, we found that 69 genes were connected (**Figure 3.2 A**). Next, we calculated a normalized depletion score for each sgRNA, and the median value was used to represent the gene

score. Depleted genes in C57BL/6J and NSG mice showed an overall good correlation ($R^2=0.65$). Among the genes which did not correlate were components of the antigen processing machinery (*Tapbp*, *B2m*, *Tap1* and *Tap2*), which we expected to not drop out in B-, T, and NK cell depleted mouse model (**Figure 3.2 B, D**). Furthermore, we found that the complement receptor (*Cr1l*) and the leukocyte surface antigen (*CD47*) were depleted in both arms, but AML cells were more vulnerable in immune-competent mice (*Cr1l* Log₂FC, -3,86 in NSG and -6.14 in C57BL/6J; *CD47* Log₂FC, -2,36 in NSG and -4.6 in C57BL/6J). Known AML dependencies such as the transcription factor *Myb*, *Runx1* and *Cbfb* dropped out in both models (**Figure 3.2 C**). Next, we examined the context of immune response by calculating the difference in Log₂FC between NSG and C57BL/6J mice. We took as a cut-off for immune-specific candidate genes all genes > -1.5 (**Figure 3. 2E**). This approach identified five genes with specific depletion in MA cells in the context of immune dependency: the solute carrier family 25 member 19 (*Slc25a19*), Caspase8 and FADD-like apoptosis regulator (*Cflar*), Ankyrin repeat domain 52 (*Ankrd52*), Granulocyte colony-stimulating factor receptor (*Csf3r*) and coat complex subunit gamma 1 (*Copg1*) (**Figure 3.2F**). *Slc25a19* was the top candidate that ranked as highly as the genes of the antigen processing machinery (**Figure 3. 2E**). *Slc25a19* is a mitochondrial transporter which shuttles the active form of thiamine (thiamine pyrophosphate, TPP) through the inner membrane. TPP is an essential cofactor for pyruvate dehydrogenase (*Pdh*), α -ketoglutarate dehydrogenase (*Okgdh*) in the TCA cycle and branched-chain α -ketoacid dehydrogenase (*Bckdh*) in the catabolism of branched-chain amino acids (**Supplementary figure 3.2 B**). Despite its known function as a mitochondrial gene, *Slc25a19* appears to be essential only in an immune-competent microenvironment, in contrast to other mitochondrial genes screened, such as dihydrolipoyl dehydrogenase, mitochondrial (*Dld*), 2-oxoglutarate dehydrogenase E2 component (*Dlst*), Aconitate hydratase (*Aco2*),

Lipoyltransferase 1 (*Lipt*) and Lipoyltransferase 2 (*Lipt2*), which did not show any immune dependency (**Supplementary figure 3.2 A**). Furthermore, we investigated the essentiality of other thiamine transporters in our CRISPR/Cas9-based genome-wide screen and found that *Slc25a19* was the only essential gene (data not shown). To validate the focused CRISPR screen, we performed an *in vivo* competition assay, in which we transduced MA cells with sgGFP-mCherry and sgSlc25a19-BFP and transplanted the cells in C57BL/6J and NSG mice (**Figure 3. 3A**). Approximately two weeks after, we sacrificed the mice. We found that sgSlc25a19-BFP targeted MA cells were depleted almost entirely (> 0.5%) in C57BL/6J recipients, whereas in NSG, we found approximately 30% of sgSlc25a19-BFP cells remaining, validating our focused screen (**Figure 3. 3B, C**). These data suggest a novel link between the mitochondrial thiamine transporter *Slc25a19* and AML immune biology.

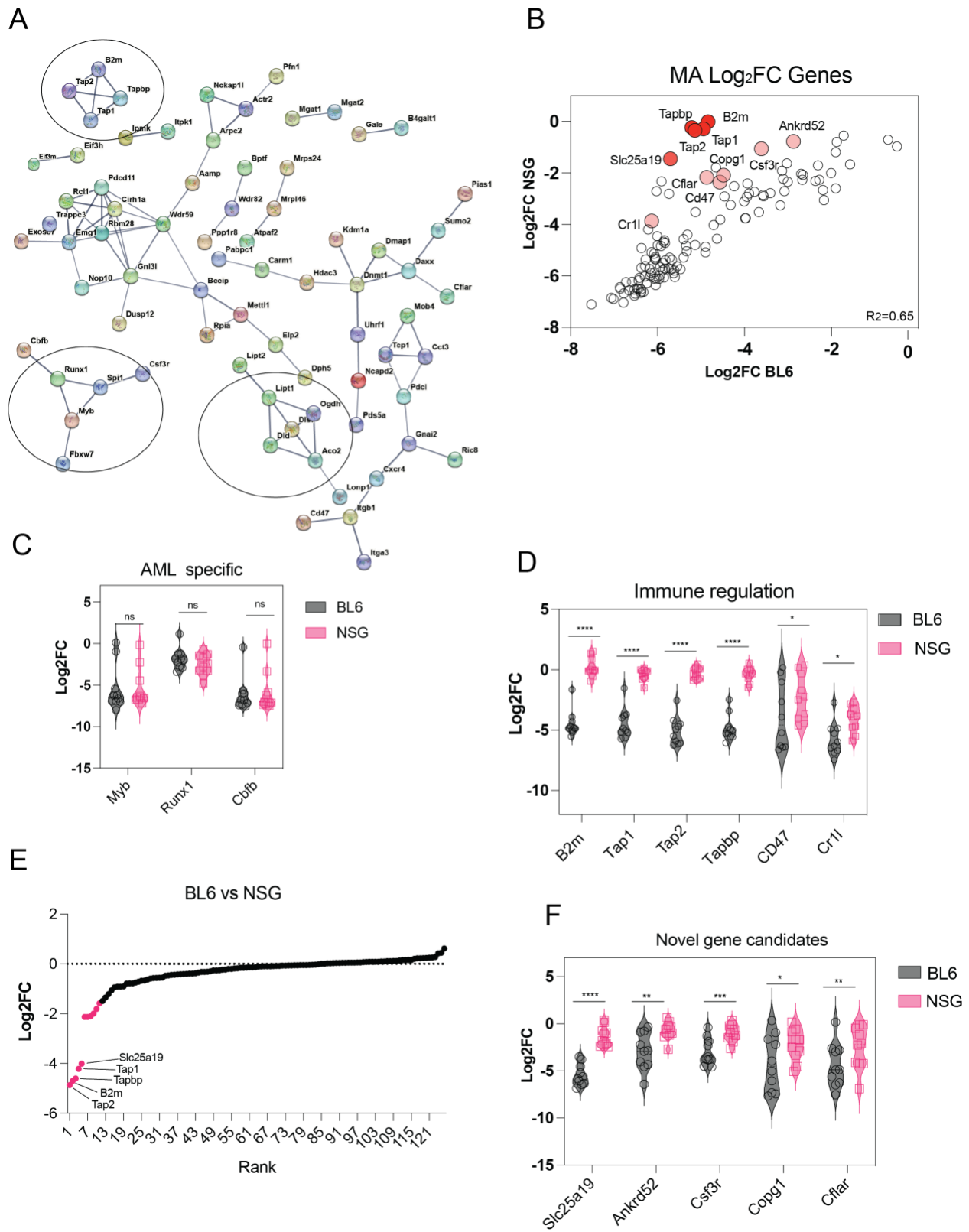


Figure 3.2 *In vivo* CRISPR/Cas9 library targets different components of AML biology.

- (A) STRING functional protein association of all complexes in the focused library.
- (B) log₂fold-change representation of every gene in MA- cells. The Log₂fold-change was determined for every gene, by the median log₂fold-change of sgRNA representation relative to day 0 (plasmid).
- (C) Drop out of known essential genes in AML. Log₂fold-change of *Myb*, *Runx1* and *Cbfb* in C57BL/6J and NSG mice significance was tested between groups by a paired multiple t-test ($p < 0.05 = *$).
- (D) Drop out of immune regulatory genes in AML. Log₂fold-change of *B2m*, *Tap1*, *Tap2*, *Tapbp*, *CD47*, *Cr11* in C57BL/6J and NSG mice, significance was tested between groups by a paired multiple t-test ($p < 0.05 = *$).
- (E) Rank of all tested in genes in focused library. Dots highlighted in red represent immune essential immune regulatory genes with log₂fold-change > 1.5.
- (F) Drop out of essential immune regulatory genes. Log₂fold-change of *Slc25a19*, *Ankrd52*, *Csf3r*, *Copg1*, *Cflar* in C57BL/6J and NSG mice, significance was tested between groups by a paired multiple t-test ($p < 0.05 = *$). BL6, C57BL/6J mice.

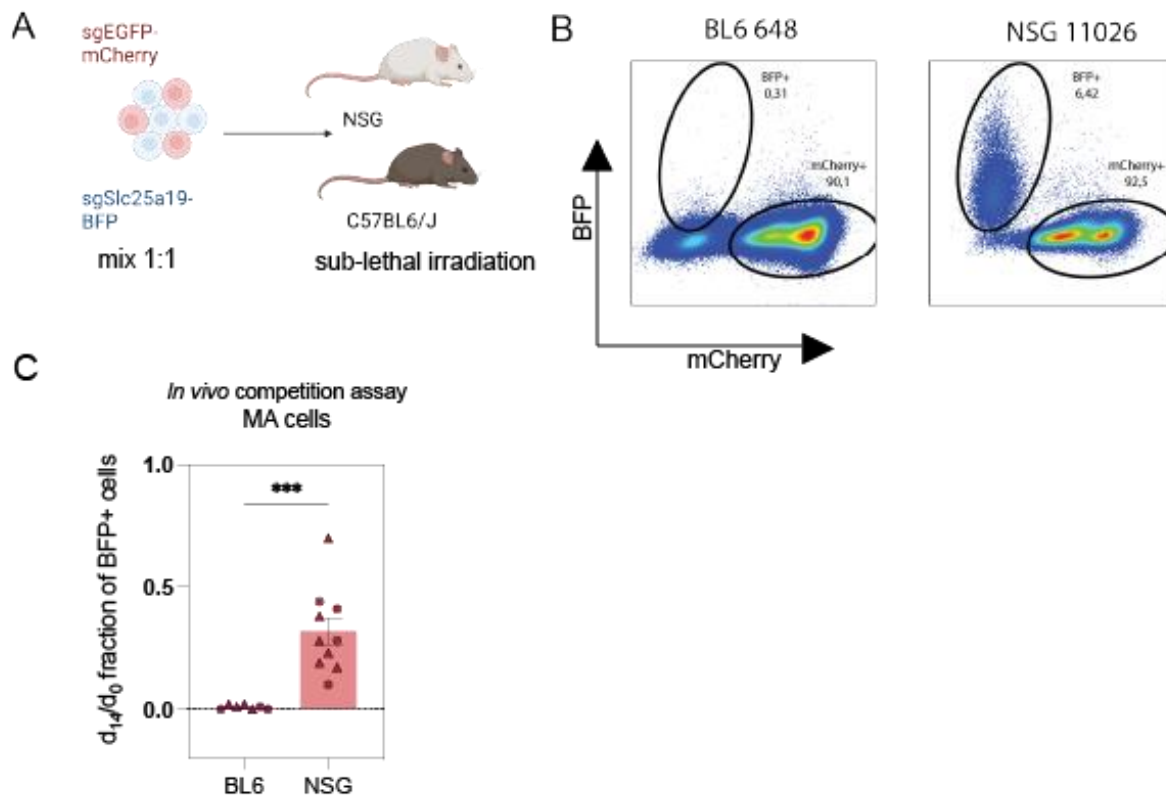


Figure 3.3 CRISPR/Cas9 mediated KO of Slc25a19 is lethal in immune competent mice.

(A) Schematic of *in vivo* competition experiment. sgEGFP-mCherry cells and sgSlc25a19-BFP cells were combined in a 1:1 ratio before transplantation. A mix of 1×10^6 cells was transplanted in sub-lethally irradiated C57BL/6J and NSG mice. Created with BioRender.com.

(B) Representation of flow cytometry analysis of BM 14 days after transplantation, as described in (A). (C) Representation of *in vivo* competition experiment displayed in (B) for MA cells. Values represent one mouse ($n = 10$, NSG and $n=7$, C57BL/6J). Significance was determined using paired t-test. $*P \leq 0.0001$. MA cells were normalized to day 0, 2 independent experiments are indicated by the symbol shape.

3.5 Discussion

3.5.1 Slc25a19 and thiamine metabolism in the immune-related biology of AML

Immune-related AML biology is still poorly understood but could provide a promising therapeutic avenue for the treatment of AML patients. To systematically discover AML-intrinsic immune-specific pathways in the tumor microenvironment, we designed a focused *in vivo* CRISPR screen in immune-competent and immune-compromised mice. We identified five genes which have not been described in AML in the context of immune dependency *Slc25a19*, *Cflar*, *Ankrd52*, *Copg1* and *Csf3r*. *Slc25a19* was the only metabolic candidate which was essential in immune-competent mice. Work by others has demonstrated that the loss of *Slc25a19* is embryonic lethal in mice, impairing the TCA cycle, mainly PDH and OGDH function [32]. Recent studies found that mitochondrial apoptosis plays an essential role in NK-cell-mediated killing, which could be a potential link for our study. Others have established the link between mitochondrial stress and antigen presentation. For instance, elevated OXPHOS increases the expression of MHC class I presentation by activating extracellular signal-regulated kinase 5 (ERK5) [33, 34]. A study in sarcoma mouse models found that Hypoxia-inducible factor-1a (HIF-1a), a master regulator of glycolysis, was recently shown to downregulate MHC class I and TAP proteins [35]. Proteomic analysis of 116 melanoma tumors revealed that high mitochondrial metabolism led to higher antigen presentation and IFN signaling [36]. Others have recently reported vitamin C and Vitamin B6 as important regulators in AML [37-39]. In our screen, we confirmed vulnerability to loss of pyroxidase (*Pdxk*) (Vitamin B6) and loss of the reduced folate transporter (*Slc19a1*) but not in the context of immune regulation.

3.5.2 Role of mitochondrial genes in the pathobiology of AML

We furthermore confirmed vulnerability to other mitochondrial genes (*Dld*, *Dlst*, *Aco2*, *Lipt1*, *Lipt2*). However, none of them showed significant differences between BL6 and NSG mice. It is possible that loss of *Dld*, *Dlst*, *Aco2*, *Lipt1*, *Lipt2* targets AML cells which are highly dependent on OXPHOS such as dormant LSCs [40] Lagadinou et al. and others have shown that dormant LSCs contrast with proliferating AML blasts and HSCs are highly reliant on mitochondrial OXPHOS, and less on glycolysis which could explain the overall essentiality *in vivo*. Remarkably, CRISPR/Cas9-based knock-out screens conducted in human AML, when combined with the BCL-2 inhibitor ABT-199 (venetoclax), have revealed significant synthetic lethality upon genetic targeting of *Dld*, *Dlst*, and *Aco2*. This discovery provides compelling evidence that the loss of these genes creates a metabolic vulnerability, rendering AML cells highly susceptible to metabolic stress. [41, 42].

3.5.3 Additional players in the immune-related biology of AML

We identified four other genes *Ankrd52*, *Csfr3r*, *Copg1*, *Cflar* providing resistance to the immune compartment. *Ankrd52* was found in another study, in which they performed CRISPR/Cas9-based screening under different immune pressures. *Ankrd52* mediated miRNA pathway was exploited by colon cancer cells to escape from T cell-mediated elimination and immune therapy [43]. Genetic deletion of *Copg1* in another study induced type I IFN activation via the cGas/STING pathway [44]. One limitation of our study was the use of NSG mice as an immune-compromised model. While this model is commonly used, other mouse models are available that exhibit fewer degrees of immune dysfunction, which could provide additional insights. Further research using human CRISPR/Cas9-based genetic screening with co-culture assays or humanized mouse models

will yield additional information. We developed a CRISPR/Cas9-screening platform, allowing us to discover genes contributing to immune dysregulation in AML. We identified several immune regulatory axes which could potentially be exploited in AML, loss of *Tap1*, *Tap2*, *Tapbp* and *B2m* suggest that NK cells could be exploited as cellular therapy. With the discovery of *Slc25a19* we found that mitochondrial thiamine metabolism could be linked to the immune compartment. Further validation will be needed to follow up on the link.

3.6 Acknowledgments

M.J. is a recipient of a Cole Foundation doctoral scholarship and Lady Davis Institute/TD Bank Studentship Award. Work in the F.E.M. laboratory was supported by an operating grant from the Cancer Research Society (#23604) and grants from the Cole Foundation, Richard and Edith Strauss Foundation, and Jewish General Hospital Foundation.

3.7 Authorship

Contribution: M.J. designed, performed most of the functional experiments, analyzed the data, and wrote the manuscript. W.P. assisted with sgRNA design. C.D. assisted with library preparation. D.X. contributed to the analysis of the data under the supervision of J.S. A.O. contributed to the analysis of the data and provided supervision. F.E.M. designed the research, provided supervision.

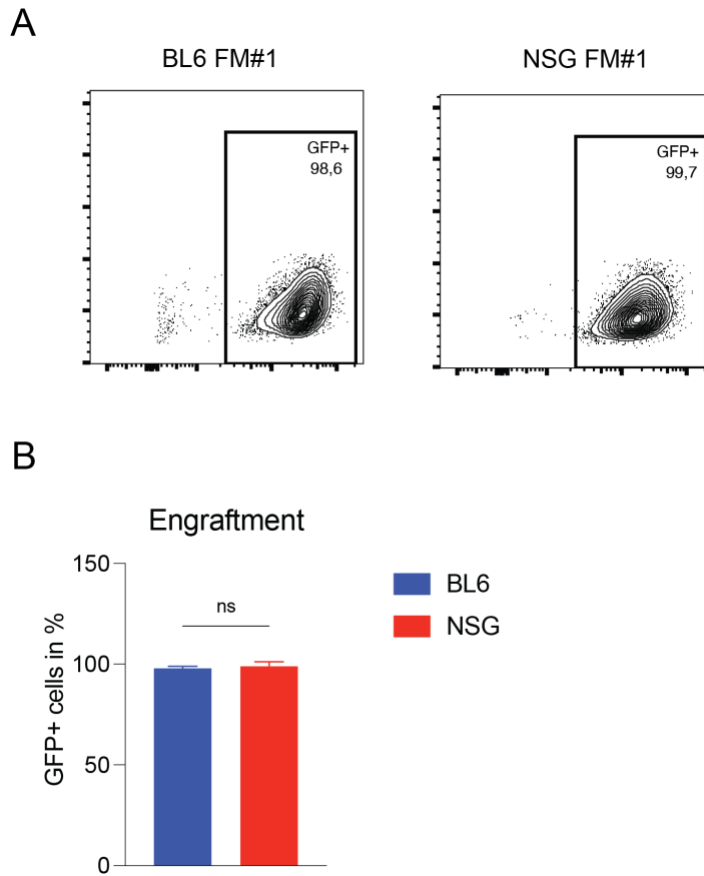
3.8 References

1. Lichtman, M.A., *A historical perspective on the development of the cytarabine (7days) and daunorubicin (3days) treatment regimen for acute myelogenous leukemia: 2013 the 40th anniversary of 7+3*. Blood Cells, Molecules, and Diseases, 2013.
2. Schuh, A.C., et al., *Azacitidine in adult patients with acute myeloid leukemia*. Crit Rev Oncol Hematol, 2017. **116**: p. 159-177.
3. Dhillon, S., *Ivosidenib: First Global Approval*. Drugs, 2018. **78**(14): p. 1509-1516.
4. Norsworthy, K.J., et al., *FDA Approval Summary: Mylotarg for Treatment of Patients with Relapsed or Refractory CD33-Positive Acute Myeloid Leukemia*. Oncologist, 2018. **23**(9): p. 1103-1108.
5. Stone, R.M., R.A. Larson, and H. Dohner, *Midostaurin in FLT3-Mutated Acute Myeloid Leukemia*. N Engl J Med, 2017. **377**(19): p. 1903.
6. Letai, A., *Functional precision cancer medicine-moving beyond pure genomics*. Nat Med, 2017. **23**(9): p. 1028-1035.
7. Global Burden of Disease Cancer, C., et al., *Cancer Incidence, Mortality, Years of Life Lost, Years Lived With Disability, and Disability-Adjusted Life Years for 29 Cancer Groups From 2010 to 2019: A Systematic Analysis for the Global Burden of Disease Study 2019*. JAMA Oncol, 2022. **8**(3): p. 420-444.
8. Daver, N., et al., *T-cell-based immunotherapy of acute myeloid leukemia: current concepts and future developments*. Leukemia, 2021. **35**(7): p. 1843-1863.
9. Majeti, R., et al., *CD47 is an adverse prognostic factor and therapeutic antibody target on human acute myeloid leukemia stem cells*. Cell, 2009. **138**(2): p. 286-99.
10. Jaiswal, S., et al., *CD47 is upregulated on circulating hematopoietic stem cells and leukemia cells to avoid phagocytosis*. Cell, 2009. **138**(2): p. 271-85.
11. Jaiswal, S., et al., *Macrophages as mediators of tumor immunosurveillance*. Trends Immunol, 2010. **31**(6): p. 212-9.
12. Edris, B., et al., *Antibody therapy targeting the CD47 protein is effective in a model of aggressive metastatic leiomyosarcoma*. Proc Natl Acad Sci U S A, 2012. **109**(17): p. 6656-61.
13. Liu, J., et al., *Pre-Clinical Development of a Humanized Anti-CD47 Antibody with Anti-Cancer Therapeutic Potential*. PLoS One, 2015. **10**(9): p. e0137345.
14. Sikic, B.I., et al., *First-in-Human, First-in-Class Phase I Trial of the Anti-CD47 Antibody Hu5F9-G4 in Patients With Advanced Cancers*. J Clin Oncol, 2019. **37**(12): p. 946-953.
15. Hope, K.J., L. Jin, and J.E. Dick, *Acute myeloid leukemia originates from a hierarchy of leukemic stem cell classes that differ in self-renewal capacity*. Nat Immunol, 2004. **5**(7): p. 738-43.
16. Dick, J.E., *Acute myeloid leukemia stem cells*. Ann N Y Acad Sci, 2005. **1044**: p. 1-5.
17. Sanchez-Aguilera, A. and S. Mendez-Ferrer, *The hematopoietic stem-cell niche in health and leukemia*. Cell Mol Life Sci, 2017. **74**(4): p. 579-590.
18. Vilaplana-Lopera, N., et al., *Crosstalk between AML and stromal cells triggers acetate secretion through the metabolic rewiring of stromal cells*. eLife, 2022. **11**: p. e75908.
19. Williams, R.T., et al., *ZBTB1 Regulates Asparagine Synthesis and Leukemia Cell Response to L-Asparaginase*. Cell Metab, 2020. **31**(4): p. 852-861 e6.

20. van Gastel, N., et al., *Induction of a Timed Metabolic Collapse to Overcome Cancer Chemoresistance*. Cell Metabolism, 2020. **32**(3): p. 391-403.e6.
21. Gordon, P.M., S. Dias, and D.A. Williams, *Cytokines secreted by bone marrow stromal cells protect c-KIT mutant AML cells from c-KIT inhibitor-induced apoptosis*. Leukemia, 2014. **28**(11): p. 2257-60.
22. Mercier, F.E., et al., *In vivo genome-wide CRISPR screening in murine acute myeloid leukemia uncovers microenvironmental dependencies*. Blood Adv, 2022. **6**(17): p. 5072-5084.
23. Kroon, E., et al., *Hoxa9 transforms primary bone marrow cells through specific collaboration with Meis1a but not Pbx1b*. EMBO Journal, 1998.
24. Krivtsov, A.V., et al., *Transformation from committed progenitor to leukaemia stem cell initiated by MLL-AF9*. Nature, 2006. **442**(7104): p. 818-22.
25. Doench, J.G., et al., *Optimized sgRNA design to maximize activity and minimize off-target effects of CRISPR-Cas9*. Nat Biotechnol, 2016. **34**(2): p. 184-191.
26. Sanson, K.R., et al., *Optimized libraries for CRISPR-Cas9 genetic screens with multiple modalities*. Nat Commun, 2018. **9**(1): p. 5416.
27. Sanjana, N.E., O. Shalem, and F. Zhang, *Improved vectors and genome-wide libraries for CRISPR screening*. 2014.
28. Read, A., et al., *Flexible CRISPR library construction using parallel oligonucleotide retrieval*. Nucleic Acids Res, 2017. **45**(11): p. e101.
29. Li, W., et al., *MAGeCK enables robust identification of essential genes from genome-scale CRISPR/Cas9 knockout screens*. Genome Biol, 2014. **15**(12): p. 554.
30. Szklarczyk, D., et al., *STRING v10: protein-protein interaction networks, integrated over the tree of life*. Nucleic Acids Res, 2015. **43**(Database issue): p. D447-52.
31. Li, W., et al., *Quality control, modeling, and visualization of CRISPR screens with MAGeCK-VISPR*. Genome Biology, 2015.
32. Lindhurst, M.J., et al., *Knockout of *Slc25a19* causes mitochondrial thiamine pyrophosphate depletion, embryonic lethality, CNS malformations, and anemia*. Proceedings of the National Academy of Sciences, 2006. **103**(43): p. 15927-15932.
33. Charni, S., et al., *ERK5 Knockdown Generates Mouse Leukemia Cells with Low MHC Class I Levels That Activate NK Cells and Block Tumorigenesis1*. The Journal of Immunology, 2009. **182**(6): p. 3398-3405.
34. Charni, S., et al., *Oxidative Phosphorylation Induces De Novo Expression of the MHC Class I in Tumor Cells through the ERK5 Pathway*. The Journal of Immunology, 2010. **185**(6): p. 3498-3503.
35. Sethumadhavan, S., et al., *Hypoxia and hypoxia-inducible factor (HIF) downregulate antigen-presenting MHC class I molecules limiting tumor cell recognition by T cells*. PLOS ONE, 2017. **12**(11): p. e0187314.
36. Harel, M., et al., *Proteomics of Melanoma Response to Immunotherapy Reveals Mitochondrial Dependence*. Cell, 2019. **179**(1): p. 236-250.e18.
37. Cimmino, L., et al., *Restoration of TET2 Function Blocks Aberrant Self-Renewal and Leukemia Progression*. Cell, 2017. **170**(6): p. 1079-1095.e20.
38. Agathocleous, M., et al., *Ascorbate regulates haematopoietic stem cell function and leukaemogenesis*. Nature, 2017. **549**(7673): p. 476-481.
39. Chen, C.C., et al., *Vitamin B6 Addiction in Acute Myeloid Leukemia*. Cancer Cell, 2020. **37**(1): p. 71-84.e7.

40. Lagadinou, Eleni D., et al., *BCL-2 Inhibition Targets Oxidative Phosphorylation and Selectively Eradicates Quiescent Human Leukemia Stem Cells*. *Cell Stem Cell*, 2013. **12**(3): p. 329-341.
41. Lin, K.H., et al., *Systematic Dissection of the Metabolic-Apoptotic Interface in AML Reveals Heme Biosynthesis to Be a Regulator of Drug Sensitivity*. *Cell Metab*, 2019. **29**(5): p. 1217-1231.e7.
42. Chen, X., et al., *Targeting Mitochondrial Structure Sensitizes Acute Myeloid Leukemia to Venetoclax Treatment*. *Cancer Discov*, 2019. **9**(7): p. 890-909.
43. Shalem, O., et al., *GeCKO v2. pooled libraries*. *Science*, 2014.
44. Steiner, A., et al., *Deficiency in coatamer complex I causes aberrant activation of STING signalling*. *Nature Communications*, 2022. **13**(1): p. 2321.

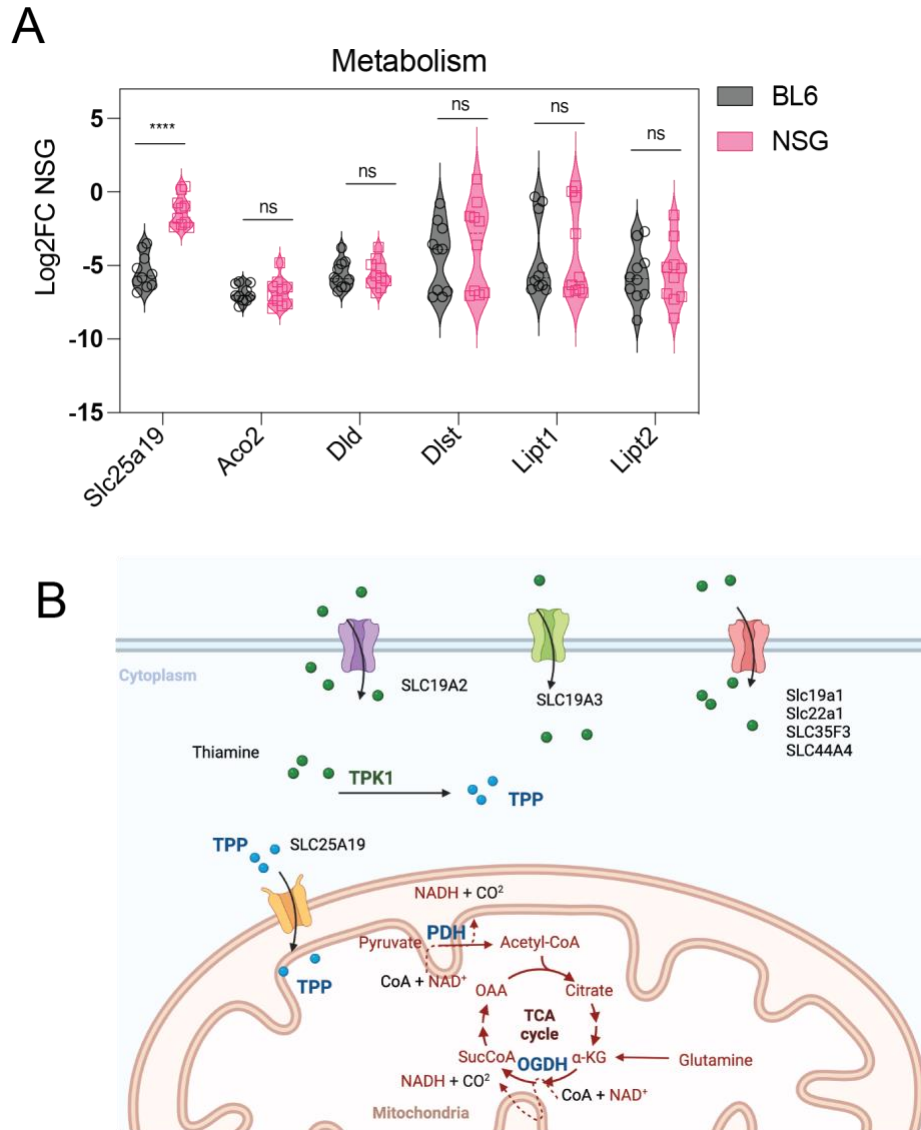
3.9 Supplementary Figures



Supplementary Figure 3. 1 Engraftment efficiency of library transduced MA-Cas9 cells.

(A) Flow cytometry example of GFP⁺ cells in BL6 and NSG mice.

(B) Engraftment efficiency of library transduced MA-Cas9 cells at day 14, significance was tested between groups by unpaired t-test.



Supplementary Figure 3. 2 Loss of *Slc25a19* is essential in immune competent BL6 mice.

(A) Drop out of essential metabolic genes. Log₂fold-change of *Slc25a19*, *Aco2*, *Dld*, *Dlst*, *Lipt1*, *Lipt2* in C576BL/6 and NSG mice, significance was tested between groups by a paired multiple t-test ($p < 0.05 = *$).

(B) Thiamine metabolism in cytosol and mitochondria. Thiamine gets transported to the cytoplasm through transporters of the Solute carrier family (SLC). Inside the cytoplasm, thiamine gets phosphorylated by Thiamin Pyrophosphokinase 1 (TPK1) to thiamine pyrophosphate (TPP). TPP gets transported inside the mitochondria, where it is used as essential cofactor for pyruvate

dehydrogenase (PDH) and α -ketoglutarate dehydrogenase (OGDH) in the Tricarboxylic acid cycle (TCA cycle). Created with BioRender.com.

4 Chapter: Discussion and Future Directions

4.1 HERC1 in AML and nucleoside analogue treatment

AML cells have a high rate of proliferation, which increases their demand for nucleotides. This dependency on nucleotides provides a therapeutic vulnerability for nucleoside analogues such as Ara-C. AML cells metabolize nucleotides through two pathways, the nucleotide *de novo* synthesis and the nucleotide salvage pathway. Nucleotide *de novo* synthesis refers to synthesizing nucleotides from glucose and the two amino acids glutamine and aspartate using ATP. The nucleotide salvage pathway allows cells to recycle nucleotides from degraded RNA and DNA molecules. The curative treatment of AML is high-dose cytotoxic therapy consisting mainly of Ara-C and Daunorubicin (7+3 induction therapy). Ara-C is recognized as a nucleotide and is metabolized through the nucleotide salvage pathway. DCK phosphorylates Ara-C to its active form Ara-CTP, which acts in the S-phase of the cell cycle. Once Ara-CTP is incorporated into DNA, it terminates DNA elongation leading to stalled replication fork and induction of mitochondrial apoptosis [329]. The principal toxicities of Ara-C induction are myelotoxicity, gastrointestinal side effects including nausea and vomiting, fever, hepatotoxicity, and sometimes severe cerebral toxicity. These major toxicities are age-related and can harm elderly AML patients, resulting in limited treatment options for elderly AML patients with comorbidities [330]. In my thesis, I focused on identifying drug-gene combinations that synergize with Ara-C to improve its efficacy. In contrast to other CRISPR/Cas9-based studies, which have mainly focused on finding mechanisms of Ara-C resistance [265, 331], I prioritized the identification of novel therapeutic targets that could be used to enhance the efficacy of Ara-C.

The CRISPR-based genome-wide screen that I performed revealed that inhibition of the E3 ligase Herc1 may represent a novel approach to improve Ara-C efficacy. Herc1 regulates at the post-transcriptional level the abundance of the rate-limiting Ara-C-activating enzyme Dck. In my

thesis, I propose a new foundation for exploring the post-transcriptional regulation of Dck and its regulation through the UPS.

4.1.1 The UPS in AML and the response to Ara-C

Numerous members of the UPS have been found to play crucial roles in AML biology, particularly in the context of disease development and progression. Recently, two separate studies have shed light on how resistance to the chemotherapy drug Ara-C in AML is mediated at the proteasomal level through distinct cellular pathways. One group revealed that the dNTP hydrolase SAMHD1 is under the control of two factors, Non-POU Domain Containing Octamer Binding (NONO) and the DDB1-DCAF1 E3 ligase. This regulation results in increased stability of SAMHD1, leading to AML cells developing resistance to Ara-C [332]. In another investigation, the DUB USP7 was found to play a pivotal role in AML chemoresistance by modulating the levels of the CHK1 protein. This modulation enables AML cells to promote the progression of replication forks and adapt to replication stress, thus contributing to resistance against Ara-C treatment [333]. These findings offer new insights into proteasomal mechanisms that can potentially enhance the effectiveness of Ara-C treatment. During my thesis, I found that the Ubiquitin E3 ligase Herc1 modulates protein levels of Dck. Overall, these findings highlight the significance of proteasomal regulation as a promising avenue to explore in the context of Ara-C treatment in AML.

4.1.2 The implication of HERC1 in AML biology

The ubiquitin ligase HERC1 is a 530-kDa protein that belongs to the large HERC protein family, which is characterized through many functional domains including the HECT-domain. HERC1 has been shown to regulate multiple cellular pathways through its ligase activity, such as

cellular proliferation, autophagy, and acts as a proteasome-quality control factor monitoring proteasome assembly [334-338]. Furthermore, it has been demonstrated that HERC1 is implicated in intracellular vesicle trafficking by interacting with ARF1 and clathrin through its RCC1-Like domain (RLD) [339, 340]. Another group found that HERC1 contains a putative BH3 domain that can bind to BAK and target it for degradation [341]. HERC1 is widely conserved among species and is highly expressed in the brain and hematopoietic- and lymphoid tissues. Loss of function mutations of HERC1 in humans and mice leads to neurological defects associated with intellectual disability and autism [341-345].

Moreover, HERC1 has been found to be mutated in hematological malignancies [346, 347], and it has been shown that HERC1 is relevant for myeloid differentiation [348]. *Herc1*-ko mice are phenotypically characterized by increased leukocyte numbers and an increase in eosinophil cell numbers and Ly6C⁺ monocytes [334, 349]. In the transcriptomic analysis that I performed, MA sgHerc1-KO cells compared to controls overexpressed several genes related to granulocyte differentiation, including Ly6C2, and pathway enrichment analysis revealed that top-upregulated pathways were involved in neutrophil degranulation and leukocyte activation. For future studies, it will be important to understand how HERC1 is regulated in AML, and how AML cells hijack HERC1 functions in the context of AML self-renewal and differentiation.

4.1.3 Proteasomal degradation of DCK as a novel regulatory step in Ara-C resistance

DCK is the rate-limiting step in Ara-C treatment. Several studies have demonstrated that genetic targeting of DCK or inhibition with small molecules result in resistance to nucleoside analogs [350-352]. Interestingly, most of the AML patients resistant to Ara-C do not show mutations in DCK, which suggests that DCK-mediated resistance is multifactorial [353]. Two

groups have independently demonstrated in Ara-C-resistant AML patients that alternative splicing results in inefficient DCK isoforms, which has been proposed as a potential mechanism for Ara-C and gemcitabine resistance [354, 355]. Until now, it is not fully understood how alternatively spliced forms of DCK are caused; however, one recent report highlights that posttranslational modification of splicing factors is contributing to Ara-C resistance [356].

In addition to alternative splicing, several research groups have demonstrated that DCK undergoes phosphorylation at Ser-74. This phosphorylation serves as an activation signal for DCK, and its activity is decreased upon dephosphorylation [357]. In the context of DNA damage, ATR and ATM phosphorylate DCK at Ser-74. ATR has been shown to control the basal activity of DCK [358, 359]. Moreover, inhibiting ATR has been found to reduce the activity of DCK by reducing its phosphorylation at Ser-74 [360] [361]. Sabine *et al.* conducted a study that provided high-resolution DCK structures bound to cytidine and nucleoside analogues. Their findings revealed the factors that determine substrate specificity and identified structural constraints that limit the efficacy of phosphorylation in nucleoside analogs [362]. In various cancer models, the relationship between the mRNA level of DCK and its activity has been explored. Notably, in pancreatic and lung cancer, it was observed that the prediction of resistance to gemcitabine treatment relied solely on the activity and protein level of DCK rather than its mRNA level [363]. My research has demonstrated that the levels of Dck are regulated through post-transcriptional mechanisms involving Herc1, which ultimately results in improved efficacy of nucleoside analogs. Subsequent investigations will be required to decipher the Herc1 and Dck interactome.

4.1.4 HERC1 as a candidate regulator of DCK activity

My research lays the groundwork for examining the post-transcriptional regulation of Dck through Herc1. Overall, I found that the depletion of Herc1 in HM and MA cells leads to elevated levels of Dck protein. The same effect was observed by administering a proteasome inhibitor, mimicking the impact of Herc1 depletion. These results are consistent with a recent report demonstrating that the proteasome controls metabolic enzymes in the nucleotide salvage pathway [361]. To obtain valuable insights into the relationship between Herc1 and Dck, it will be crucial to investigate further if Dck is ubiquitinated and investigate their physical interaction, particularly under specific circumstances such as different cell cycle states. On one side, utilizing a proximity labeling approach coupled with mass spectrometry (MS) can provide valuable insights into the proteome of Dck and help determine if Herc1 directly regulates it. On the other side, the overexpression of Herc1 will allow us in future to investigate whether Herc1 overexpression directly influences Dck.

4.1.5 The potential role of HERC1 in nucleotide metabolism at steady state and chemoresistance

AML cells can utilize the two main pathways to generate nucleotides for their increased demand: *de novo* synthesis- and the nucleotide salvage pathway. Nucleotide production is tightly regulated, and measurements of intracellular levels of dNTPs suggest that nucleotides are produced “on demand” in non-cancerous cell lines [364] [365]. In AML, it has been shown that there is a plasticity of both pathways, and AML cells “switch” for instance to nucleotide *de novo* synthesis to overcome Ara-C treatment [205]. **The precise mechanism on how AML cells alter both pathways is not fully understood, and my research suggests that proteasomal degradation**

plays a role in regulating the nucleotide demand. Furthermore, I hypothesize that Herc1 specifically plays a role in switching the cellular metabolism towards the nucleotide *de novo* synthesis by modulating the levels of Dck.

It is possible that whenever cells do not have the immediate demand for nucleotides (for instance after the S-Phase of the cycle) Dck could be targeted for proteasomal degradation by Herc1. Interestingly, I observed that the loss of *Herc1* or *Dck* at steady state did not have a significant impact on AML growth *in vitro*, and I also did not observe notable differences in the cell cycle profile. These findings suggest potential plasticity in the nucleotide salvage and nucleotide *de novo* synthesis pathways. These observations are supported by reports from other groups, in which it was shown that HSCs are more dependent on nucleotide salvage than *de novo* synthesis. However, when *Dck* or *Tk* is depleted, HSCs can switch to predominately *de novo* nucleotide synthesis [364]. It is not known if AML cells have a stronger dependency on one or the other pathway. However, work by others has shown that AML cells are vulnerable to the inhibition of both pathways [205, 366]. The degradation of Dck mediated by Herc1 may become particularly relevant in the context of resistance to Ara-C treatment. When exposed to Ara-C, it is possible that cells utilize proteasomal targeting of Dck as a mechanism to redirect their metabolism toward nucleoside synthesis. This adaptive response may allow cells to evade the effects of nucleoside analogs. For instance, a study by Van Gastel *et al.* demonstrated that AML cells exhibit a heightened dependency on nucleotide synthesis following Ara-C chemotherapy. They also revealed a metabolic bottleneck where AML cells rely on glutamine and aspartate from stroma cells immediately after Ara-C treatment. This study unveiled a novel "switch" in metabolic pathways that compensates for the increased demand for nucleotide synthesis [205, 366]. Furthermore, in pancreatic cells, the depletion of DCK leads to the enrichment of genes associated with MYC,

folate and one-carbon metabolism, and glutamine pathways. This observation suggests a shift in metabolic pathways upon DCK depletion [367].

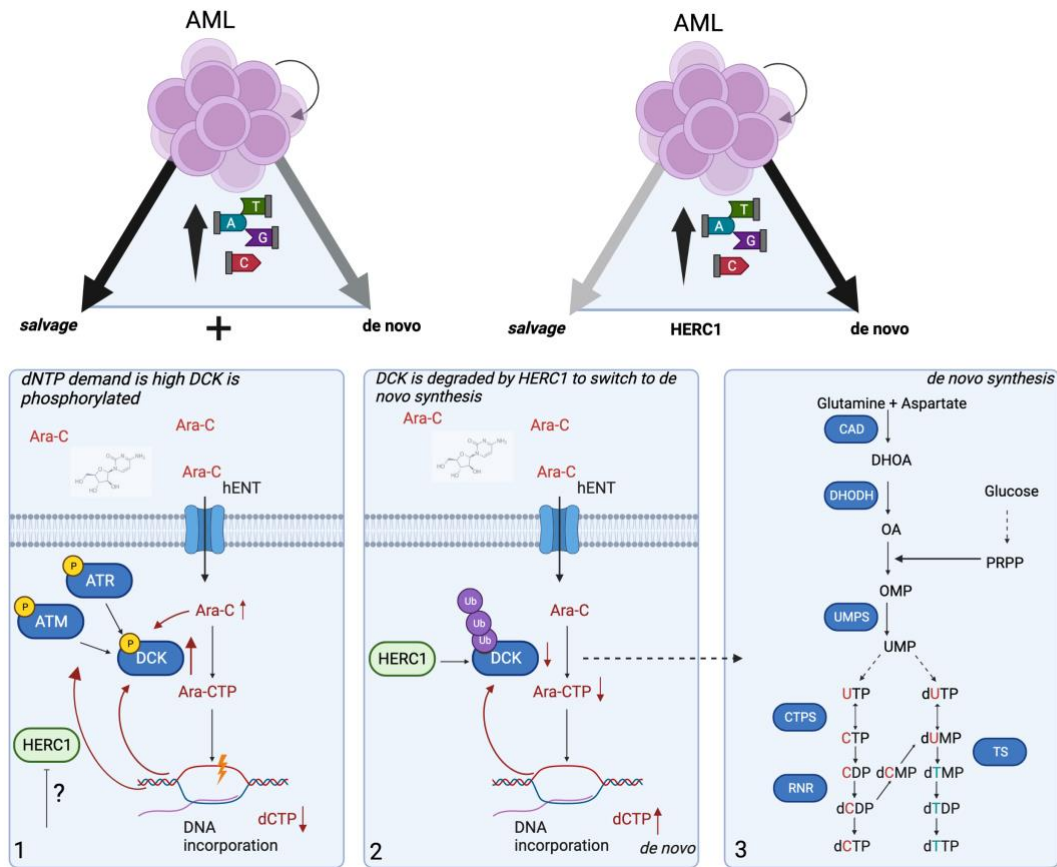


Figure 4.1 Model of the contribution of HERC1 in the nucleotide salvage pathway.

AML cells rely on nucleoside synthesis and the salvage pathway. 1) Replication stress leads to phosphorylation of ATM and ATR, which phosphorylate DCK. DCK phosphorylates Ara-C resulting in incorporation into DNA and apoptosis. 2) To turn down the activity of DCK and switch to *de novo* synthesis, HERC1 degrades DCK. This mechanism could be specifically relevant after long-time exposure of Ara-C and in the context of resistance. 3) AML cells rely predominantly on *de novo* synthesis pathway. Created with BioRender.com.

4.1.6 Potential pleiotropic effects in Herc1-depleted MA cells

Upon conducting a proteomic analysis of Herc1-depleted cells, I observed a notable increase in the levels of several proteins, which were unaltered at the transcriptomic level. In my

genome-wide CRISPR/Cas9 screen, *Dck* emerged as the strongest hit in the resistant arm. However, it is important to acknowledge that loss of *Herc1* could result in a pleiotropic effect that enhances Ara-C sensitivity. This aspect was not considered during our integrative analysis. I noticed an overexpression of proteins that play a crucial role in AML differentiation and maturation, CCAAT Enhancer Binding Protein Epsilon (Cebpe) and the lymphocyte Antigen 6 Family Member G6C) Ly6C2, which are essential for granulocyte and monocyte maturation and differentiation (**Table 2.3 and Table 2.4**) [368-370]. For instance, CEBPE, has been identified as a prognostic factor in several genetic categories of AML, and additionally, research has indicated that CEBPE regulates the expression of members of the S100 family of proteins containing 2 EF-hand calcium-binding motifs A8- and A9 (S100A8) and (S100A9) [368]. My study revealed that S100a8 and S100a9 were overexpressed both at the proteomic and transcriptomic levels, indicating that they are most likely regulated through Cebpe. Additionally, I found that *Herc1* regulates the protein level of a third S100 protein member: S100a11, without any associated changes in the transcriptome. A recent study has found that C/EBP family proteins are only degraded by the proteasome when they are not forming dimers, which could be another potential role for HERC1 in AML [371]. In the future, it will be beneficial to conduct experiments to determine if the observed phenotype is solely influenced by *Dck* or multiple proteins. It is important to mention that previous research has shown that Ara-C triggers differentiation, so there may be additive effects [372]. Furthermore, while my study focused predominantly on post-transcriptional regulation of *Herc1*, RNA-seq in *Herc1*-depleted cells showed that *Herc1* is also involved in transcriptional regulation.

4.1.7 Limitations of the study

While my project aimed to identify genetic regulators of response Ara-C, it is important to note that there are limitations to my research study. I utilized two established murine experimental models that respond to Ara-C, but they have limited genetic heterogeneity and do not fully resemble human AML. Furthermore, my screen was performed *in vitro*; it is possible that the mechanism of sensitivity and resistance is different *in vivo*. Nevertheless, the focus of my screen was to identify chemogenomic interactions rather than gene intrinsic mechanisms of resistance. Another limitation of my study was the selection of two similar murine models of AML, since HoxA9 and Meis1 are overexpressed downstream of the MLL/AF9 fusion. Even though we had <10% of shared genes between both screens, those identified genes may be essential in Hox-driven AML models. To assess whether Herc1 regulates Dck in diverse genetic contexts, additional validation experiments using other models of AML will be necessary. Furthermore, to gain a comprehensive understanding of genetic factors impacting Ara-C sensitivity in human AML, it will be necessary to account for potential inter-species differences.

4.1.8 Therapeutic implications

The findings of my study highlight the significance of proteasomal regulation of Dck by Herc1 and its implication in Ara-C resistance. This underscores the potential advantages of combining Ara-C with proteasomal inhibitors such as Bortezomib to enhance its effectiveness. Bortezomib is used in several hematological malignancies, including multiple myeloma and mantle cell lymphoma. Further studies will be needed to assess if AML patients will benefit from a combination therapy with proteasomal inhibitors. A recent study showed that Bortezomib

treatment effectively prevented the decrease in DCK levels observed in Ara-C-resistant mantle cell lymphoma, suggesting its feasibility in human cancers [373].

4.2 CRISPR/Cas9-based screening approach for the discovery of immune regulatory genes

AML cells are genetically and cellularly heterogeneous, which makes them extremely difficult to target. High-dose chemotherapy is the only curative treatment, which is sometimes combined with targeted therapies such as the FLT3 inhibitor midostaurin [225]. Other targeted therapies are available but exhibit only modest results and some patients carry mutations that are undruggable. Even though AML is very heterogeneous, AML shares unifying biological features and vulnerabilities. For instance, AML cells respond to cues from the microenvironment, which can nurture their growth, protect them from chemotherapy and the immune system. AML is organized hierarchically, with LSCs at the apex, sustaining the disease. LSCs are often difficult to identify and eradicate as they share many cell markers with non-malignant cells and are often quiescent. Recently several groups have shown that LSCs and proliferative AML blasts exhibit metabolic differences, including variations in energy utilization, such as OXPHOS and glycolysis. LSCs for instance, are highly dependent on mitochondrial OXPHOS, whereas proliferative AML utilize glycolysis and less OXPHOS. Those discoveries were highly valuable as they provided opportunities to identify LSCs based on metabolic profiles and offered new therapeutic opportunity. In our previous study, Mercier *et al.* developed a systematic CRISPR/Cas9 based screening method in murine AML *in vivo*, in which we identified valuable insights into AML

biology *in vivo*. Mercier *et al.* identified essential genes related to cell adhesion, metabolism, and immune regulation which we sought to further explore in the context of AML immune biology.

I discovered five genes (*Slc25a19*, *Ankrd52*, *Csfr3r*, *Copg1*, *Cflar*) that are essential in the context of AML immune biology. I found that genetic targeting of the mitochondrial transporter *Slc25a19* sensitizes AML cells to the immune system and further research can be built on the link between metabolic dependencies and the regulation of the immune system in AML.

I was the first to systematically screen for biological vulnerabilities in the context of immune regulation in AML, which builds the foundation for potential cellular therapies. Different groups showed that AML cells developed several strategies to escape from the immune system. I have shown that the loss of genes of the antigen-processing machinery (*Tap1*, *Tap2*, *B2m*, *Tapbp*) sensitizes AML cells to the immune compartment. Others have demonstrated that loss of MHC-I molecules sensitizes cancer cells to NK cells, and it is possible that AML cells could be sensitized through the same mechanism. Interestingly, I found that the loss of *Slc25a19*, a metabolic thiamine transporter provided a very similar immune phenotype compared to the targeting of genes of the antigen-processing machinery. *Slc25a19* has never been studied in the context of AML before, and further questions will need to be answered on how *Slc25a19* sensitizes AML to the immune compartment and how it could be relevant for AML survival. *Slc25a19* is essential to transport thiamine inside the mitochondria, where it is needed as a co-factor for two enzymatic reactions during the TCA cycle. Furthermore, I found that the loss of *Slc25a19* in other CRISPR/Cas9-based drug screens using venetoclax and in my Ara-C screen, is essential [298, 302, 305]. This suggests that loss of *Slc25a19* increases the vulnerability of AML cells to mitochondrial targeting and chemotherapy. A potential explanation could be that the reduced function of the TCA cycle caused

by reduced enzymatic activity of Pdh and Ogdh, is synergistic with metabolic- and chemotherapy by decreasing the apoptotic threshold of AML cells to go into apoptosis. Another explanation on how loss of *Slc25a19* in AML potentially modulates immunogenicity could be through changes in mitochondrial TCA cycle metabolites, causing epigenetic changes. For instance *Slc25a19-Ko* mice and *Slc25a19*-mutant patients are found with elevated levels (10–100 times) of α -ketoglutaric acid, and die, usually by 6 months of age [374, 375]. It has been shown that high levels of α -ketoglutarate (α -KG), has direct impact on gene expression and cell fate decisions in stem cells [376]. α -KG is required for chromatin modifying enzymes like the Jumonji C domain containing lysine demethylases (KDM2-7), and the ten-eleven translocation hydroxylases (TET1-3) [377]. More recently Mangalhar *et al.* have shown that manipulating the mitochondrial electron transport chain (ETC) resulted into elevated levels of succinate. Elevated level of succinate led to transcriptional and epigenetic activation of MHC-I and antigen presentation and processing genes resulting in increased immunogenicity in melanoma [378]. Mangalhar *et al.* revealed that CRISPR-mediated KO of the *ETC transporter II (succinate dehydrogenase (SDH))* caused an increase in MHC-I expression on protein level and significantly increased immune cell (CD45⁺) infiltration, especially CD8⁺ T cells, relative to control tumors. Furthermore, they showed that pharmacological inhibition of *SDH* with 3-nitropropanoic (3-NPA) lead to global epigenetic changes enriched for H3K4me3 and H3K36me3 methylation. MHC-APP genes were significantly enriched for H3K4me3 and H3K36me3 methylation. Interestingly, those epigenetic changes could be reversed through addition of α -KG. Furthermore, the addition of α -KG lead to reduced expression of MHC-I expression levels [378]. In my study, it is possible that loss of *Slc25a19* causes impairment of the enzymes Pdh and Ogdh leading to high level of α -KG, resulting into

epigenetic changes of MHC-I loci and leading to reduced expression. Those changes in MHC-I expression, can lead to increased sensitivity to NK cells.

Further investigation will be needed to determine the level of α -KG in *Slc25a19*-Ko AML cells in plasma or bone marrow. Another recent report has demonstrated that supplementation with α -KG enhances the efficacy of PD1 blockade in melanoma and leads to increased ratios of infiltrating GZMB⁺CD8⁺/CD4⁺ T cells and IFN γ ⁺CD8⁺/CD4⁺ T cells and reduction in suppressive M2 (F4/80⁺CD11b⁺CD206⁺) macrophage subsets [379]. Studies in AML patients have shown that, the immune cell composition is often altered in comparison to healthy patients, therefore it will be crucial to determine if loss of *Slc25a19* changes the composition of immune cells in the bone marrow [209]. Furthermore, our model utilized sublethal irradiation, in immune-competent and -compromised mice, which might affect the cellular BM composition after transplantation in comparison to non-irradiated mice [380].

4.2.1 New potential of cellular immune therapies in the treatment of AML

NK cells are cytotoxic cells, which can lyse various target cells. Upon activation, NK cells release granzyme and perforin to lyse cells, similar to cytotoxic T cells. Moreover, NK cells produce chemokines, cytokines, interferon-gamma (IFN- γ) and tumor necrosis factor-alpha (TNF- α) to modulate the adaptive immune response. A significant finding by Pan *et al.* revealed that AML cells can be specifically targeted for NK cell-mediated killing through the treatment with the BCL-2 inhibitor venetoclax. Pan *et al.* showed recently that mitochondrial priming is a key event regulating NK-mediated tumor cell killing. LSCs, relatively low in ROS, overexpress BCL-2, which makes them vulnerable to venetoclax [186]. LSCs protect themselves from chemotherapy

and irradiation by inhibiting the mitochondrial pro-apoptotic pathway, increasing the apoptotic threshold [186, 381]. BCL-2 protein controls apoptosis through mitochondrial outer membrane permeabilization (MOMP). MOMP can be measured through a functional assay called BH3 profiling, which uses peptides derived from the BH3 domains of proapoptotic proteins of the BCL-2 family to describe the proximity to the apoptotic threshold [382]. BH3-profiling has been used to establish the magnitude of apoptotic priming in various cancers, including AML, predicting the response of various cancer cells to chemotherapy and could be used as a biomarker for cellular NK cell therapies in future [382]. Further studies will be needed to elucidate if loss of *Slc25a19* and mitochondrial metabolic disruption can be used to target LSCs specifically to NK cell-mediated therapy.

Overall, I am curious to see if BH-3 profiling could be tested as a predictive marker on AML patients receiving NK cell therapies. In the past two decades, early clinical trials have demonstrated the overall safety of NK-cell-based immunotherapies, even in the allogeneic setting [383, 384]. Furthermore, early studies by Miller *et al.* demonstrated that NK cell infusion from HLA-haploidentical donors in combination with subcutaneous Interleukin 2 (IL-2) administration after pre-conditioning regimes with high-dose cyclophosphamide and fludarabine resulted in complete remission in 5 out of 19 patients with poor prognosis [385]. More clinical NK-cell trials in which NK cells were tested as consolidation therapy of AML provided evidence that pediatric refractory or relapsed AML patients could benefit from NK cell-based therapies [386] [387].

My CRISPR/Cas9 screen revealed that loss of *Tap1*, *Tap2* and other genes of the antigen-processing machinery sensitized AML cells to immune cells, and I hypothesize that NK cells are the effector cells, like studies in other cancer types [388].

4.2.2 Other immune targets

Nevertheless, the overall infiltration of immune cells in the BM niche and dysregulation through AML cells is another component modulating the success of chemotherapy. A recent study in AML patients found that Interferon type II (IFN- γ) -related genes improved the prediction of chemotherapy along ELN criteria [389]. I further found four other genes *Ankrd52*, *Csfr3r*, *Copg1*, *Cflar* that provide resistance to the immune department. Interestingly, those genes had a smaller dropout between C57BL/6J and NSG overall, suggesting that adaptive immune regulation is not the predominant mechanism of action. For instance, *Copg1* was found by others to negatively regulate T cells in solid cancers through type I interferon (IFN-I) response and STING pathway [390], and *Ankrd52* was found to negatively regulate MHC-I expression [391].

Similarly, with a smaller dropout, I confirmed sensitivity towards the loss of *CD47* and the complement-activating ligand *Cr11*. *Cr11* is highly expressed in HSCs and inhibits complement activation. It has been previously demonstrated that certain members of the complement pathway are connected to the outcomes of patients with AML. This emphasizes the importance of this pathway in the pathobiology of AML [392]. The validation of the CD47-SIRP axis and Cr11 in immune-competent and -compromised mice further support their involvement in the adaptive immune regulation of AML [393, 394].

4.2.3 Limitations of the study

NSG mice lack mature lymphocytes, NK cells and show other impairments of innate immunity, providing a controlled environment to study the effects of immune cell depletion on tumor response [395]. Although this model is frequently used, other mouse models of immune-compromised mice, such as NOD or NUDE mice, may offer opportunities to selectively screen for

T and NK cell-specific markers, thereby expanding the range of potential therapeutic targets. As reported by Vadakekolathu *et al.* the infiltration and landscape of immune cells play a significant role in predicting the success of chemotherapy, survival, and potential immune targeting, further systematic studies will be needed to understand their role in AML biology [389].

4.2.4 Therapeutic implications

The discovery of Slc25a19 holds significant biological importance, as it opens avenues to investigate whether the induction of metabolic stress ultimately results in apoptotic priming *in vivo*, thereby enhancing the recognition of AML cells by the immune system. Notably, the combination of venetoclax with low-dose Ara-C or HMA has shown success in patients who are not eligible for induction therapy. For the future, a potential therapeutic strategy could involve utilizing allogeneic NK cells for adoptive transfer, combined with pre-treatment of AML cells using venetoclax or chemotherapy. This approach could hold promise for enhancing the effectiveness of immune-based therapies in AML.

4.3 Conclusion and summary

In my study, I employed two distinct experimental models of murine AML in conjunction with CRISPR/Cas9-based genetic screening. Through these approaches, I made the significant discovery that proteasomal regulation plays a pivotal role in determining the response of AML cells to Ara-C drug treatment. Furthermore, I successfully identified that the response to Ara-C can be augmented by increasing the protein levels, which is mediated by the ubiquitin ligase Herc1. Consequently, it is possible that stabilizing Dck protein through inhibiting proteasomal activity could serve as a promising therapeutic strategy. This approach holds the potential in reducing the

toxicity associated with Ara-C treatment in elderly patients, or even mitigate the development of drug resistance in AML. In addition, I curated a CRISPR/Cas9-based library, focusing on targeting various components of AML biology *in vivo*. I found that the loss of the mitochondrial transporter *Slc25a19* provides sensitivity to immune cells, which represents a novel finding that may open new avenues for investigating the interplay between AML and immune biology.

5 References

1. Kaushansky, K., *Lineage-specific hematopoietic growth factors*. N Engl J Med, 2006. **354**(19): p. 2034-45.
2. Fliedner, T.M., et al., *Structure and function of bone marrow hemopoiesis: mechanisms of response to ionizing radiation exposure*. Cancer Biother Radiopharm, 2002. **17**(4): p. 405-26.
3. Lee-Six, H., et al., *Population dynamics of normal human blood inferred from somatic mutations*. Nature, 2018. **561**(7724): p. 473-478.
4. Challen, G.A., et al., *Mouse hematopoietic stem cell identification and analysis*. Cytometry A, 2009. **75**(1): p. 14-24.
5. Till, J.E. and E.A. McCulloch, *A Direct Measurement of the Radiation Sensitivity of Normal Mouse Bone Marrow Cells*. Radiation Research, 1961. **14**(2): p. 213-222.
6. Thomas, E.D., et al., *Intravenous Infusion of Bone Marrow in Patients Receiving Radiation and Chemotherapy*. New England Journal of Medicine, 1957. **257**(11): p. 491-496.
7. Hulett, H.R., et al., *Cell sorting: automated separation of mammalian cells as a function of intracellular fluorescence*. Science, 1969. **166**(3906): p. 747-9.
8. Köhler, G. and C. Milstein, *Continuous cultures of fused cells secreting antibody of predefined specificity*. Nature, 1975. **256**(5517): p. 495-7.
9. Baum, C.M., et al., *Isolation of a candidate human hematopoietic stem-cell population*. Proc Natl Acad Sci U S A, 1992. **89**(7): p. 2804-8.
10. Morrison, S.J., N. Uchida, and I.L. Weissman, *The Biology of Hematopoietic Stem Cells*. Annual Review of Cell and Developmental Biology, 1995. **11**(1): p. 35-71.
11. Doulatov, S., et al., *Revised map of the human progenitor hierarchy shows the origin of macrophages and dendritic cells in early lymphoid development*. Nat Immunol, 2010. **11**(7): p. 585-93.
12. Wilson, A., et al., *Hematopoietic Stem Cells Reversibly Switch from Dormancy to Self-Renewal during Homeostasis and Repair*. Cell, 2008. **135**(6): p. 1118-1129.
13. Foudi, A., et al., *Analysis of histone 2B-GFP retention reveals slowly cycling hematopoietic stem cells*. Nat Biotechnol, 2009. **27**(1): p. 84-90.
14. Cabezas-Wallscheid, N., et al., *Identification of regulatory networks in HSCs and their immediate progeny via integrated proteome, transcriptome, and DNA methylome analysis*. Cell Stem Cell, 2014. **15**(4): p. 507-522.
15. Bowie, M.B., et al., *Hematopoietic stem cells proliferate until after birth and show a reversible phase-specific engraftment defect*. J Clin Invest, 2006. **116**(10): p. 2808-16.
16. Ganuza, M., et al., *Murine foetal liver supports limited detectable expansion of life-long haematopoietic progenitors*. Nat Cell Biol, 2022. **24**(10): p. 1475-1486.
17. Bowie, M.B., et al., *Identification of a new intrinsically timed developmental checkpoint that reprograms key hematopoietic stem cell properties*. Proc Natl Acad Sci U S A, 2007. **104**(14): p. 5878-82.
18. Busch, K., et al., *Fundamental properties of unperturbed haematopoiesis from stem cells in vivo*. Nature, 2015. **518**(7540): p. 542-6.

19. Sun, J., et al., *Clonal dynamics of native haematopoiesis*. Nature, 2014. **514**(7522): p. 322-327.
20. Wang, J.C. and J.E. Dick, *Cancer stem cells: lessons from leukemia*. Trends Cell Biol, 2005. **15**(9): p. 494-501.
21. Rodriguez-Fraticelli, A.E., et al., *Clonal analysis of lineage fate in native haematopoiesis*. Nature, 2018. **553**(7687): p. 212-216.
22. Notta, F., et al., *Distinct routes of lineage development reshape the human blood hierarchy across ontogeny*. Science, 2016. **351**(6269): p. aab2116.
23. Wang, J.C.Y., M. Doedens, and J.E. Dick, *Primitive Human Hematopoietic Cells Are Enriched in Cord Blood Compared With Adult Bone Marrow or Mobilized Peripheral Blood as Measured by the Quantitative In Vivo SCID-Repopulating Cell Assay*. Blood, 1997. **89**(11): p. 3919-3924.
24. Mayle, A., et al., *Flow cytometry analysis of murine hematopoietic stem cells*. Cytometry A, 2013. **83**(1): p. 27-37.
25. Kiel, M.J., et al., *Spatial differences in hematopoiesis but not in stem cells indicate a lack of regional patterning in definitive hematopoietic stem cells*. Dev Biol, 2005. **283**(1): p. 29-39.
26. Kiel, M.J., et al., *SLAM family receptors distinguish hematopoietic stem and progenitor cells and reveal endothelial niches for stem cells*. Cell, 2005. **121**(7): p. 1109-21.
27. Schofield, R., *The relationship between the spleen colony-forming cell and the haemopoietic stem cell*. Blood cells, 1978. **4**(1-2): p. 7-25.
28. Pinho, S. and P.S. Frenette, *Haematopoietic stem cell activity and interactions with the niche*. Nat Rev Mol Cell Biol, 2019. **20**(5): p. 303-320.
29. Kricun, M.E., *Red-yellow marrow conversion: Its effect on the location of some solitary bone lesions*. Skeletal Radiology, 1985. **14**(1): p. 10-19.
30. Ding, L., et al., *Endothelial and perivascular cells maintain haematopoietic stem cells*. Nature, 2012. **481**(7382): p. 457-62.
31. Greenbaum, A., et al., *CXCL12 in early mesenchymal progenitors is required for haematopoietic stem-cell maintenance*. Nature, 2013. **495**(7440): p. 227-30.
32. Ding, L. and S.J. Morrison, *Haematopoietic stem cells and early lymphoid progenitors occupy distinct bone marrow niches*. Nature, 2013. **495**(7440): p. 231-235.
33. Scadden, David T., *Nice Neighborhood: Emerging Concepts of the Stem Cell Niche*. Cell, 2014. **157**(1): p. 41-50.
34. Asada, N., et al., *Differential cytokine contributions of perivascular haematopoietic stem cell niches*. Nat Cell Biol, 2017. **19**(3): p. 214-223.
35. Bruns, I., et al., *Megakaryocytes regulate hematopoietic stem cell quiescence through CXCL4 secretion*. Nat Med, 2014. **20**(11): p. 1315-20.
36. Zhao, M., et al., *Megakaryocytes maintain homeostatic quiescence and promote post-injury regeneration of hematopoietic stem cells*. Nat Med, 2014. **20**(11): p. 1321-6.
37. Yamazaki, S., et al., *Nonmyelinating Schwann cells maintain hematopoietic stem cell hibernation in the bone marrow niche*. Cell, 2011. **147**(5): p. 1146-58.
38. Hirata, Y., et al., *CD150(high) Bone Marrow Tregs Maintain Hematopoietic Stem Cell Quiescence and Immune Privilege via Adenosine*. Cell Stem Cell, 2018. **22**(3): p. 445-453.e5.
39. Fujisaki, J., et al., *In vivo imaging of Treg cells providing immune privilege to the haematopoietic stem-cell niche*. Nature, 2011. **474**(7350): p. 216-9.

40. Kuppusamy, P. and J.L. Zweier, *Characterization of free radical generation by xanthine oxidase. Evidence for hydroxyl radical generation.* J Biol Chem, 1989. **264**(17): p. 9880-4.
41. Kino, K., et al., *Generation, repair and replication of guanine oxidation products.* Genes and Environment, 2017. **39**(1): p. 21.
42. Pontel, L.B., et al., *Endogenous Formaldehyde Is a Hematopoietic Stem Cell Genotoxin and Metabolic Carcinogen.* Mol Cell, 2015. **60**(1): p. 177-88.
43. Rossi, D.J., et al., *Deficiencies in DNA damage repair limit the function of haematopoietic stem cells with age.* Nature, 2007. **447**(7145): p. 725-729.
44. Mulderrig, L., et al., *Aldehyde-driven transcriptional stress triggers an anorexic DNA damage response.* Nature, 2021. **600**(7887): p. 158-163.
45. Mohrin, M., et al., *Hematopoietic Stem Cell Quiescence Promotes Error-Prone DNA Repair and Mutagenesis.* Cell Stem Cell, 2010. **7**(2): p. 174-185.
46. Ferrari, G., et al., *Perceived urban environment attributes and obesity indices in adults: an 8-Nation study from Latin America.* Sci Rep, 2022. **12**(1): p. 19598.
47. Mohrin, M., et al., *Hematopoietic stem cell quiescence promotes error-prone DNA repair and mutagenesis.* Cell Stem Cell, 2010. **7**(2): p. 174-85.
48. Beerman, I., et al., *Quiescent hematopoietic stem cells accumulate DNA damage during aging that is repaired upon entry into cell cycle.* Cell Stem Cell, 2014. **15**(1): p. 37-50.
49. Smith, S.M., et al., *Clinical-cytogenetic associations in 306 patients with therapy-related myelodysplasia and myeloid leukemia: the University of Chicago series.* Blood, 2003. **102**(1): p. 43-52.
50. Fischer, K., et al., *Molecular cytogenetic delineation of deletions and translocations involving chromosome band 7q22 in myeloid leukemias.* Blood, 1997. **89**(6): p. 2036-41.
51. Dohner, K., et al., *Molecular cytogenetic characterization of a critical region in bands 7q35-q36 commonly deleted in malignant myeloid disorders.* Blood, 1998. **92**(11): p. 4031-5.
52. Kayser, S., et al., *The impact of therapy-related acute myeloid leukemia (AML) on outcome in 2853 adult patients with newly diagnosed AML.* Blood, 2011. **117**(7): p. 2137-45.
53. Ceccaldi, R., P. Sarangi, and A.D. D'Andrea, *The Fanconi anaemia pathway: new players and new functions.* Nat Rev Mol Cell Biol, 2016. **17**(6): p. 337-49.
54. Hodskinson, M.R., et al., *Alcohol-derived DNA crosslinks are repaired by two distinct mechanisms.* Nature, 2020. **579**(7800): p. 603-608.
55. Ito, K., et al., *Regulation of oxidative stress by ATM is required for self-renewal of haematopoietic stem cells.* Nature, 2004. **431**(7011): p. 997-1002.
56. Young, A.L., et al., *Clonal haematopoiesis harbouring AML-associated mutations is ubiquitous in healthy adults.* Nat Commun, 2016. **7**: p. 12484.
57. Welch, John S., et al., *The Origin and Evolution of Mutations in Acute Myeloid Leukemia.* Cell, 2012. **150**(2): p. 264-278.
58. Jaiswal, S. and B.L. Ebert, *Clonal hematopoiesis in human aging and disease.* Science, 2019. **366**(6465): p. eaan4673.
59. Xie, M., et al., *Age-related mutations associated with clonal hematopoietic expansion and malignancies.* Nat Med, 2014. **20**(12): p. 1472-8.
60. Genovese, G., et al., *Clonal hematopoiesis and blood-cancer risk inferred from blood DNA sequence.* N Engl J Med, 2014. **371**(26): p. 2477-87.

61. Jaiswal, S., et al., *Age-related clonal hematopoiesis associated with adverse outcomes*. N Engl J Med, 2014. **371**(26): p. 2488-98.
62. Buscarlet, M., et al., *DNMT3A and TET2 dominate clonal hematopoiesis and demonstrate benign phenotypes and different genetic predispositions*. Blood, 2017. **130**(6): p. 753-762.
63. Cimmino, L., et al., *Restoration of TET2 Function Blocks Aberrant Self-Renewal and Leukemia Progression*. Cell, 2017. **170**(6): p. 1079-1095.e20.
64. Guillaumot, M., L. Cimmino, and I. Aifantis, *The Impact of DNA Methylation in Hematopoietic Malignancies*. Trends Cancer, 2016. **2**(2): p. 70-83.
65. Gillis, N.K., et al., *Clonal haemopoiesis and therapy-related myeloid malignancies in elderly patients: a proof-of-concept, case-control study*. Lancet Oncol, 2017. **18**(1): p. 112-121.
66. Gibson, C.J., et al., *Clonal Hematopoiesis Associated With Adverse Outcomes After Autologous Stem-Cell Transplantation for Lymphoma*. J Clin Oncol, 2017. **35**(14): p. 1598-1605.
67. Takahashi, K., et al., *Preleukaemic clonal haemopoiesis and risk of therapy-related myeloid neoplasms: a case-control study*. Lancet Oncol, 2017. **18**(1): p. 100-111.
68. Hormaechea-Agulla, D., et al., *Chronic infection drives Dnmt3a-loss-of-function clonal hematopoiesis via IFN γ signaling*. Cell Stem Cell, 2021. **28**(8): p. 1428-1442.e6.
69. Arber, D.A., et al., *International Consensus Classification of Myeloid Neoplasms and Acute Leukemias: integrating morphologic, clinical, and genomic data*. Blood, 2022. **140**(11): p. 1200-1228.
70. Mughal, T.I., et al., *Current pre-clinical and clinical advances in the BCR-ABL1-positive and -negative chronic myeloproliferative neoplasms*. Haematologica, 2014. **99**(5): p. 797-801.
71. Soverini, S., et al., *Chronic myeloid leukemia: the paradigm of targeting oncogenic tyrosine kinase signaling and counteracting resistance for successful cancer therapy*. Molecular Cancer, 2018. **17**(1): p. 49.
72. Hochhaus, A., et al., *European LeukemiaNet 2020 recommendations for treating chronic myeloid leukemia*. Leukemia, 2020. **34**(4): p. 966-984.
73. Rowley, J.D., *A New Consistent Chromosomal Abnormality in Chronic Myelogenous Leukaemia identified by Quinacrine Fluorescence and Giemsa Staining*. Nature, 1973. **243**(5405): p. 290-293.
74. Sawyers, C.L., *Chronic Myeloid Leukemia*. New England Journal of Medicine, 1999. **340**(17): p. 1330-1340.
75. Greenfield, G., M.F. McMullin, and K. Mills, *Molecular pathogenesis of the myeloproliferative neoplasms*. Journal of Hematology & Oncology, 2021. **14**(1): p. 103.
76. Estey, E., R.P. Hasserjian, and H. Dohner, *Distinguishing AML from MDS: a fixed blast percentage may no longer be optimal*. Blood, 2022. **139**(3): p. 323-332.
77. Leone, G., et al., *The incidence of secondary leukemias*. Haematologica, 1999. **84**(10): p. 937-45.
78. Bonnet, D. and J.E. Dick, *Human acute myeloid leukemia is organized as a hierarchy that originates from a primitive hematopoietic cell*. Nat Med, 1997. **3**(7): p. 730-7.
79. Dohner, H., et al., *Diagnosis and management of AML in adults: 2022 recommendations from an international expert panel on behalf of the ELN*. Blood, 2022. **140**(12): p. 1345-1377.

80. SEER. *Surveillance, Epidemiology, and End Results (SEER) Program* (www.seer.cancer.gov) *SEER*Stat Database: Incidence - SEER Research Data, 8 Registries, Nov 2021 Sub (1975-2020) - Linked To County Attributes - Time Dependent (1990-2020) Income/Rurality, 1969-2020 Counties, National Cancer Institute, DCCPS, Surveillance Research Program, released April 2023, based on the November 2022 submission.* 2021.
81. Bolouri, H., et al., *The molecular landscape of pediatric acute myeloid leukemia reveals recurrent structural alterations and age-specific mutational interactions.* *Nature Medicine*, 2018. **24**(1): p. 103-112.
82. Papaemmanuil, E., et al., *Genomic Classification and Prognosis in Acute Myeloid Leukemia.* *N Engl J Med*, 2016. **374**(23): p. 2209-2221.
83. Vassiliou, G.S., et al., *Mutant nucleophosmin and cooperating pathways drive leukemia initiation and progression in mice.* *Nat Genet*, 2011. **43**(5): p. 470-5.
84. Challen, G.A., et al., *Dnmt3a is essential for hematopoietic stem cell differentiation.* *Nat Genet*, 2011. **44**(1): p. 23-31.
85. Mallardo, M., et al., *NPMc+ and FLT3_ITD mutations cooperate in inducing acute leukaemia in a novel mouse model.* *Leukemia*, 2013. **27**(11): p. 2248-2251.
86. Shlush, L.I., et al., *Identification of pre-leukaemic haematopoietic stem cells in acute leukaemia.* *Nature*, 2014. **506**(7488): p. 328-33.
87. Kirtonia, A., et al., *A comprehensive review of genetic alterations and molecular targeted therapies for the implementation of personalized medicine in acute myeloid leukemia.* *Journal of Molecular Medicine*, 2020. **98**(8): p. 1069-1091.
88. TCGA, *Genomic and Epigenomic Landscapes of Adult De Novo Acute Myeloid Leukemia.* *New England Journal of Medicine*, 2013. **368**(22): p. 2059-2074.
89. Ma, X., et al., *Pan-cancer genome and transcriptome analyses of 1,699 paediatric leukaemias and solid tumours.* *Nature*, 2018. **555**(7696): p. 371-376.
90. Dang, L., et al., *Cancer-associated IDH1 mutations produce 2-hydroxyglutarate.* *Nature*, 2009. **462**(7274): p. 739-44.
91. Ostrander, E.L., et al., *Divergent Effects of Dnmt3a and Tet2 Mutations on Hematopoietic Progenitor Cell Fitness.* *Stem Cell Reports*, 2020. **14**(4): p. 551-560.
92. Yagi, M., et al., *Identification of distinct loci for de novo DNA methylation by DNMT3A and DNMT3B during mammalian development.* *Nature Communications*, 2020. **11**(1): p. 3199.
93. Doi, A., et al., *Differential methylation of tissue- and cancer-specific CpG island shores distinguishes human induced pluripotent stem cells, embryonic stem cells and fibroblasts.* *Nat Genet*, 2009. **41**(12): p. 1350-3.
94. Moran-Crusio, K., et al., *Tet2 loss leads to increased hematopoietic stem cell self-renewal and myeloid transformation.* *Cancer Cell*, 2011. **20**(1): p. 11-24.
95. Quivoron, C., et al., *TET2 inactivation results in pleiotropic hematopoietic abnormalities in mouse and is a recurrent event during human lymphomagenesis.* *Cancer Cell*, 2011. **20**(1): p. 25-38.
96. Ko, M., et al., *Ten-Eleven-Translocation 2 (TET2) negatively regulates homeostasis and differentiation of hematopoietic stem cells in mice.* *Proc Natl Acad Sci U S A*, 2011. **108**(35): p. 14566-71.
97. Li, Z., et al., *Deletion of Tet2 in mice leads to dysregulated hematopoietic stem cells and subsequent development of myeloid malignancies.* *Blood*, 2011. **118**(17): p. 4509-18.

98. Buscarlet, M., et al., *Lineage restriction analyses in CHIP indicate myeloid bias for TET2 and multipotent stem cell origin for DNMT3A*. Blood, 2018. **132**(3): p. 277-280.
99. Steudel, C., et al., *Comparative analysis of MLL partial tandem duplication and FLT3 internal tandem duplication mutations in 956 adult patients with acute myeloid leukemia*. Genes Chromosomes Cancer, 2003. **37**(3): p. 237-51.
100. Caligiuri, M.A., et al., *Molecular rearrangement of the ALL-1 gene in acute myeloid leukemia without cytogenetic evidence of 11q23 chromosomal translocations*. Cancer Res, 1994. **54**(2): p. 370-3.
101. Tkachuk, D.C., S. Kohler, and M.L. Cleary, *Involvement of a homolog of Drosophila trithorax by 11q23 chromosomal translocations in acute leukemias*. Cell, 1992. **71**(4): p. 691-700.
102. Meyer, C., et al., *The KMT2A recombinome of acute leukemias in 2023*. Leukemia, 2023. **37**(5): p. 988-1005.
103. Krivtsov, A.V., et al., *Cell of origin determines clinically relevant subtypes of MLL-rearranged AML*. Leukemia, 2013. **27**(4): p. 852-60.
104. Alexander, F.E., et al., *Transplacental chemical exposure and risk of infant leukemia with MLL gene fusion*. Cancer Res, 2001. **61**(6): p. 2542-6.
105. Bariar, B., et al., *Bioflavonoids promote stable translocations between MLL-AF9 breakpoint cluster regions independent of normal chromosomal context: Model system to screen environmental risks*. Environ Mol Mutagen, 2019. **60**(2): p. 154-167.
106. Ford, A.M., et al., *In utero rearrangements in the trithorax-related oncogene in infant leukaemias*. Nature, 1993. **363**(6427): p. 358-360.
107. Abdel-Wahab, O., et al., *Deletion of Asx11 results in myelodysplasia and severe developmental defects in vivo*. J Exp Med, 2013. **210**(12): p. 2641-59.
108. Abdel-Wahab, O., et al., *Deletion of Asx11 results in myelodysplasia and severe developmental defects in vivo*. Journal of Experimental Medicine, 2013. **210**(12): p. 2641-2659.
109. Abdel-Wahab, O., et al., *ASXL1 mutations promote myeloid transformation through loss of PRC2-mediated gene repression*. Cancer Cell, 2012. **22**(2): p. 180-93.
110. Falini, B., et al., *Altered nucleophosmin transport in acute myeloid leukaemia with mutated NPM1: molecular basis and clinical implications*. Leukemia, 2009. **23**(10): p. 1731-43.
111. Network, T.C.G.A., *Genomic and Epigenomic Landscapes of Adult De Novo Acute Myeloid Leukemia*. New England Journal of Medicine, 2013. **368**(22): p. 2059-2074.
112. Okuda, M., et al., *Nucleophosmin/B23 is a target of CDK2/cyclin E in centrosome duplication*. Cell, 2000. **103**(1): p. 127-40.
113. Okuwaki, M., *The structure and functions of NPM1/Nucleophosmin/B23, a multifunctional nucleolar acidic protein*. J Biochem, 2008. **143**(4): p. 441-8.
114. Yu, Y., et al., *Nucleophosmin is essential for ribosomal protein L5 nuclear export*. Mol Cell Biol, 2006. **26**(10): p. 3798-809.
115. Nachmani, D., et al., *Germline NPM1 mutations lead to altered rRNA 2'-O-methylation and cause dyskeratosis congenita*. Nat Genet, 2019. **51**(10): p. 1518-1529.
116. Mitrea, D.M., et al., *Nucleophosmin integrates within the nucleolus via multi-modal interactions with proteins displaying R-rich linear motifs and rRNA*. eLife, 2016. **5**: p. e13571.

117. Feric, M., et al., *Coexisting Liquid Phases Underlie Nucleolar Subcompartments*. Cell, 2016. **165**(7): p. 1686-1697.
118. Mitrea, D.M., et al., *Self-interaction of NPM1 modulates multiple mechanisms of liquid-liquid phase separation*. Nature Communications, 2018. **9**(1): p. 842.
119. Gu, X., et al., *Leukemogenic nucleophosmin mutation disrupts the transcription factor hub that regulates granulomonocytic fates*. The Journal of Clinical Investigation, 2018. **128**(10): p. 4260-4279.
120. Alcalay, M., et al., *Acute myeloid leukemia bearing cytoplasmic nucleophosmin (NPMc+ AML) shows a distinct gene expression profile characterized by up-regulation of genes involved in stem-cell maintenance*. Blood, 2005. **106**(3): p. 899-902.
121. Brunetti, L., et al., *Mutant NPM1 Maintains the Leukemic State through HOX Expression*. Cancer Cell, 2018. **34**(3): p. 499-512.e9.
122. Falini, B., et al., *NPM1-mutated acute myeloid leukemia: from bench to bedside*. Blood, 2020. **136**(15): p. 1707-1721.
123. Tzelepis, K., et al., *A CRISPR Dropout Screen Identifies Genetic Vulnerabilities and Therapeutic Targets in Acute Myeloid Leukemia*. Cell Rep, 2016. **17**(4): p. 1193-1205.
124. Dovey, O.M., et al., *Molecular synergy underlies the co-occurrence patterns and phenotype of NPM1-mutant acute myeloid leukemia*. Blood, 2017. **130**(17): p. 1911-1922.
125. Wang, T., et al., *Gene Essentiality Profiling Reveals Gene Networks and Synthetic Lethal Interactions with Oncogenic Ras*. Cell, 2017. **168**(5): p. 890-903.e15.
126. Wiktorin, H.G., et al., *Mutated NPM1 in combination with overexpression of Meis1 or Hoxa9 is not sufficient to induce acute myeloid leukemia*. Experimental Hematology & Oncology, 2016. **5**(1): p. 25.
127. Mupo, A., et al., *A powerful molecular synergy between mutant Nucleophosmin and Flt3-ITD drives acute myeloid leukemia in mice*. Leukemia, 2013. **27**(9): p. 1917-1920.
128. Kiyoi, H., et al., *Mechanism of constitutive activation of FLT3 with internal tandem duplication in the juxtamembrane domain*. Oncogene, 2002. **21**(16): p. 2555-63.
129. Chu, S.H., et al., *FLT3-ITD knockin impairs hematopoietic stem cell quiescence/homeostasis, leading to myeloproliferative neoplasm*. Cell Stem Cell, 2012. **11**(3): p. 346-58.
130. Niparuck, P., et al., *TP53 mutation in newly diagnosed acute myeloid leukemia and myelodysplastic syndrome*. Diagnostic Pathology, 2021. **16**(1): p. 100.
131. Seifert, H., et al., *The prognostic impact of 17p (p53) deletion in 2272 adults with acute myeloid leukemia*. Leukemia, 2009. **23**(4): p. 656-663.
132. Papaemmanuil, E., et al., *Genomic Classification and Prognosis in Acute Myeloid Leukemia*. N Engl J Med, 2016. **374**(23): p. 2209-2221.
133. Patel, J.P., et al., *Prognostic Relevance of Integrated Genetic Profiling in Acute Myeloid Leukemia*. New England Journal of Medicine, 2012. **366**(12): p. 1079-1089.
134. Pan, X., et al., *Prognostic Impact of WT1 Mutation on AML of Different Risk Groups Based on 2022 European Leukemianet (ELN) Risk Classification*. Blood, 2022. **140**(Supplement 1): p. 3216-3217.
135. Downing, J.R., *The core-binding factor leukemias: lessons learned from murine models*. Curr Opin Genet Dev, 2003. **13**(1): p. 48-54.

136. Ogawa, E., et al., *PEBP2/PEA2 represents a family of transcription factors homologous to the products of the Drosophila runt gene and the human AML1 gene*. Proc Natl Acad Sci U S A, 1993. **90**(14): p. 6859-63.
137. Ogawa, E., et al., *Molecular cloning and characterization of PEBP2 beta, the heterodimeric partner of a novel Drosophila runt-related DNA binding protein PEBP2 alpha*. Virology, 1993. **194**(1): p. 314-31.
138. Wang, S., et al., *Cloning and characterization of subunits of the T-cell receptor and murine leukemia virus enhancer core-binding factor*. Mol Cell Biol, 1993. **13**(6): p. 3324-39.
139. Pabst, T., et al., *AML1-ETO downregulates the granulocytic differentiation factor C/EBPalpha in t(8;21) myeloid leukemia*. Nat Med, 2001. **7**(4): p. 444-51.
140. Lukasik, S.M., et al., *Altered affinity of CBFβ-SMMHC for Runx1 explains its role in leukemogenesis*. Nature Structural Biology, 2002. **9**(9): p. 674-679.
141. de The, H., et al., *The t(15;17) translocation of acute promyelocytic leukaemia fuses the retinoic acid receptor alpha gene to a novel transcribed locus*. Nature, 1990. **347**(6293): p. 558-61.
142. Grignani, F., et al., *The acute promyelocytic leukemia-specific PML-RAR alpha fusion protein inhibits differentiation and promotes survival of myeloid precursor cells*. Cell, 1993. **74**(3): p. 423-31.
143. Grignani, F., et al., *Fusion proteins of the retinoic acid receptor-alpha recruit histone deacetylase in promyelocytic leukaemia*. Nature, 1998. **391**(6669): p. 815-8.
144. Wang, K., et al., *PML/RARalpha targets promoter regions containing PU.1 consensus and RARE half sites in acute promyelocytic leukemia*. Cancer Cell, 2010. **17**(2): p. 186-97.
145. Martens, J.H., et al., *PML-RARalpha/RXR Alters the Epigenetic Landscape in Acute Promyelocytic Leukemia*. Cancer Cell, 2010. **17**(2): p. 173-85.
146. Hadjimichael, C., et al., *Promyelocytic Leukemia Protein Is an Essential Regulator of Stem Cell Pluripotency and Somatic Cell Reprogramming*. Stem Cell Reports, 2017. **8**(5): p. 1366-1378.
147. Huang, M., et al., *Use of all-trans retinoic acid in the treatment of acute promyelocytic leukemia*. Blood, 1988. **72**(2): p. 567-572.
148. Zhu, J., et al., *Arsenic-induced PML targeting onto nuclear bodies: implications for the treatment of acute promyelocytic leukemia*. Proc Natl Acad Sci U S A, 1997. **94**(8): p. 3978-83.
149. Zhu, J., et al., *Retinoic acid induces proteasome-dependent degradation of retinoic acid receptor alpha (RARalpha) and oncogenic RARalpha fusion proteins*. Proc Natl Acad Sci U S A, 1999. **96**(26): p. 14807-12.
150. Zhang, X.-W., et al., *Arsenic Trioxide Controls the Fate of the PML-RAR β Oncoprotein by Directly Binding PML*. Science, 2010. **328**(5975): p. 240-243.
151. Godley, L.A., *Inherited predisposition to acute myeloid leukemia*. Semin Hematol, 2014. **51**(4): p. 306-21.
152. Papaemmanuil, E., H. Dohner, and P.J. Campbell, *Genomic Classification in Acute Myeloid Leukemia*. N Engl J Med, 2016. **375**(9): p. 900-1.
153. Koschmieder, S., et al., *Dysregulation of the C/EBPalpha differentiation pathway in human cancer*. J Clin Oncol, 2009. **27**(4): p. 619-28.

154. Gerritsen, M., et al., *RUNX1 mutations enhance self-renewal and block granulocytic differentiation in human in vitro models and primary AMLs*. Blood Advances, 2019. **3**(3): p. 320-332.
155. Shih, A.H., et al., *Mutational analysis of therapy-related myelodysplastic syndromes and acute myelogenous leukemia*. Haematologica, 2013. **98**(6): p. 908-12.
156. Kim, E., et al., *SRSF2 Mutations Contribute to Myelodysplasia by Mutant-Specific Effects on Exon Recognition*. Cancer Cell, 2015. **27**(5): p. 617-30.
157. Lindsley, R.C., et al., *Acute myeloid leukemia ontogeny is defined by distinct somatic mutations*. Blood, 2015. **125**(9): p. 1367-1376.
158. Reinig, E., et al., *Targeted Next-Generation Sequencing in Myelodysplastic Syndrome and Chronic Myelomonocytic Leukemia Aids Diagnosis in Challenging Cases and Identifies Frequent Spliceosome Mutations in Transformed Acute Myeloid Leukemia*. American Journal of Clinical Pathology, 2016. **145**(4): p. 497-506.
159. Yoshida, K., et al., *Frequent pathway mutations of splicing machinery in myelodysplasia*. Nature, 2011. **478**(7367): p. 64-69.
160. Wahl, M.C., C.L. Will, and R. Lührmann, *The Spliceosome: Design Principles of a Dynamic RNP Machine*. Cell, 2009. **136**(4): p. 701-718.
161. Rivera, O.D., et al., *Alternative splicing redefines landscape of commonly mutated genes in acute myeloid leukemia*. Proceedings of the National Academy of Sciences, 2021. **118**(15): p. e2014967118.
162. Yoshimi, A., et al., *Coordinated alterations in RNA splicing and epigenetic regulation drive leukaemogenesis*. Nature, 2019. **574**(7777): p. 273-277.
163. Waldman, T., *Emerging themes in cohesin cancer biology*. Nature Reviews Cancer, 2020. **20**(9): p. 504-515.
164. Mullenders, J., et al., *Cohesin loss alters adult hematopoietic stem cell homeostasis, leading to myeloproliferative neoplasms*. Journal of Experimental Medicine, 2015. **212**(11): p. 1833-1850.
165. Viny, A.D., et al., *Dose-dependent role of the cohesin complex in normal and malignant hematopoiesis*. Journal of Experimental Medicine, 2015. **212**(11): p. 1819-1832.
166. Kfoury, Y., F. Mercier, and D.T. Scadden, *SnapShot: The hematopoietic stem cell niche*. Cell, 2014. **158**(1): p. 228-228.e1.
167. Baryawno, N., et al., *A Cellular Taxonomy of the Bone Marrow Stroma in Homeostasis and Leukemia*. Cell, 2019. **177**(7): p. 1915-1932.e16.
168. Bonnet, D., et al., *Cytokine treatment or accessory cells are required to initiate engraftment of purified primitive human hematopoietic cells transplanted at limiting doses into NOD/SCID mice*. Bone Marrow Transplant, 1999. **23**(3): p. 203-9.
169. Méndez-Ferrer, S., et al., *Bone marrow niches in haematological malignancies*. Nat Rev Cancer, 2020. **20**(5): p. 285-298.
170. Forte, D., et al., *Bone Marrow Mesenchymal Stem Cells Support Acute Myeloid Leukemia Bioenergetics and Enhance Antioxidant Defense and Escape from Chemotherapy*. Cell Metabolism, 2020. **32**(5): p. 829-843.e9.
171. Ishikawa, F., et al., *Chemotherapy-resistant human AML stem cells home to and engraft within the bone-marrow endosteal region*. Nat Biotechnol, 2007. **25**(11): p. 1315-21.
172. Griessinger, E., et al., *A niche-like culture system allowing the maintenance of primary human acute myeloid leukemia-initiating cells: a new tool to decipher their*

- chemoresistance and self-renewal mechanisms*. Stem Cells Transl Med, 2014. **3**(4): p. 520-9.
173. Duarte, D., et al., *Inhibition of Endosteal Vascular Niche Remodeling Rescues Hematopoietic Stem Cell Loss in AML*. Cell Stem Cell, 2018. **22**(1): p. 64-77.e6.
 174. Hanoun, M., et al., *Acute Myelogenous Leukemia-Induced Sympathetic Neuropathy Promotes Malignancy in an Altered Hematopoietic Stem Cell Niche*. Cell Stem Cell, 2014. **15**(3): p. 365-375.
 175. Forte, D., et al., *Bone Marrow Mesenchymal Stem Cells Support Acute Myeloid Leukemia Bioenergetics and Enhance Antioxidant Defense and Escape from Chemotherapy*. Cell Metab, 2020. **32**(5): p. 829-843 e9.
 176. Ho, Y.H., et al., *Remodeling of Bone Marrow Hematopoietic Stem Cell Niches Promotes Myeloid Cell Expansion during Premature or Physiological Aging*. Cell Stem Cell, 2019. **25**(3): p. 407-418.e6.
 177. Mitchell, C.A., et al., *Stromal niche inflammation mediated by IL-1 signalling is a targetable driver of haematopoietic ageing*. Nat Cell Biol, 2023. **25**(1): p. 30-41.
 178. Flores-Figueroa, E., et al., *In vitro characterization of hematopoietic microenvironment cells from patients with myelodysplastic syndrome*. Leuk Res, 2002. **26**(7): p. 677-86.
 179. Raaijmakers, M.H., et al., *Bone progenitor dysfunction induces myelodysplasia and secondary leukaemia*. Nature, 2010. **464**(7290): p. 852-7.
 180. Zambetti, N.A., et al., *Mesenchymal Inflammation Drives Genotoxic Stress in Hematopoietic Stem Cells and Predicts Disease Evolution in Human Pre-leukemia*. Cell Stem Cell, 2016. **19**(5): p. 613-627.
 181. Kode, A., et al., *Leukaemogenesis induced by an activating β -catenin mutation in osteoblasts*. Nature, 2014. **506**(7487): p. 240-4.
 182. Bhagat, T.D., et al., *Epigenetically Aberrant Stroma in MDS Propagates Disease via Wnt/ β -Catenin Activation*. Cancer Res, 2017. **77**(18): p. 4846-4857.
 183. Sala-Torra, O., et al., *Evidence of donor-derived hematologic malignancies after hematopoietic stem cell transplantation*. Biol Blood Marrow Transplant, 2006. **12**(5): p. 511-7.
 184. Hanahan, D., *Hallmarks of Cancer: New Dimensions*. Cancer Discovery, 2022. **12**(1): p. 31-46.
 185. Poulain, L., et al., *High mTORC1 activity drives glycolysis addiction and sensitivity to G6PD inhibition in acute myeloid leukemia cells*. Leukemia, 2017. **31**(11): p. 2326-2335.
 186. Lagadinou, Eleni D., et al., *BCL-2 Inhibition Targets Oxidative Phosphorylation and Selectively Eradicates Quiescent Human Leukemia Stem Cells*. Cell Stem Cell, 2013. **12**(3): p. 329-341.
 187. Herst, P.M., et al., *The level of glycolytic metabolism in acute myeloid leukemia blasts at diagnosis is prognostic for clinical outcome*. Journal of Leukocyte Biology, 2010. **89**(1): p. 51-55.
 188. Mesbahi, Y., et al., *Exploring the Metabolic Landscape of AML: From Haematopoietic Stem Cells to Myeloblasts and Leukaemic Stem Cells*. Front Oncol, 2022. **12**: p. 807266.
 189. Wang, Y.-H., et al., *Cell-State-Specific Metabolic Dependency in Hematopoiesis and Leukemogenesis*. Cell, 2014. **158**(6): p. 1309-1323.
 190. Tirado, H.A., et al., *Metabolic crosstalk between stromal and malignant cells in the bone marrow niche*. Bone Rep, 2023. **18**: p. 101669.

191. Hao, X., et al., *Metabolic Imaging Reveals a Unique Preference of Symmetric Cell Division and Homing of Leukemia-Initiating Cells in an Endosteal Niche*. *Cell Metabolism*, 2019. **29**(4): p. 950-965.e6.
192. Mercier, F.E., et al., *In vivo genome-wide CRISPR screening in murine acute myeloid leukemia uncovers microenvironmental dependencies*. *Blood Adv*, 2022. **6**(17): p. 5072-5084.
193. Nelson, M.A.M., et al., *Intrinsic OXPHOS limitations underlie cellular bioenergetics in leukemia*. *eLife*, 2021. **10**: p. e63104.
194. Jones, C.L., et al., *Inhibition of Amino Acid Metabolism Selectively Targets Human Leukemia Stem Cells*. *Cancer Cell*, 2018. **34**(5): p. 724-740.e4.
195. Pei, S., et al., *AMPK/FIS1-Mediated Mitophagy Is Required for Self-Renewal of Human AML Stem Cells*. *Cell Stem Cell*, 2018. **23**(1): p. 86-100.e6.
196. Saito, Y., et al., *AMPK Protects Leukemia-Initiating Cells in Myeloid Leukemias from Metabolic Stress in the Bone Marrow*. *Cell Stem Cell*, 2015. **17**(5): p. 585-96.
197. Chan, S.M., et al., *Isocitrate dehydrogenase 1 and 2 mutations induce BCL-2 dependence in acute myeloid leukemia*. *Nat Med*, 2015. **21**(2): p. 178-84.
198. German, N.J., et al., *PHD3 Loss in Cancer Enables Metabolic Reliance on Fatty Acid Oxidation via Deactivation of ACC2*. *Mol Cell*, 2016. **63**(6): p. 1006-20.
199. Tcheng, M., et al., *Very long chain fatty acid metabolism is required in acute myeloid leukemia*. *Blood*, 2021. **137**(25): p. 3518-3532.
200. Samudio, I., et al., *Pharmacologic inhibition of fatty acid oxidation sensitizes human leukemia cells to apoptosis induction*. *J Clin Invest*, 2010. **120**(1): p. 142-56.
201. Stevens, B.M., et al., *Fatty acid metabolism underlies venetoclax resistance in acute myeloid leukemia stem cells*. *Nat Cancer*, 2020. **1**(12): p. 1176-1187.
202. Tabe, Y., et al., *Bone Marrow Adipocytes Facilitate Fatty Acid Oxidation Activating AMPK and a Transcriptional Network Supporting Survival of Acute Monocytic Leukemia Cells*. *Cancer Res*, 2017. **77**(6): p. 1453-1464.
203. Shafat, M.S., et al., *Leukemic blasts program bone marrow adipocytes to generate a protumoral microenvironment*. *Blood*, 2017. **129**(10): p. 1320-1332.
204. Lu, W., et al., *Growth differentiation factor 15 contributes to marrow adipocyte remodeling in response to the growth of leukemic cells*. *J Exp Clin Cancer Res*, 2018. **37**(1): p. 66.
205. van Gastel, N., et al., *Induction of a Timed Metabolic Collapse to Overcome Cancer Chemoresistance*. *Cell Metabolism*, 2020. **32**(3): p. 391-403.e6.
206. Zhao, E., et al., *Bone marrow and the control of immunity*. *Cellular & Molecular Immunology*, 2012. **9**(1): p. 11-19.
207. Khaldoyanidi, S., et al., *Immune Biology of Acute Myeloid Leukemia: Implications for Immunotherapy*. *Journal of Clinical Oncology*, 2021. **39**(5): p. 419-432.
208. Vago, L. and I. Gojo, *Immune escape and immunotherapy of acute myeloid leukemia*. *The Journal of Clinical Investigation*, 2020. **130**(4): p. 1552-1564.
209. Serroukh, Y., et al., *Blasts in context: the impact of the immune environment on acute myeloid leukemia prognosis and treatment*. *Blood Rev*, 2023. **57**: p. 100991.
210. Curti, A., et al., *Modulation of tryptophan catabolism by human leukemic cells results in the conversion of CD25⁻ into CD25⁺ T regulatory cells*. *Blood*, 2006. **109**(7): p. 2871-2877.

211. Rutella, S., et al., *Immune dysfunction signatures predict outcomes and define checkpoint blockade-unresponsive microenvironments in acute myeloid leukemia*. J Clin Invest, 2022. **132**(21).
212. Lion, E., et al., *Natural killer cell immune escape in acute myeloid leukemia*. Leukemia, 2012. **26**(9): p. 2019-2026.
213. Kate, S., et al., *Leukemia-induced phenotypic and functional defects in natural killer cells predict failure to achieve remission in acute myeloid leukemia*. Haematologica, 2014. **99**(5): p. 836-847.
214. Paczulla, A.M., et al., *Absence of NKG2D ligands defines leukaemia stem cells and mediates their immune evasion*. Nature, 2019. **572**(7768): p. 254-259.
215. Christopher, M.J., et al., *Immune Escape of Relapsed AML Cells after Allogeneic Transplantation*. New England Journal of Medicine, 2018. **379**(24): p. 2330-2341.
216. Khoury, J.D., et al., *The 5th edition of the World Health Organization Classification of Haematolymphoid Tumours: Myeloid and Histiocytic/Dendritic Neoplasms*. Leukemia, 2022. **36**(7): p. 1703-1719.
217. Dillon, R., et al., *How we use molecular minimal residual disease (MRD) testing in acute myeloid leukaemia (AML)*. Br J Haematol, 2021. **193**(2): p. 231-244.
218. Walter, R.B., et al., *Measurable residual disease as a biomarker in acute myeloid leukemia: theoretical and practical considerations*. Leukemia, 2021. **35**(6): p. 1529-1538.
219. Tazi, Y., et al., *Unified classification and risk-stratification in Acute Myeloid Leukemia*. Nat Commun, 2022. **13**(1): p. 4622.
220. Dombret, H., E. Raffoux, and C. Gardin, *Acute myeloid leukemia in the elderly*. Semin Oncol, 2008. **35**(4): p. 430-8.
221. Lichtman, M.A., *A historical perspective on the development of the cytarabine (7days) and daunorubicin (3days) treatment regimen for acute myelogenous leukemia: 2013 the 40th anniversary of 7+3*. Blood Cells, Molecules, and Diseases, 2013.
222. Zwelling, L.A., *DNA topoisomerase II as a target of antineoplastic drug therapy*. Cancer Metastasis Rev, 1985. **4**(4): p. 263-76.
223. Pommier, Y., et al., *Effects of DNA intercalating agents on topoisomerase II induced DNA strand cleavage in isolated mammalian cell nuclei*. Biochemistry, 1985. **24**(23): p. 6406-10.
224. Minotti, G., et al., *Anthracyclines: molecular advances and pharmacologic developments in antitumor activity and cardiotoxicity*. Pharmacol Rev, 2004. **56**(2): p. 185-229.
225. Stone, R.M., et al., *Midostaurin plus Chemotherapy for Acute Myeloid Leukemia with a FLT3 Mutation*. N Engl J Med, 2017. **377**(5): p. 454-464.
226. Dohner, H., et al., *Midostaurin plus intensive chemotherapy for younger and older patients with AML and FLT3 internal tandem duplications*. Blood Adv, 2022. **6**(18): p. 5345-5355.
227. Mayer, L.D., P. Tardi, and A.C. Louie, *CPX-351: a nanoscale liposomal co-formulation of daunorubicin and cytarabine with unique biodistribution and tumor cell uptake properties*. Int J Nanomedicine, 2019. **14**: p. 3819-3830.
228. Lancet, J.E., et al., *CPX-351 versus 7+3 cytarabine and daunorubicin chemotherapy in older adults with newly diagnosed high-risk or secondary acute myeloid leukaemia: 5-year results of a randomised, open-label, multicentre, phase 3 trial*. Lancet Haematol, 2021. **8**(7): p. e481-e491.

229. Cortes, J.E., et al., *Efficacy and safety of CPX-351 versus 7 + 3 chemotherapy by European LeukemiaNet 2017 risk subgroups in older adults with newly diagnosed, high-risk/secondary AML: post hoc analysis of a randomized, phase 3 trial.* J Hematol Oncol, 2022. **15**(1): p. 155.
230. DiNardo, C.D., et al., *Venetoclax combined with decitabine or azacitidine in treatment-naive, elderly patients with acute myeloid leukemia.* Blood, 2019. **133**(1): p. 7-17.
231. DiNardo, C.D., et al., *Azacitidine and Venetoclax in Previously Untreated Acute Myeloid Leukemia.* N Engl J Med, 2020. **383**(7): p. 617-629.
232. Maiti, A., et al., *Outcomes of relapsed or refractory acute myeloid leukemia after frontline hypomethylating agent and venetoclax regimens.* Haematologica, 2021. **106**(3): p. 894-898.
233. Wei, A.H., et al., *Venetoclax plus LDAC for newly diagnosed AML ineligible for intensive chemotherapy: a phase 3 randomized placebo-controlled trial.* Blood, 2020. **135**(24): p. 2137-2145.
234. Montesinos, P., et al., *Ivosidenib and Azacitidine in IDH1-Mutated Acute Myeloid Leukemia.* New England Journal of Medicine, 2022. **386**(16): p. 1519-1531.
235. Cortes, J.E., et al., *Randomized comparison of low dose cytarabine with or without glasdegib in patients with newly diagnosed acute myeloid leukemia or high-risk myelodysplastic syndrome.* Leukemia, 2019. **33**(2): p. 379-389.
236. Crossnohere, N.L., et al., *Side effects from acute myeloid leukemia treatment: results from a national survey.* Current Medical Research and Opinion, 2019. **35**(11): p. 1965-1970.
237. Ganzel, C., et al., *Very poor long-term survival in past and more recent studies for relapsed AML patients: The ECOG-ACRIN experience.* Am J Hematol, 2018. **93**(8): p. 1074-1081.
238. Yilmaz, M., et al., *Late relapse in acute myeloid leukemia (AML): clonal evolution or therapy-related leukemia?* Blood Cancer Journal, 2019. **9**(2): p. 7.
239. Ding, L., et al., *Clonal evolution in relapsed acute myeloid leukaemia revealed by whole-genome sequencing.* Nature, 2012. **481**(7382): p. 506-10.
240. Wong, T.N., et al., *Role of TP53 mutations in the origin and evolution of therapy-related acute myeloid leukaemia.* Nature, 2015. **518**(7540): p. 552-555.
241. Lechman, E.R., et al., *miR-126 Regulates Distinct Self-Renewal Outcomes in Normal and Malignant Hematopoietic Stem Cells.* Cancer Cell, 2016. **29**(2): p. 214-28.
242. Naldini, M.M., et al., *Longitudinal single-cell profiling of chemotherapy response in acute myeloid leukemia.* Nature Communications, 2023. **14**(1): p. 1285.
243. Jordheim, L.P., et al., *Advances in the development of nucleoside and nucleotide analogues for cancer and viral diseases.* Nature Reviews Drug Discovery, 2013. **12**(6): p. 447-464.
244. Wang, E., et al., *The Emerging Role of Gemcitabine in Conditioning Regimens for Hematopoietic Stem Cell Transplantation.* Biology of Blood and Marrow Transplantation, 2014. **20**(9): p. 1382-1389.
245. Burris, H.A., 3rd, et al., *Improvements in survival and clinical benefit with gemcitabine as first-line therapy for patients with advanced pancreas cancer: a randomized trial.* J Clin Oncol, 1997. **15**(6): p. 2403-13.
246. Sandler, A. and D.S. Ettinger, *Gemcitabine: single-agent and combination therapy in non-small cell lung cancer.* Oncologist, 1999. **4**(3): p. 241-51.

247. Drenberg, C.D., et al., *A high-throughput screen indicates gemcitabine and JAK inhibitors may be useful for treating pediatric AML*. Nature Communications, 2019. **10**(1): p. 2189.
248. Borthakur, G.M., et al., *Fludarabine, Cytarabine, G-CSF and Gemtuzumab Ozogamicin (FLAG-GO) Regimen Results in Better Molecular Response and Relapse-Free Survival in Core Binding Factor Acute Myeloid Leukemia Than FLAG and Idarubicin (FLAG-Ida)*. Blood, 2019. **134**(Supplement_1): p. 290-290.
249. Cheng, J.C., et al., *Inhibition of DNA methylation and reactivation of silenced genes by zebularine*. J Natl Cancer Inst, 2003. **95**(5): p. 399-409.
250. Antonsson, B.E., et al., *Effect of 5-azacytidine and congeners on DNA methylation and expression of deoxycytidine kinase in the human lymphoid cell lines CCRF/CEM/0 and CCRF/CEM/dCk-1*. Cancer Res, 1987. **47**(14): p. 3672-8.
251. Qin, T., et al., *Effect of cytarabine and decitabine in combination in human leukemic cell lines*. Clinical Cancer Research, 2007.
252. Qin, T., et al., *Mechanisms of resistance to 5-aza-2'-deoxycytidine in human cancer cell lines*. Blood, 2009. **113**(3): p. 659-67.
253. Cano-Soldado, P. and M. Pastor-Anglada, *Transporters that translocate nucleosides and structural similar drugs: structural requirements for substrate recognition*. Med Res Rev, 2012. **32**(2): p. 428-57.
254. Tsismetzis, N., et al., *Nucleobase and Nucleoside Analogues: Resistance and Re-Sensitisation at the Level of Pharmacokinetics, Pharmacodynamics and Metabolism*. Cancers (Basel), 2018. **10**(7).
255. Bester, A.C., et al., *Nucleotide deficiency promotes genomic instability in early stages of cancer development*. Cell, 2011. **145**(3): p. 435-46.
256. Hartman, S.C. and J.M. Buchanan, *Nucleic acids, purines, pyrimidines (nucleotide synthesis)*. Annu Rev Biochem, 1959. **28**: p. 365-410.
257. Newsholme, P., et al., *Glutamine and glutamate--their central role in cell metabolism and function*. Cell Biochem Funct, 2003. **21**(1): p. 1-9.
258. Avramis, V.I., et al., *Pharmacodynamic and DNA methylation studies of high-dose 1-beta-D-arabinofuranosyl cytosine before and after in vivo 5-azacytidine treatment in pediatric patients with refractory acute lymphocytic leukemia*. Cancer Chemother Pharmacol, 1989. **24**(4): p. 203-10.
259. Carpinelli, P., et al., *Antiproliferative effects and DNA hypomethylation by 5-aza-2'-deoxycytidine in human neuroblastoma cell lines*. Anticancer Drugs, 1993. **4**(6): p. 629-35.
260. Raynal, N.J., et al., *3-Deazauridine enhances the antileukemic action of 5-aza-2'-deoxycytidine and targets drug-resistance due to deficiency in deoxycytidine kinase*. Leuk Res, 2011. **35**(1): p. 110-8.
261. Rathe, S.K., et al., *Using RNA-seq and targeted nucleases to identify mechanisms of drug resistance in acute myeloid leukemia*. Sci Rep, 2014. **4**: p. 6048.
262. Kurata, M., et al., *Using genome-wide CRISPR library screening with library resistant DCK to find new sources of Ara-C drug resistance in AML*. Sci Rep, 2016. **6**: p. 36199.
263. Schneider, C., et al., *SAMHD1 is a biomarker for cytarabine response and a therapeutic target in acute myeloid leukemia*. Nat Med, 2017. **23**(2): p. 250-255.

264. Gruber, T.A., et al., *An Inv(16)(p13.3q24.3)-encoded CBFA2T3-GLIS2 fusion protein defines an aggressive subtype of pediatric acute megakaryoblastic leukemia*. *Cancer Cell*, 2012. **22**(5): p. 683-97.
265. Ling, V.Y., et al., *Targeting cell cycle and apoptosis to overcome chemotherapy resistance in acute myeloid leukemia*. *Leukemia*, 2022.
266. Tibaldi, C., et al., *Correlation of cytidine deaminase polymorphisms and activity with clinical outcome in gemcitabine-/platinum-treated advanced non-small-cell lung cancer patients*. *Ann Oncol*, 2012. **23**(3): p. 670-677.
267. Yonemori, K., et al., *Severe drug toxicity associated with a single-nucleotide polymorphism of the cytidine deaminase gene in a Japanese cancer patient treated with gemcitabine plus cisplatin*. *Clin Cancer Res*, 2005. **11**(7): p. 2620-4.
268. Fanciullino, R., et al., *CDA as a predictive marker for life-threatening toxicities in patients with AML treated with cytarabine*. *Blood Adv*, 2018. **2**(5): p. 462-469.
269. Chinwalla, A.T., et al., *Initial sequencing and comparative analysis of the mouse genome*. *Nature*, 2002. **420**(6915): p. 520-562.
270. Zheng-Bradley, X., et al., *Large scale comparison of global gene expression patterns in human and mouse*. *Genome Biology*, 2010. **11**(12): p. R124.
271. Zuber, J., et al., *Mouse models of human AML accurately predict chemotherapy response*. *Genes and Development*, 2009.
272. Krivtsov, A.V., et al., *Transformation from committed progenitor to leukaemia stem cell initiated by MLL-AF9*. *Nature*, 2006. **442**(7104): p. 818-22.
273. Kroon, E., et al., *Hoxa9 transforms primary bone marrow cells through specific collaboration with Meis1a but not Pbx1b*. *EMBO Journal*, 1998.
274. Wong, P., et al., *Meis1 is an essential and rate-limiting regulator of MLL leukemia stem cell potential*. *Genes Dev*, 2007. **21**(21): p. 2762-74.
275. Argiropoulos, B., et al., *Linkage of the potent leukemogenic activity of Meis1 to cell-cycle entry and transcriptional regulation of cyclin D3*. *Blood*, 2010. **115**(20): p. 4071-82.
276. Gibbs, K.D., Jr., et al., *Decoupling of tumor-initiating activity from stable immunophenotype in HoxA9-Meis1-driven AML*. *Cell Stem Cell*, 2012. **10**(2): p. 210-7.
277. George, J., et al., *Leukaemia cell of origin identified by chromatin landscape of bulk tumour cells*. *Nat Commun*, 2016. **7**: p. 12166.
278. Bernt, Kathrin M., et al., *MLL-Rearranged Leukemia Is Dependent on Aberrant H3K79 Methylation by DOT1L*. *Cancer Cell*, 2011. **20**(1): p. 66-78.
279. Dawson, M.A., et al., *Inhibition of BET recruitment to chromatin as an effective treatment for MLL-fusion leukaemia*. *Nature*, 2011. **478**(7370): p. 529-533.
280. Grembecka, J., et al., *Menin-MLL inhibitors reverse oncogenic activity of MLL fusion proteins in leukemia*. *Nature Chemical Biology*, 2012. **8**(3): p. 277-284.
281. Collins, E.C., et al., *Inter-chromosomal recombination of Mll and Af9 genes mediated by cre-loxP in mouse development*. *EMBO reports*, 2000. **1**(2): p. 127-132.
282. Hartner, J.C., et al., *ADAR1 is essential for the maintenance of hematopoiesis and suppression of interferon signaling*. *Nature Immunology*, 2009. **10**(1): p. 109-115.
283. Sinha, R., et al., *Development of embryonic and adult leukemia mouse models driven by MLL-ENL translocation*. *Experimental Hematology*, 2020. **85**: p. 13-19.
284. Sarrou, E., et al. *CRISPR Gene Editing of Murine Blood Stem and Progenitor Cells Induces MLL-AF9 Chromosomal Translocation and MLL-AF9 Leukaemogenesis*. *International Journal of Molecular Sciences*, 2020. **21**, DOI: 10.3390/ijms21124266.

285. Mojica, F.J., et al., *Intervening sequences of regularly spaced prokaryotic repeats derive from foreign genetic elements*. J Mol Evol, 2005. **60**(2): p. 174-82.
286. Bolotin, A., et al., *Clustered regularly interspaced short palindrome repeats (CRISPRs) have spacers of extrachromosomal origin*. Microbiology (Reading), 2005. **151**(Pt 8): p. 2551-2561.
287. Marraffini, L.A. and E.J. Sontheimer, *CRISPR interference limits horizontal gene transfer in staphylococci by targeting DNA*. Science, 2008. **322**(5909): p. 1843-5.
288. Evers, B., et al., *CRISPR knockout screening outperforms shRNA and CRISPRi in identifying essential genes*. Nature Biotechnology, 2016. **34**(6): p. 631-633.
289. Konermann, S., et al., *Genome-scale transcriptional activation by an engineered CRISPR-Cas9 complex*. Nature, 2015. **517**(7536): p. 583-8.
290. Chavez, A., et al., *Highly efficient Cas9-mediated transcriptional programming*. Nat Methods, 2015. **12**(4): p. 326-8.
291. Alerasool, N., et al., *An efficient KRAB domain for CRISPRi applications in human cells*. Nat Methods, 2020. **17**(11): p. 1093-1096.
292. Xu, X. and L.S. Qi, *A CRISPR-dCas Toolbox for Genetic Engineering and Synthetic Biology*. J Mol Biol, 2019. **431**(1): p. 34-47.
293. Shalem, O., et al., *GeCKO v2. pooled libraries*. Science, 2014.
294. Shalem, O., et al., *Genome-scale CRISPR-Cas9 knockout screening in human cells*. Science, 2014.
295. Doench, J.G., et al., *Rational design of highly active sgRNAs for CRISPR-Cas9-mediated gene inactivation*. Nat Biotechnol, 2014. **32**(12): p. 1262-7.
296. Doench, J.G., et al., *Optimized sgRNA design to maximize activity and minimize off-target effects of CRISPR-Cas9*. Nat Biotechnol, 2016. **34**(2): p. 184-191.
297. Arroyo, J.D., et al., *A Genome-wide CRISPR Death Screen Identifies Genes Essential for Oxidative Phosphorylation*. Cell Metab, 2016. **24**(6): p. 875-885.
298. Chen, X., et al., *Targeting Mitochondrial Structure Sensitizes Acute Myeloid Leukemia to Venetoclax Treatment*. Cancer Discov, 2019. **9**(7): p. 890-909.
299. Lin, S., et al., *An In Vivo CRISPR Screening Platform for Prioritizing Therapeutic Targets in AML*. Cancer Discov, 2022. **12**(2): p. 432-449.
300. Vujovic, A., et al., *In Vivo Screening Unveils Pervasive RNA-Binding Protein Dependencies in Leukemic Stem Cells and Identifies ELAVL1 as a Therapeutic Target*. Blood Cancer Discov, 2023. **4**(3): p. 180-207.
301. Hartenian, E. and J.G. Doench, *Genetic screens and functional genomics using CRISPR/Cas9 technology*. FEBS J, 2015. **282**(8): p. 1383-93.
302. Sharon, D., et al., *Inhibition of mitochondrial translation overcomes venetoclax resistance in AML through activation of the integrated stress response*. Sci Transl Med, 2019. **11**(516).
303. Bass, D. and T. Both, *Monitoring Line Specifications*. p. 12--17.
304. Lin, K.H., et al., *Systematic Dissection of the Metabolic-Apoptotic Interface in AML Reveals Heme Biosynthesis to Be a Regulator of Drug Sensitivity*. Cell Metab, 2019. **29**(5): p. 1217-1231.e7.
305. Nechiporuk, T., et al., *The TP53 Apoptotic Network Is a Primary Mediator of Resistance to BCL2 Inhibition in AML Cells*. Cancer Discov, 2019. **9**(7): p. 910-925.

306. Damnernasawad, A., et al., *Genome-wide CRISPR screen identifies regulators of MAPK and MTOR pathways mediating sorafenib resistance in acute myeloid leukemia*. *Haematologica*, 2022. **107**(1): p. 77-85.
307. Deng, L., et al., *The role of ubiquitination in tumorigenesis and targeted drug discovery*. *Signal Transduction and Targeted Therapy*, 2020. **5**(1): p. 11.
308. Ciechanover, A., et al., *Activation of the heat-stable polypeptide of the ATP-dependent proteolytic system*. *Proc Natl Acad Sci U S A*, 1981. **78**(2): p. 761-5.
309. Stewart, M.D., et al., *E2 enzymes: more than just middle men*. *Cell Research*, 2016. **26**(4): p. 423-440.
310. Hoeller, D. and I. Dikic, *Targeting the ubiquitin system in cancer therapy*. *Nature*, 2009. **458**(7237): p. 438-44.
311. Komander, D., M.J. Clague, and S. Urbé, *Breaking the chains: structure and function of the deubiquitinases*. *Nature Reviews Molecular Cell Biology*, 2009. **10**(8): p. 550-563.
312. Yuan, J., et al., *USP10 regulates p53 localization and stability by deubiquitinating p53*. *Cell*, 2010. **140**(3): p. 384-96.
313. Stevenson, L.F., et al., *The deubiquitinating enzyme USP2a regulates the p53 pathway by targeting Mdm2*. *Embo j*, 2007. **26**(4): p. 976-86.
314. Sun, X.X., K.B. Challagundla, and M.S. Dai, *Positive regulation of p53 stability and activity by the deubiquitinating enzyme Otubain 1*. *Embo j*, 2012. **31**(3): p. 576-92.
315. Rajalingam, K. and I. Dikic, *SnapShot: Expanding the Ubiquitin Code*. *Cell*, 2016. **164**(5): p. 1074-1074.e1.
316. Gregory, R.C., T. Taniguchi, and A.D. D'Andrea, *Regulation of the Fanconi anemia pathway by monoubiquitination*. *Semin Cancer Biol*, 2003. **13**(1): p. 77-82.
317. Wang, X., P.R. Andreassen, and A.D. D'Andrea, *Functional interaction of monoubiquitinated FANCD2 and BRCA2/FANCD1 in chromatin*. *Mol Cell Biol*, 2004. **24**(13): p. 5850-62.
318. Geng, L., C.J. Huntoon, and L.M. Karnitz, *RAD18-mediated ubiquitination of PCNA activates the Fanconi anemia DNA repair network*. *J Cell Biol*, 2010. **191**(2): p. 249-57.
319. Al-Hakim, A., et al., *The ubiquitous role of ubiquitin in the DNA damage response*. *DNA Repair (Amst)*, 2010. **9**(12): p. 1229-40.
320. Pickart, C.M., *Mechanisms underlying ubiquitination*. *Annu Rev Biochem*, 2001. **70**: p. 503-33.
321. Chi, S.-W., et al., *Structural Details on mdm2-p53 Interaction**. *Journal of Biological Chemistry*, 2005. **280**(46): p. 38795-38802.
322. Poyurovsky, M.V., et al., *The Mdm2 RING domain C-terminus is required for supramolecular assembly and ubiquitin ligase activity*. *Embo j*, 2007. **26**(1): p. 90-101.
323. Weber, J., S. Polo, and E. Maspero, *HECT E3 Ligases: A Tale With Multiple Facets*. *Front Physiol*, 2019. **10**: p. 370.
324. Mund, T. and H.R. Pelham, *Control of the activity of WW-HECT domain E3 ubiquitin ligases by NDFIP proteins*. *EMBO Rep*, 2009. **10**(5): p. 501-7.
325. Mund, T., et al., *Peptide and small molecule inhibitors of HECT-type ubiquitin ligases*. *Proceedings of the National Academy of Sciences*, 2014. **111**(47): p. 16736-16741.
326. Zhang, W., et al., *System-Wide Modulation of HECT E3 Ligases with Selective Ubiquitin Variant Probes*. *Mol Cell*, 2016. **62**(1): p. 121-36.
327. Morrison, S.J. and D.T. Scadden, *The bone marrow niche for haematopoietic stem cells*. 2014.

328. Majeti, R., et al., *Clonal Expansion of Stem/Progenitor Cells in Cancer, Fibrotic Diseases, and Atherosclerosis, and CD47 Protection of Pathogenic Cells*. *Annu Rev Med*, 2022. **73**: p. 307-320.
329. Sampath, D., V.A. Rao, and W. Plunkett, *Mechanisms of apoptosis induction by nucleoside analogs*. *Oncogene*, 2003. **22**(56): p. 9063-9074.
330. Stentoft, J., *The Toxicity of Cytarabine*. *Drug Safety*, 1990. **5**(1): p. 7-27.
331. Gu, X., et al., *Decitabine- and 5-azacytidine resistance emerges from adaptive responses of the pyrimidine metabolism network*. *Leukemia*, 2021. **35**(4): p. 1023-1036.
332. Zhang, F., et al., *Stabilization of SAMHD1 by NONO is crucial for Ara-C resistance in AML*. *Cell Death Dis*, 2022. **13**(7): p. 590.
333. Cartel, M., et al., *Inhibition of ubiquitin-specific protease 7 sensitizes acute myeloid leukemia to chemotherapy*. *Leukemia*, 2021. **35**(2): p. 417-432.
334. Pedrazza, L., et al., *HERC1 deficiency causes osteopenia through transcriptional program dysregulation during bone remodeling*. *Cell Death Dis*, 2023. **14**(1): p. 17.
335. Zavodszky, E., et al., *Identification of a quality-control factor that monitors failures during proteasome assembly*. *Science*, 2021. **373**(6558): p. 998-1004.
336. Chong-Kopera, H., et al., *TSC1 stabilizes TSC2 by inhibiting the interaction between TSC2 and the HERC1 ubiquitin ligase*. *Journal of Biological Chemistry*, 2006.
337. Diouf, B., et al., *Somatic deletions of genes regulating MSH2 protein stability cause DNA mismatch repair deficiency and drug resistance in human leukemia cells*. *Nature Medicine*, 2011.
338. Schneider, T., et al., *The E3 ubiquitin ligase HERC1 controls the ERK signaling pathway targeting C-RAF for degradation*. *Oncotarget*, 2018. **9**(59): p. 31531-31548.
339. Rosa, J.L., et al., *p619, a giant protein related to the chromosome condensation regulator RCC1, stimulates guanine nucleotide exchange on ARF1 and Rab proteins*. *Embo j*, 1996. **15**(16): p. 4262-73.
340. Rosa, J.L. and M. Barbacid, *A giant protein that stimulates guanine nucleotide exchange on ARF1 and Rab proteins forms a cytosolic ternary complex with clathrin and Hsp70*. *Oncogene*, 1997. **15**(1): p. 1-6.
341. Holloway, A., et al., *Resistance to UV-induced apoptosis by β -HPV5 E6 involves targeting of activated BAK for proteolysis by recruitment of the HERC1 ubiquitin ligase*. *International Journal of Cancer*, 2015.
342. Mashimo, T., et al., *Progressive Purkinje Cell Degeneration in tambaleante Mutant Mice Is a Consequence of a Missense Mutation in HERC1 E3 Ubiquitin Ligase*. *PLOS Genetics*, 2009. **5**(12): p. e1000784.
343. Bachiller, S., et al., *The HERC1 E3 Ubiquitin Ligase is essential for normal development and for neurotransmission at the mouse neuromuscular junction*. *Cellular and Molecular Life Sciences*, 2015.
344. Nguyen, L.S., et al., *A nonsense variant in HERC1 is associated with intellectual disability, megalencephaly, thick corpus callosum and cerebellar atrophy*. *European Journal of Human Genetics*, 2016.
345. Utine, G.E., et al., *HERC1 mutations in idiopathic intellectual disability*. *European Journal of Medical Genetics*, 2017.
346. Johansson, P., et al., *SAMHD1 is recurrently mutated in T-cell prolymphocytic leukemia*. *Blood Cancer Journal*, 2018.

347. Opatz, S., et al., *The clinical mutator of core binding factor leukemia*. *Leukemia*, 2020. **34**(6): p. 1553-1562.
348. Ali, M.S., et al., *The Downregulation of Both Giant HERCs, HERC1 and HERC2, Is an Unambiguous Feature of Chronic Myeloid Leukemia, and HERC1 Levels Are Associated with Leukemic Cell Differentiation*. *J Clin Med*, 2022. **11**(2).
349. Blake, J.A., et al., *Mouse Genome Database (MGD): Knowledgebase for mouse-human comparative biology*. *Nucleic Acids Res*, 2021. **49**(D1): p. D981-d987.
350. Yang, H., et al., *Genome-Wide CRISPR Screening Identifies DCK and CCNLI as Genes That Contribute to Gemcitabine Resistance in Pancreatic Cancer*. *Cancers (Basel)*, 2022. **14**(13).
351. Prajapati, S.C., et al., *Validation of CRISPR targeting for proliferation and cytarabine resistance control genes in the acute myeloid leukemia cell line MOLM-13*. *Biotechniques*, 2022. **72**(3): p. 81-84.
352. Poddar, S., et al., *Development and preclinical pharmacology of a novel dCK inhibitor, DI-87*. *Biochem Pharmacol*, 2020. **172**: p. 113742.
353. Wu, B., et al., *Deoxycytidine Kinase (DCK) Mutations in Human Acute Myeloid Leukemia Resistant to Cytarabine*. *Acta Haematol*, 2021. **144**(5): p. 534-541.
354. Veuger, M.J.T., et al., *High incidence of alternatively spliced forms of deoxycytidine kinase in patients with resistant acute myeloid leukemia*. *Blood*, 2000. **96**(4): p. 1517-1524.
355. Al-Madhoun, A.S., et al., *Detection of an alternatively spliced form of deoxycytidine kinase mRNA in the 2'-2'-difluorodeoxycytidine (gemcitabine)-resistant human ovarian cancer cell line AG6000*. *Biochem Pharmacol*, 2004. **68**(4): p. 601-9.
356. Wang, E., et al., *Modulation of RNA splicing enhances response to BCL2 inhibition in leukemia*. *Cancer Cell*, 2023. **41**(1): p. 164-180 e8.
357. Amsailale, R., et al., *Protein phosphatase 2A regulates deoxycytidine kinase activity via Ser-74 dephosphorylation*. *FEBS Lett*, 2014. **588**(5): p. 727-32.
358. Beyaert, M., et al., *A crucial role for ATR in the regulation of deoxycytidine kinase activity*. *Biochem Pharmacol*, 2016. **100**: p. 40-50.
359. Yang, C., et al., *Deoxycytidine kinase regulates the G2/M checkpoint through interaction with cyclin-dependent kinase 1 in response to DNA damage*. *Nucleic Acids Res*, 2012. **40**(19): p. 9621-32.
360. Le, T.M., et al., *ATR inhibition facilitates targeting of leukemia dependence on convergent nucleotide biosynthetic pathways*. *Nat Commun*, 2017. **8**(1): p. 241.
361. Sugitani, N., et al., *Thymidine rescues ATR kinase inhibitor-induced deoxyuridine contamination in genomic DNA, cell death, and interferon- α/β expression*. *Cell Rep*, 2022. **40**(12): p. 111371.
362. Sabini, E., et al., *Structure of human dCK suggests strategies to improve anticancer and antiviral therapy*. *Nature Structural & Molecular Biology*, 2003. **10**(7): p. 513-519.
363. Kroep, J.R., et al., *Pretreatment deoxycytidine kinase levels predict in vivo gemcitabine sensitivity*. *Mol Cancer Ther*, 2002. **1**(6): p. 371-6.
364. Austin, W.R., et al., *Nucleoside salvage pathway kinases regulate hematopoiesis by linking nucleotide metabolism with replication stress*. *Journal of Experimental Medicine*, 2012. **209**(12): p. 2215-2228.

365. Cohen, A., et al., *Purine metabolism in human T lymphocytes: role of the purine nucleoside cycle*. Canadian Journal of Biochemistry and Cell Biology, 1984. **62**(7): p. 577-583.
366. Sykes, D.B., et al., *Inhibition of Dihydroorotate Dehydrogenase Overcomes Differentiation Blockade in Acute Myeloid Leukemia*. Cell, 2016. **167**(1): p. 171-186.e15.
367. Dash, S., et al., *MYC/Glutamine Dependency Is a Therapeutic Vulnerability in Pancreatic Cancer with Deoxycytidine Kinase Inactivation-Induced Gemcitabine Resistance*. Mol Cancer Res, 2023. **21**(5): p. 444-457.
368. Shyamsunder, P., et al., *Identification of a novel enhancer of CEBPE essential for granulocytic differentiation*. Blood, 2019. **133**(23): p. 2507-2517.
369. Laouedj, M., et al., *S100A9 induces differentiation of acute myeloid leukemia cells through TLR4*. Blood, 2017. **129**(14): p. 1980-1990.
370. Mildner, A., et al., *Genomic Characterization of Murine Monocytes Reveals C/EBP β ; Transcription Factor Dependence of Ly6C⁺ Cells*. Immunity, 2017. **46**(5): p. 849-862.e7.
371. Hattori, T., et al., *C/EBP family transcription factors are degraded by the proteasome but stabilized by forming dimer*. Oncogene, 2003. **22**(9): p. 1273-80.
372. Tomic, B., et al., *Cytarabine-induced differentiation of AML cells depends on Chk1 activation and shares the mechanism with inhibitors of DHODH and pyrimidine synthesis*. Sci Rep, 2022. **12**(1): p. 11344.
373. Freiburghaus, C., et al., *Bortezomib prevents cytarabine resistance in MCL, which is characterized by down-regulation of dCK and up-regulation of SPIB resulting in high NF-kappaB activity*. BMC Cancer, 2018. **18**(1): p. 466.
374. Lindhurst, M.J., et al., *Knockout of *Slc25a19* causes mitochondrial thiamine pyrophosphate depletion, embryonic lethality, CNS malformations, and anemia*. Proceedings of the National Academy of Sciences, 2006. **103**(43): p. 15927-15932.
375. Kelley, R.I., et al., *Amish lethal microcephaly: a new metabolic disorder with severe congenital microcephaly and 2-ketoglutaric aciduria*. Am J Med Genet, 2002. **112**(4): p. 318-26.
376. Carey, B.W., et al., *Intracellular α -ketoglutarate maintains the pluripotency of embryonic stem cells*. Nature, 2015. **518**(7539): p. 413-6.
377. Martínez-Reyes, I. and N.S. Chandel, *Mitochondrial TCA cycle metabolites control physiology and disease*. Nature Communications, 2020. **11**(1): p. 102.
378. Mangalhara, K.C., et al., *Manipulating mitochondrial electron flow enhances tumor immunogenicity*. Science, 2023. **381**(6664): p. 1316-1323.
379. Liu, N., et al., *Supplementation with α -ketoglutarate improved the efficacy of anti-PD1 melanoma treatment through epigenetic modulation of PD-L1*. Cell Death & Disease, 2023. **14**(2): p. 170.
380. Hochman, P.S., G. Cudkowicz, and J. Dausset, *Decline of Natural Killer Cell Activity in Sublethally Irradiated Mice*. JNCI: Journal of the National Cancer Institute, 1978. **61**(1): p. 265-268.
381. Del Poeta, G., et al., *Amount of spontaneous apoptosis detected by Bax/Bcl-2 ratio predicts outcome in acute myeloid leukemia (AML)*. Blood, 2003. **101**(6): p. 2125-31.
382. Chonghaile, T.N., et al., *Pretreatment Mitochondrial Priming Correlates with Clinical Response to Cytotoxic Chemotherapy*. Science, 2011. **334**(6059): p. 1129-1133.

383. Rubnitz, J.E., et al., *NKAML: a pilot study to determine the safety and feasibility of haploidentical natural killer cell transplantation in childhood acute myeloid leukemia*. J Clin Oncol, 2010. **28**(6): p. 955-9.
384. Iliopoulou, E.G., et al., *A phase I trial of adoptive transfer of allogeneic natural killer cells in patients with advanced non-small cell lung cancer*. Cancer Immunol Immunother, 2010. **59**(12): p. 1781-9.
385. Miller, J.S., et al., *Successful adoptive transfer and in vivo expansion of human haploidentical NK cells in patients with cancer*. Blood, 2005. **105**(8): p. 3051-7.
386. Vela, M., et al., *Haploidentical IL-15/41BBL activated and expanded natural killer cell infusion therapy after salvage chemotherapy in children with relapsed and refractory leukemia*. Cancer Letters, 2018. **422**: p. 107-117.
387. Gómez García, L.M., et al., *Phase 2 Clinical Trial of Infusing Haploidentical K562-mb15-41BBL-Activated and Expanded Natural Killer Cells as Consolidation Therapy for Pediatric Acute Myeloblastic Leukemia*. Clin Lymphoma Myeloma Leuk, 2021. **21**(5): p. 328-337.e1.
388. Smyth, M.J., et al., *Activation of NK cell cytotoxicity*. Molecular Immunology, 2005. **42**(4): p. 501-510.
389. Vadakekolathu, J., et al., *Immune landscapes predict chemotherapy resistance and immunotherapy response in acute myeloid leukemia*. Science Translational Medicine, 2020. **12**(546): p. eaaz0463.
390. Steiner, A., et al., *Deficiency in coatomer complex I causes aberrant activation of STING signalling*. Nature Communications, 2022. **13**(1): p. 2321.
391. Song, T.-Y., et al., *Tumor evolution selectively inactivates the core microRNA machinery for immune evasion*. Nature Communications, 2021. **12**(1): p. 7003.
392. Laverdière, I., et al., *Complement cascade gene expression defines novel prognostic subgroups of acute myeloid leukemia*. Experimental Hematology, 2016. **44**(11): p. 1039-1043.e10.
393. Majeti, R., et al., *CD47 is an adverse prognostic factor and therapeutic antibody target on human acute myeloid leukemia stem cells*. Cell, 2009. **138**(2): p. 286-99.
394. Jaiswal, S., et al., *CD47 is upregulated on circulating hematopoietic stem cells and leukemia cells to avoid phagocytosis*. Cell, 2009. **138**(2): p. 271-85.
395. Shultz, L.D., et al., *Human Lymphoid and Myeloid Cell Development in NOD/LtSz-scid IL2R γ null Mice Engrafted with Mobilized Human Hemopoietic Stem Cells 12*. The Journal of Immunology, 2005. **174**(10): p. 6477-6489.